SEVER INSTITUTE OF TECHNOLOGY

Doctor of Science Degree

DISSERTATION ACCEPTANCE
(To be submitted by the graduation approval deadline)

DATE: September 9, 1993

STUDENT'S NAME: Muthanna Al-Dahhan

E.R.S. CODE: _____

This student's dissertation, entitled Effects of High Pressure and Fines on the Hydrodynamics of Trickle-Bed Reactors

has been examined by the undersigned committee of three faculty members and has received full approval for acceptance in partial fulfillment of the requirements for the degree Doctor of Science.

Signatures: _____ Chairman
_____
_____
_____

Distribution:

5 - Dissertation copies
1 - Candidate
1 - Department
1 - Dean's Office
1 - Registrar

WASHINGTON UNIVERSITY
SEVER INSTITUTE OF TECHNOLOGY

EFFECTS OF HIGH PRESSURE AND FINES ON THE HYDRODYNAMICS OF TRICKLE-BED REACTORS

by

Muthanna H. Al-Dahhan

Prepared under the direction of Professors M. P. Dudukovic′ and P. A. Ramachandran

---

A dissertation presented to Sever Institute of Washington University in partial fulfillment of the requirements for the degree of

DOCTOR OF SCIENCE

December, 1993

Saint Louis, Missouri

WASHINGTON UNIVERSITY

SEVER INSTITUTE OF TECHNOLOGY

ABSTRACT

EFFECTS OF HIGH PRESSURE AND FINES ON THE HYDRODYNAMICS OF TRICKLE-BED REACTORS

ADVISORS : Professor M. P. Dudukovic'
Professor P. A. Ramachandran

December, 1993
Saint Louis, Missouri

Trickle-bed reactors are widely used in industry. These reactors generally are operated at high pressure. In the literature the studies on the design and scale-up parameters have been mainly performed under atmospheric conditions. It is unknown whether the findings of these studies can be extrapolated to much higher pressure. It is noteworthy that such reactors are usually designed and scaled-up based on data obtained in laboratory scale units. In such small scale reactors, which use the same catalyst sizes and shapes of the commercial units, wall effect, axial dispersion and liquid maldistribution and hence incomplete catalyst wetting are encountered due to low liquid velocities. Diluting the bed with fines (small, inert and nonporous particles) is recommended to overcome these shortcomings. No study has appeared in the literature which quantifies the effect of fines on liquid-solid contacting efficiency, pressure drop and liquid holdup.

In this study a high pressure trickle-bed reactor facility has been designed and developed. The effects of high pressure and gas flow rate on pressure drop, liquid holdup and liquid-solid contacting efficiency have been investigated. It was found that at high pressure operation and high gas flow rate, pressure drop increases considerably, liquid holdup decreases significantly, and liquid-solid contacting efficiency improves noticeably. A phenomenological analysis has been developed in this study which describes these effects properly. A new model based on phenomenological consideration

to predict liquid-solid contacting efficiency at high pressure has been developed. It predicts the measured contacting efficiency at elevated pressure to within ± 10% margin. Holub's phenomenological model (1990) for pressure drop and liquid holdup prediction was found to predict these parameters at high pressure better than the recently reported empirical correlations based on high pressure data.

Effects of fines on liquid-solid contacting efficiency, pressure drop and liquid holdup have been investigated. A reproducible procedure to pack the bed with a mixture of catalyst and fines has been developed which is based on filling the bed voidage with fines. Its reproducibility was quantified by pressure drop and liquid holdup measurements. It was found that fines improve liquid-solid contacting efficiency as well as increase pressure drop and liquid holdup. The effect of the degree of the bed dilution on contacting efficiency, pressure drop, and liquid holdup was also investigated . The contacting efficiency in a highly diluted bed was found to be approximately similar to that obtained in a diluted bed packed according to the developed reproducible procedure.

TABLE OF CONTENTS

	Page
List of Tables	v
List of Figures	vii
Dedication	xiii
Chapter	
1. Introduction	1
Scope	1
Motivation	7
Research objectives	10
2. Design of high pressure trickle-bed reactor facility	11
High pressure trickle-bed reactors set-up	11
Reactor's packed bed	11
Liquid / gas distributor	17
Packed bed support	20
Gas / liquid separator	21
Liquid delivery system	23
Gas delivery system	24
Tracer technique set-up	26
Data acquisition system	28
3. Effect of high pressure on pressure drop and liquid holdup	32
Background	32
Holub's phenomenological model	39
Phenomenological analysis of the effect of reactor pressure and gas flow rate on pressure drop and liquid holdup	44

Experimental investigation 47

Pressure drop and liquid holdup measurements 47

Operating conditions investigated 51

Results and data analysis 54

Validity of Holub's model and of other recent correlations 74

4. Effect of high pressure on external liquid-solid contacting efficiency 82

Background 82

Phenomenological model and analysis 87

Experimental investigation 93

External liquid-solid contacting efficiency determination 93

Operating conditions investigated 106

Results and data analysis 108

The effect of high pressure and gas flow rate on contacting efficiency 112

The developed model 118

5. Effect of fines on external liquid-solid contacting efficiency, pressure drop, and liquid holdup 122

Background 122

A reproducible procedure for packing a laboratory trickle-bed reactor with a mixture of catalyst and fines 125

The developed procedure 127

Portion of catalyst by portion of fines packing procedure 127

Whole bed packing procedure 129

Quantification of reproducibility of the developed procedure 130

Experimental investigation 137
Parameter determination 137
Pressure drop and liquid holdup measurements 137
Liquid-solid contacting efficiency determination 137
Operating conditions investigated 142
Results and data analysis 144
Effect of fines on pressure drop and liquid holdup 144
Effect of fines on liquid-solid contacting efficiency 149
6. Conclusions and recommendations 157
Conclusions 157
Recommendations 160
7. Appendices 162
Sample of a data acquisition program 163
Getting started 163
DPT.BAS program 164
Trickle-bed reactor operating procedure 167
8. Nomenclature 171
9. References 174
10. Acknowledgments 184
11. Vita 186

LIST OF TABLES

Page

1.1 Characteristic parameters of a trickle-bed reactors 2

1.2 The main advantages and disadvantages of trickle-bed reactors 3

1.3 Macroscale and microscale design parameters 5

2.1 Hardware for the data acquisition system 30

2.2 Instruments connected to the data acquisition system 31

3.1 Recent correlations for pressure drop and liquid holdup based on data obtained at high pressure and Holub's (1990) model 37

3.2 Experimental methods used to measure liquid holdup in packed-beds 48

3.3 Range of covered operating conditions 52

3.4 Physical properties of liquid-gas systems at 298 K and 1 atm 53

3.5 Packed bed characeteristics 53

3.6 Measured Ergun constants 74

3.7 Comparison of Holub's model (1990) prediction and high pressure data for pressure drop and liquid holdup 75

3.8 Comparison of models to data 77

4.1 External contacting efficiency review 84

4.2 Methods used to evaluate the external contacting efficiency 94

4.3 Expressions for the moments of infinite cylinder catalyst for a nonvolatile and nonadsorbing tracer (El-Hisnawi, 1981) 100

4.4 Expressions for the moments of spherical particles for a nonvolatile and nonadsorbing tracer (Mills and Dudukovic',1981) ... 102

4.5 Range of covered operating conditions 107

4.6 Packed bed characteristics 107

4.7 Liquid-filled effective diffusivities and the bed moments 108

5.1 Some typical data for reactors of different size 123

5.2 Methods tested for packing a bed with mixture of catalyst and fines 126

5.3 Expressions for the moments in a diluted bed of cylindrical catalyst for a nonvolatile and nonadsorbing tracer 140

5.4 Expressions for the moments in a diluted bed of spherical catalyst for a nonvolatile and nonadsorbing tracer 141

5.5 Range of covered operating conditions 142

5.6 Packed bed characteristics 143

LIST OF FIGURES

Page

1.1 Schematic diagram of a trickle-bed reactor 1

2.1 Process and instrumentation diagram (PID) of the high pressure trickle-bed reactor facility 12

2.2 (a) Front view of the high pressure trickle-bed reactor facility 13
(b) Rear view of the high pressure trickle-bed reactor facility 14

2.3 Schematic diagram of 1 inch trickle-bed reactor with acrylic window 15

2.4 Reactor's liquid / gas distributors.
(a) Distributor for two phase flow operation 18
(b) Top view of the distributor's tubes and holes 18
(c) Distributor for tracer liquid-filled operation 19

2.5 Packed bed support 20

2.6 Gas / liquid separator 22

2.7 Schematic diagram of the data acquisition system 29

3.1 Trickle-flow regime of fully wetted particles 39

3.2 Slit model representation of the geometry of a single pore in the bed (Holub, 1990) 40

3.3 Comparison of Holub's model (1990) and data for dimensionless gas phase pressure drop (ψ_G) and liquid holdup (ε_L) 43

3.4 Region of trickle flow regime covered experimentally in this study (flow map based on Fukushima And Kusaka (1977)) 51

3.5 Effect of reactor pressure and gas flow rate on pressure drop and liquid holdup. System: hexane / nitrogen ; nonporous spherical glass beads; $d_r / d_p = 20$ 57

3.6 Effect of reactor pressure and gas flow rate on pressure drop and liquid holdup. System: hexane / helium ; nonporous spherical glass beads; $d_r / d_p = 20$ 58

3.7 Effect of reactor pressure and gas flow rate on pressure drop and liquid holdup. System: water / nitrogen ; nonporous spherical glass beads; $d_r / d_p = 20$ 59

3.8 Effect of reactor pressure and gas flow rate on pressure drop and liquid holdup. System: hexane / nitrogen; porous spherical silica shell; $d_r / d_p = 14.6$ 60

3.9 Effect of reactor pressure and gas flow rate on pressure drop and liquid holdup. System: hexane / nitrogen; porous extrudate of 0.5% Pd on alumina; $d_r / d_p = 11$ 61

3.10 Effect of reactor pressure and gas flow rate on pressure drop and liquid holdup. System: water / nitrogen; porous extrudate of 0.5% Pd on alumina;$d_r / d_p = 11$ 62

3.11 Effect of reactor pressure on pressure drop and liquid holdup at $U_G \approx 4$ cm/s. System: hexane / nitrogen; nonporous spherical glass beads;$d_r / d_p = 20$ 63

3.12 Effect of reactor pressure on pressure drop and liquid holdup at $U_G \approx 8.75$ cm/s. System: hexane / nitrogen; nonporous spherical glass beads;$d_r / d_p = 20$ 64

3.13 Effect of reactor pressure on pressure drop and liquid holdup at $U_G \approx 8.75$ cm/s. System: water / nitrogen; porous extrudate of 0.5% Pd on alumina; $d_r / d_p = 11$ 65

3.14 Effect of gas density on pressure drop and liquid holdup. System: hexane / nitrogen and helium; nonporous spherical glass beads; $d_r / d_p = 20$ 66

3.15 Effect of liquid physical properties on pressure drop and liquid holdup. System: hexane/nitrogen and water/nitrogen; nonporous spherical glass beads; $d_r / d_p = 20$ 67

3.16 Effect of liquid physical properties on pressure drop and liquid holdup. System: hexane/nitrogen and water/nitrogen; porous extrudate of 0.5% Pd on alumina; $d_r / d_p = 11$ 69

3.17 Effect of bed characteristics on pressure drop and liquid holdup. System: water/nitrogen; GB: glass beads (d_p=0.114 cm); Cyl: extrudate ((d_p)$_{eq}$ = 0.199 cm) 71

3.18 Effect of bed characteristics on pressure drop and liquid holdup. System: hexane/nitrogen; GB: glass beads (d_p=0.114 cm); Cyl: extrudate ((d_p)$_{eq}$ = 0.199 cm); Sph: spherical silica shell (d_p=0.152 cm) 72

3.19 Comparison between liquid holdup measured by draining and tracer methods 73

3.20 Comparison of Holub's model (1990) prediction and high pressure data obtained in beds of d_r/d_p = 11, 14.6, 20 78

3.21 Comparison of Holub's model (1990) prediction and high pressure data obtained in the bed of d_r/d_p = 20 79

3.22 Trend of Holub's model (1990) prediction versus the experimental observation. System: water / nitrogen; nonporous glass beads; d_r/d_p = 20 80

3.23 Holub's model (1990) prediction of the effect of gas density on pressure drop and liquid holdup. System: hexane / nitrogen-helium; nonporous Glass Beads; d_r/d_p = 20 81

4.1 Flow pattern of flowing liquid and gas in trickle flow regime for externally completely wetted and partially wetted particles 87

4.2 (a) Typical differential refractometer voltage output in liquid-filled operation. Bed: silica shell sphere; L = 1.306 (kg/m^2 s).
(b) Normalized curve E(t) of the response in (a) 104

4.3 (a) Typical GC output in two-phase flow operation. Pressure = 0.31 MPa (30 psig); U_G = 1 cm/s; L = 1.777 (kg/m^2 s).
(b) Normalized curve E(t) of the response in (a) 105

4.4 Bed first moments for extrudate and spherical catalyst in liquid-filled operation 109

4.5 Bed variance for extrudate and spherical catalyst in liquid-filled operation 110

4.6 Bed dimensionless variance for extrudate and spherical catalyst in liquid-filled operation 111

4.7 Effect of high pressure and gas flow rate on liquid-solid contacting efficiency and pressure drop in extrudate bed. Solvent: hexane; tracer: heptane; gas: nitrogen; $(d_p)_{eq}$ (extrudate) = 0.199 cm 114

4.8 Effect of high pressure and gas flow rate on liquid-solid contacting efficiency and pressure drop in spherical bed. Solvent: hexane; tracer: heptane; gas: nitrogen; d_p (sphere) = 0.152 cm 115

4.9 Comparison between the contacting efficiency in extrudate and spherical beds. Solvent: hexane; tracer: heptane; gas: nitrogen; $(d_p)_{eq}$ (extrudate) = 0.199 cm ; d_p (sphere) = 0.152 cm 116

4.10 Comparison between the data of this work obtained at low pressure and El-Hisnawi's data obtained at atomspheric pressure. This work data: solvent: hexane; tracer: heptane, El-Hisnawi's data: solvent: hexane; tracer: pentane 117

4.11 A comparison of the developed model prediction and data for liquid-solid contacting efficiency 120

4.12 The trend of the developed model prediction of the effect of high pressure and gas flow rate on the contacting efficiency in the extrudate bed ($(d_p)_{eq}$ = 0.199 cm) 121

5.1 Schematic diagram of diluted bed with fines 124

5.2 The reproducibility of pressure drop using gas phase flow only in a diluted extrudate bed packed by the developed procedure (A). Gas: nitrogen; catalyst: 0.5% Pd extrudate (0.157 x 4.3 cm); fines: silicon carbide (d_f =0.21mm); vol. fines/ vol. cat. = 0.54; ε_{Bf} = 0.22; reactor: stainless steel (d_r = 2.19 cm), pressure: 0.31 MPa (30 psig). Error bars are contained within the points 132

5.3 The reproducibility of pressured drop using gas phase flow in a diluted bed packed by the developed procedure (A) and (B).
(a) Portion by portion packing (A). Gas: nitrogen; catalyst: extrudate (0.143 x 6.14 cm); fines: silicon carbide (d_f =0.21mm); vol. fines/ vol. cat.= 0.78; ε_{Bf} = 0.16; reactor: acrylic (d_r=1.587 cm); pressure: 0.31 MPa (30 psig).
(b) Whole bed packing (B). Gas: nitrogen; catalyst: sphere (d_p = 0.17 cm); vol. fines/vol. cat. =0.7; ε_{Bf} =0.19; reactor: acrylic (d_r=1.587 cm); pressure: 0.31 MPa (30 psig).
Error bars are contained within the points 133

5.4 Comparison between the reproducibility of the developed procedure (A) and wet method (E) in pressure drop measurements using gas phase flow only.
(a) Portion by portion packing (A). Gas: nitrogen; catalyst: sphere (d_p=0.17 cm); fines: silicon carbide (d_f =0.21mm);Vol. Fines/ Vol. Cat.= 0.62; ε_{Bf} = 0.22; reactor: acrylic (d_r=2.2 cm); pressure: 0.31 MPa(30 psig).
(b) Wet method packing (E). Gas: nitrogen; catalyst: sphere (d_p = 0.17 cm); vol. fines/vol. cat. =0.62; ε_{Bf} =0.346; reactor: acrylic: (d_r=2.2 cm); pressure: 0.31 MPa (30 psig).
Error bars are contained within the points 134

5.5 Comparison of pressure drop in different reactor sizes packed by the developed procedure (B) (whole bed packing procedure) with the same mixture of catalyst and fines. Gas: nitrogen; catalyst: sphere (d_p=0.17 cm); fines: silicon carbide (d_f=0.21mm); pressure : 0.31 MPa (30 psig). The points represent the average of three experiments with error bars contained within the points 135

5.6 The reproducibility of pressure drop and liquid holdup achieved by the developed preocedure (A) in two phase flow operation. System: hexane/nitrogen; catalyst: 0.5% Pd extrudate (0.157 x 4.3 cm): fines: silicon carbide (d_f = 0.21 mm); vol. fines/vol. cat. =0.61; ε_{Bf} =0.2; reactor: stainless steel; (d_r=1.55 cm); pressure: 0.31 MPa (30 psig) 136

5.7 Effect of fines on pressure drop and liquid holdup in a diluted bed of extrudates. System: hexane/nitrogen; porous 0.5% Pd ($(d_p)_{eq}$=0.199 cm); vol. fines/vol. cat. = 0.54 (developed procedure A); ε_{Bf} =0.22 145

5.8 Effect of fines on pressure drop and liquid holdup in a diluted bed of spheres with less fines than that required by the developed procedure. System: hexane/nitrogen; porous silica shell (d_p=0.152 cm); vol. fines/vol. cat.=0.4; ε_{Bf} =0.305 (the developed procedure requires vol. fines/vol. cat. = 0.7) 146

5.9 Effect of reactor pressure and gas flow rate on pressure drop and liquid holdup in a diluted bed of extrudates. System: hexane/nitrogen; porous 0.5% Pd ($(d_p)_{eq}$=0.199 cm); vol. fines/vol. cat. = 0.54 (developed procedure A); ε_{Bf} =0.22 147

5.10 A comparison among pressure drop and liquid holdup obtained in a nondiluted bed of extrudates, diluted bed with vol. fines/vol. cat.=0.54 (developed procedure A) and diluted bed with vol. fines/vol. cat.= 2 packed by wet method (G), pressure: 0.31 MPa (30 psig) ; U_G =1.0 cm/s 148

5.11 Effect of fines on liquid-solid contacting efficiency. System: hexane/nitrogen; tracer: heptane; porous 0.5% Pd extrudate; vol. fines/vol. cat.= 0.54 (developed procedure A) 150

5.12 Effect of degree of bed dilution on liquid-solid contacting efficiency. System: hexane/nitrogen; tracer: heptane; porous 0.5% Pd extrudate 151

5.13 Effect of fines on liquid-solid contacting efficiency in a diluted spherical bed packed by dry method (A) with vol. fines/vol. cat.=0.4 which is less than that determined by the developed procedure (vol. fines/vol. cat.= 0.7) 152

5.14 Koros (1976) findings of the effect of fines (sand) on catalyst utilization efficiency 153

5.15 Effect of wetting efficiency on the overall effectiveness factor. d_p =0.15 cm; ε_B =0.4 (Herskowitz and Smith, 1983) 156

بسم الله الرحمن الرحيم

" Glory to Thee (GOD) : of knowledge , We have none, save what Thou Hast taught us : in truth it is Thou who art perfect in knowledge and wisdom "

DEDICATION

TO

MY PARENTS , MY WIFE ETIHAD
AND OUR LOVELY CHILDREN RAWAN AND OMAR

EFFECTS OF HIGH PRESSURE AND FINES ON THE HYDRODYNAMICS OF TRICKLE-BED REACTORS

1. INTRODUCTION

1.1 SCOPE

A trickle-bed reactor (TBR), schematically shown in Figure 1.1, is a fixed bed of catalyst particles, contacted by the cocurrent downflow of gas and liquid. The vast majority of commercial cocurrent trickle-bed reactors operate at high pressure, up to about 20-30 MPa (3000-4500 psig), in order to improve the solubility of the gaseous reactant and/or achieve better heat transfer. The catalyst particles are always porous, except for immobilized cells or enzymes on nonporous ceramic beads, and usually are in the form of extrudates, granules, spheres, or tablets of diameter ranging from 0.1 cm to 0.32 cm (Mills,1978; Gianetto and Specchia, 1992).

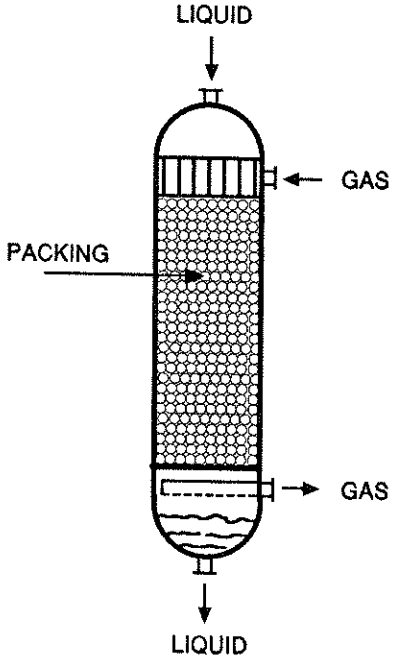

Figure 1.1 : Schematic diagram of a trickle-bed reactor

In commercial trickle-bed reactors, liquid superficial mass velocity, L, (liquid mass flow rate divided by the cross-sectional area of the empty reactor) can be up to 50 (kg/m^2s), while the superficial gas mass velocity , G, reaches up to 25 (kg/m^2s). In a laboratory reactor usually $L < 0.1$ (kg/m^2s) , while $10^{-5} < G < 10^{-2}$ (kg/m^2s). It is evident that liquid superficial velocities are changed dramatically with scale-up.

Trickle-bed reactors are usually used for heterogeneous gas-liquid reactions catalyzed by the solid and for solid-catalyzed gas reactions in an inert liquid phase. Since trickle-bed reactors have a greater throughput range, less pressure drop, no flooding limitations and prevent liquid back-up into gas lines, they are preferred over upflow packed-bed reactors (i.e. packed bubble column) unless there is a need to have high liquid holdup at low liquid mass velocities and/or to protect the catalyst from direct contact with the gas. Trickle-beds are also preferred over countercurrent packed-bed reactors (Ramachandran and Chaudhari, 1983; Shah, 1979). The characteristic parameters of trickle-bed reactors are shown in Table 1.1 (Gianetto and Specchia, 1992).

Table 1.1 : Characteristic parameters of a trickle-bed reactors

Catalyst loading % b. v.	0.55 - 0.65
Particle size , mm	1.0-3.2
Catalyst external area , m^2/m^3	400 - 1500
Catalyst effectiveness factor	< 1
Liquid holdup	0.05 - 0.2
Gas holdup	0.3 - 0.45
Gas-liquid interfacial area , m^{-1}	200 - 900
Reactor volume , m^3	150 - 200
Bed height , m	up to 20
Liquid hourly space velocity , hr^{-1}	0.5 - 10
Operating pressure , MPa	up to 30 (4500 psig)
Power consumption , W/m^3	10^2 - 10^3

The main advantages and disadvantages of trickle-bed reactors are listed in Table 1.2. The comparison among three phase reactor types are discussed by many authors (Shah, 1979 ; Ramachandran and Chaudhari, 1983 ; Gianetto and Silveston, ed., 1986; Rodrigues et al., 1981; Satterfield, 1975; Gianetto and Specchia, 1992; etc.).

Table 1.2 : The main advantages and disadvantages of trickle-bed reactors

- Advantages

1 - Liquid flow approaches plug flow.
2 - Low catalyst loss : important when costly catalyst are used.
3 - No moving parts.
4 - Possibility of operating at higher pressure and temperature.
5 - Longer reactor sizes.
6 - Low liquid-solid volume ratio : less occurrence of homogeneous side reactions (undesired non catalytic reaction).
7 - Lower investment and operating costs.
8 - Flexibility of operation : possibility of varying the liquid rate according to catalyst wetting, heat and mass transfer resistance.
9 - Lower power requirements.

- Disadvantages

1 - Lower catalyst effectiveness factor due to the large catalyst particle size.
2 - Limitations on the use of viscous or foaming liquids.
3 - Risk of increasing pressure drop or obstructing catalyst pores when side reactions lead to fouling products
4 - Scale-up is difficult and poor design may lead to incomplete wetting, hot spot formation, and instability.
5 - Sensitivity to thermal effects, although this drawback can be limited by recycling part of the outlet liquid or injecting cooled gas.
6 - Difficulties in the recovery of the reaction heat.
7 - Long term catalyst stability and high crushing strength are required.
8 - Incomplete catalyst wetting in laboratory scale reactor with low liquid flow rates and reactor diameter to particle size ratio less than 20 which cause wall effects and liquid maldistribution.

Trickle-bed reactors are widely used in petroleum industries (e.g. hydrocracking, hydrodesulfurization, hydrodenitrogenation, etc.) petrochemical industries (e.g. hydrogenation, oxidation, etc.), and chemical industries (e.g. hydrogenation of higher aldehydes, reductive ammination, liquid phase oxidation, syngas conversion, etc.). In recent years, importance of trickle-bed reactors has increased due to their application in waste treatment processes (e.g. oxidation of dilute aqueous and organic pollutants, etc.), biochemical processes (e.g. immobilized enzymes or cells. etc.) and electrochemical processing.

Because of the industrial significance of this reactor, a large number of technical review papers and monographs have appeared in the literature (Gianetto and Specchia, 1992 ; Zhukova et al., 1990; Ng and Chu, 1987; Charpentier, 1988, 1976; Ramachandran et al., 1987; Dudukovic′ and Mills, 1986; Levec and Goto, 1986; Herskowitz and Smith, 1983; Hofmann, 1978; Satterfield, 1975; Goto et al., 1977; Rodrigues et al., 1981; Delasa, 1986; Ramachandran and Chaudhari, 1983; etc.) .

Various flow regimes exist in a trickle-bed reactor depending on the superficial mass velocities, fluid properties and bed characteristics. Usually two broad regimes are classified which are : a low gas-liquid interaction regime, LIR , where gas-liquid shear does not affect the flow pattern, and a high gas-liquid interaction regime, HIR, where gas-liquid shear affects the flow pattern. LIR includes the trickle flow regime which is also called gas continuous flow regime, while HIR includes pulse, spray, wavy, bubble, and dispersed bubble flow regimes. The last two regimes are also called liquid continuous flow regime. The transition between the trickle and pulse flow regime is sharp, while the transitions to spray , bubble and dispersed bubble flow regime are more gradual. The design and scale-up parameters are affected differently in each flow regime as the hydrodynamics change from one regime to another (Wammes, 1990). The choice of the particular regime depends on the nature of the reaction and the process

conditions. In general, the trickle flow regime, the pulse flow regime, and the transition region between them are of particular interest in industry. (Hofmann, 1978 ; Levec et al., 1986 ; Tosun, 1984; Fukushima and Kusaka, 1977,1978,1979; Talmor, 1977; Chou et. al., 1977; Midoux et al., 1976; Charpentier and Favier, 1975; Sato et al., 1973 ; Wammes and Westerterp, 1990; Holub,1990).

The design and scale-up of a trickle-bed reactor involve predicting the reactor performance in terms of global rates, conversion and selectivity. The performance is affected by a number of complex phenomena which can be divided into those that are observed on reactor scale (macroscale) and those that occur on particle scale (microscale). Therefore macroscale and microscale design parameters shown in Table 1.3 need to be predicted correctly for a successful trickle-bed reactor design and scale-up (Dudukovic' and Mills, 1986; L'Homme,1979). Accurate prediction of such parameters in trickle-bed reactors is extremely difficult due to the complex interaction between the flowing phases and stationary packing, which makes the flow field in such reactors poorly understood. Accordingly, the prediction of most design parameters relies on empirical approaches rather than on a fundamental basis.

Table 1.3 : Macroscale and microscale design parameters

- Macroscale parameters

Liquid holdup ; pressure drop ; liquid-solid contacting efficiency ; flow regimes and their transition ; intrinsic kinetics ; the extent of catalyst volatilization ; flow distribution of both phases; residence time distribution, gas-liquid interfacial area ; volumetric mass transfer coefficients (gas-liquid, liquid-solid, gas-liquid coefficients) ; heat transfer ; energy dissipation.

- Microscale parameters

Local irrigation and external catalyst wetting ; local texture of the liquid (flowing film, rivulet, stagnant pocket); local liquid holdup in catalyst particles pores ; local mass transfer coefficients ; exchange coefficients between stagnant and flowing liquid ; local gas-liquid interfacial area.

A basic understanding of the hydrodynamics of trickle-bed reactors is essential to their design, scale-up and performance. Liquid holdup, pressure drop and external liquid-solid contacting efficiency are important hydrodynamics parameters which have to be known prior to reactor design , scale-up , and operation.

Liquid holdup, which partially occupies the void volume of the packed bed, is a basic parameter for the reactor design because it is related to other important parameters: the pressure gradient, gas-liquid interfacial area, the mean residence time of the liquid phase, catalyst loading per unit liquid volume, axial dispersion coefficient, and heat transfer coefficient at the wall. Pressure drop is important in determining the energy losses, the sizing of the compression equipment, liquid holdup, external contacting efficiency, gas-liquid interfacial area and mass transfer coefficients (Al-Dahhan, 1991; Wammes et al., 1991; Holub, 1990).

The low liquid velocities in a laboratory scale reactor, which uses the same catalyst size and shape as the commercial reactor, can give rise to incomplete wetting. Therefore, external liquid-solid contacting efficiency, which is the fraction of the particles external area wetted by the flowing liquid, is an important design and scale-up parameter for prediction of reactor performance. This can be seen in terms of its effect on the apparent reaction rate. The reaction rate over incompletely wetted packing can be greater or smaller than the rate observed over completely wetted packing. This depends upon whether the limiting reactant is present only in the liquid phase or in both gas and liquid phases. If the limiting reactant is nonvolatile, such as occurs in many hydrogenation processes, then a decrease in the solid-liquid contacting reduces the surface for mass transfer between the liquid and solid material causing a decrease in the reaction rate. However, if the liquid reactants are volatile and significant heat effects are also present, then a gas phase reaction can occur on the dry area of the catalyst and

consequently a higher reaction rate will be observed. Moreover, if the degree of wetting is below unity, the conventional concept of an effectiveness factor becomes useless, since the concentration of the reactants does not remain constant over the entire external surface of the catalyst particles (Zhukova et al., 1990; El-Hisnawi, 1981; Mills, 1978).

1.2 MOTIVATION

In contrast to the industrial trickle-bed reactors, which are usually operated at high pressure , most of the research reported in the literature concerning various aspects of trickle-bed reactors has been performed at atmospheric pressure . High pressure data is scarce. All reported studies on liquid-solid contacting efficiency and most of the published results on liquid holdup and pressure drop have been performed at atmospheric pressure. It is not known whether models that have been verified by experiments at atmospheric pressure and parameters determined at this pressure can be extrapolated to much higher pressure which is of industrial interest.

Recently , few investigations concerned with liquid holdup and pressure drop in pressurized trickle-bed reactors have been reported (Wammes, 1990; Wammes et al.,1990,1991; Marquez et al., 1992; Gianetto and Specchia, 1992; Larachi et al., 1991,1992). Their experimental observations show that at high pressure operation , liquid holdup decreases considerably, while pressure drop increases significantly. In these studies empirical correlations were developed to predict liquid holdup and pressure drop at elevated pressure. Other available models for liquid holdup and pressure drop, are also based on either empirical, semitheoretical, or phenomenological approaches, because a quantitative description of two phase flow through a packed-bed based on fundamental principles has not yet been successfully achieved (Wammes, et al.,1991; Holub,1990; Larachi, 1991,1992). In absence of a fundamental approach, a

phenomenological (or mechanistic) model or approach is preferred to strictly empirical correlations and often is very useful.

Holub (1990) derived such a phenomenological model in the form of a modified Ergun equation, based on a mechanistic representation of two phase flow in a single slit, to predict liquid holdup and pressure drop simultaneously in the trickle-flow regime. Holub's model (1990) was tested for experimental data obtained at atmospheric pressure and showed better agreement with liquid holdup and pressure drop data than previous models and correlations (Holub, 1990; Holub et al.,1992). Unfortunately, the validity of Holub's model (1990) at elevated pressure has not been tested. However, all recently reported correlations established for high pressure data, as mentioned above, are entirely empirical. Therefore, Holub's model (1990) and its phenomenological representation are of sufficient interest to be studied further.

All the available data for liquid-solid contacting efficiency has been obtained at atmospheric pressure, while the operating condition of interest is at high pressure . Liquid holdup and gas-liquid interfacial area, which reflect the degree of the liquid spreading over the external surface of the catalyst, affect both the degree of catalyst wetting and the thickness of the liquid film around the particles (Schubert et al., 1986; El-Hisnawi et al., 1982; El-Hisnawi, 1981; Wammes, 1990; Wammes and Westerterp; 1990, 1991, Marquez et al., 1992). Recently, it was found that high pressure operation increases gas-liquid interfacial area (Larachi, 1992 ; Marquez et al., 1992; Wammes, 1990). Accordingly, it is doubtful whether the current data and correlations obtained at atmospheric pressure can be utilized to predict properly the contacting efficiency at high pressure. Unfortunately, no study up to date investigated the effect of high pressure on the external liquid-solid contacting efficiency.

Commercial trickle-bed reactors are often designed based on data from laboratory scale reactors. In a laboratory reactor the velocities of liquid and gas are

lower than in commercial reactor by a factor of 10 to 100 (Van Klinken, 1979; Sie, 1991). The same catalyst size and type employed in commercial reactors is used in small high pressure laboratory reactors of inside diameter between 1 to 3 cm (Anderson and Pratt, 1985). Such conditions cause wall effects and liquid flow maldistribution, which reduce the external liquid-particles contacting efficiency and hence lead to inefficient use of the catalyst bed. Therefore, since the laboratory reactor state is uncertain, scale-up could lead to a bad commercial design (Lazzaroni et al., 1988; Herskowitz and Smith, 1978; Dudukovic′ and Mills, 1986; Sie, 1991). Accordingly, catalyst bed dilution with fines which are small , inert and nonporous particles of about 0.1 of the catalyst particles diameter, is recommended in kinetic studies and catalyst testing to remedy the shortcomings of small reactors. Dilution of the catalyst bed with fines is known to have a beneficial effect on the contacting efficiency, by improving liquid distribution, reducing the wall effect and by minimizing axial dispersion. Hence, the performance of the commercial reactor can be approached, and the obtained data in laboratory reactors can be utilized for scale-up and/or scale-down with increased confidence (Van Klinken, 1979; Van Klinken and Van Dongen, 1980; Sie, 1991; Carruthers and DiCamillo,1988; Gierman, 1988; Sedriks and Kenney, 1973; Koros, 1976; Dudukovic′ and Mills, 1986). Van Klinken (1979) and Van Klinken and Van Dongen(1980) found that fines increase liquid holdup and qualitatively deduced that increasing liquid holdup results in increasing liquid-solid contacting efficiency. Unfortunately, no study appeared in the literature which measured external liquid-solid contacting efficiency in a bed of a mixture of catalyst and fines to confirm quantitatively the effect of fines on the contacting efficiency. Packing the reactor bed with the mixture of catalyst and fines reproducibly is also an important issue since only if one achieves reproducibility can one rely on the obtained kinetic data for scale-up or in scale-down. Yet no study in the literature

proposed, or quantified, a reproducible procedure to pack the laboratory reactors with a mixture of catalyst and fines.

1.3 RESEARCH OBJECTIVES

The primary goals of this research are to develop a phenomenological model to predict external liquid-solid contacting efficiency in trickle-flow regime at high pressure operation, to test the validity of Holub's phenomenological model (1990) for liquid holdup and pressure drop prediction at high pressure operation, and to investigate experimentally the effect of high pressure and fines on the hydrdrodynamics parameters (external liquid-solid contacting efficiency, liquid holdup, and pressure drop) in the trickle flow regime. The specific objectives, as covered sequentially in this thesis, are :

1 - Design and constructed a high pressure trickle-bed reactor facility.
2 - Investigate the effect of high pressure and gas flow rate on pressure drop and liquid holdup in trickle flow regime as follows :
  I - Describe phenomenologically the effect of high pressure and gas flow rate on pressure drop and liquid holdup.
  II - Investigate experimentally such effects.
  III - Test the validity of Holub's phenomenological model (1990) for prediction of liquid holdup and pressure drop at high pressure.
3 - Investigate the effect of high pressure and gas flow rate on external liquid-solid contacting efficiency in trickle flow regime as follows :
  I - Develop a new phenomenologically based model to predict the external contacting efficiency at high pressure operation.
  II - Investigate experimentally the effect of high pressure and gas flow rate via tracer technique.
4 - Investigate the effect of fines on external liquid-solid contacting efficiency, liquid holdup and pressure drop in trickle-flow regime as follows :
  I - Develop a reproducible procedure to pack the laboratory scale trickle-bed reactors with a mixture of catalyst and fines.
  II - Investigate experimentally the effect of fines on external liquid-solid contacting efficiency, liquid holdup and pressure drop.

2. DESIGN OF HIGH PRESSURE TRICKLE-BED REACTOR FACILITY

High pressure trickle-bed reactor facility has been designed and developed to operate at a pressure up to 7 MPa (~ 1000 psig). Figure 2.1 shows the process and instrumentation diagram (PID) of the facility, while Figures 2.2a and 2.2b present the front and rear view of the installation, respectively. The facility consists of a high pressure trickle-bed reactor set-up, liquid and gas delivery systems, tracer technique components, and data acquisition system. It has the ability to perform low and high pressure experiments and is well suited for different kinetic and tracer investigations. The experimental set-up is capable of measuring liquid holdup and pressure drop simultaneously over a broad range of operating conditions.

2.1 HIGH PRESSURE TRICKLE-BED REACTORS SET-UP

The main components of the high pressure trickle-bed reactor setup are the reactor's packed bed compartment, liquid/gas distributor (reactor head), packing support (reactor bottom) and gas/liquid separator.

2.1.1 Reactor's Packed Bed

Four high pressure reactors have been designed and constructed. They are a 1 inch outer diameter (O.D.) acrylic reactor and 1", 3/4", and 1/2" inch O.D. stainless steel reactors. The total length of each of these reactors is 22.5 inch (57.15 cm).

In order to observe the two phase flow at high pressure at least at the wall of the packing, the middle section of one of the reactors was made of clear acrylic as a window. The bed with the acrylic window consists of three sections as shown in Figure 2.3. The upper and the lower sections were constructed with 1 inch stainless steel tubing of inside diameter (I.D.) equal to 2.22 cm.

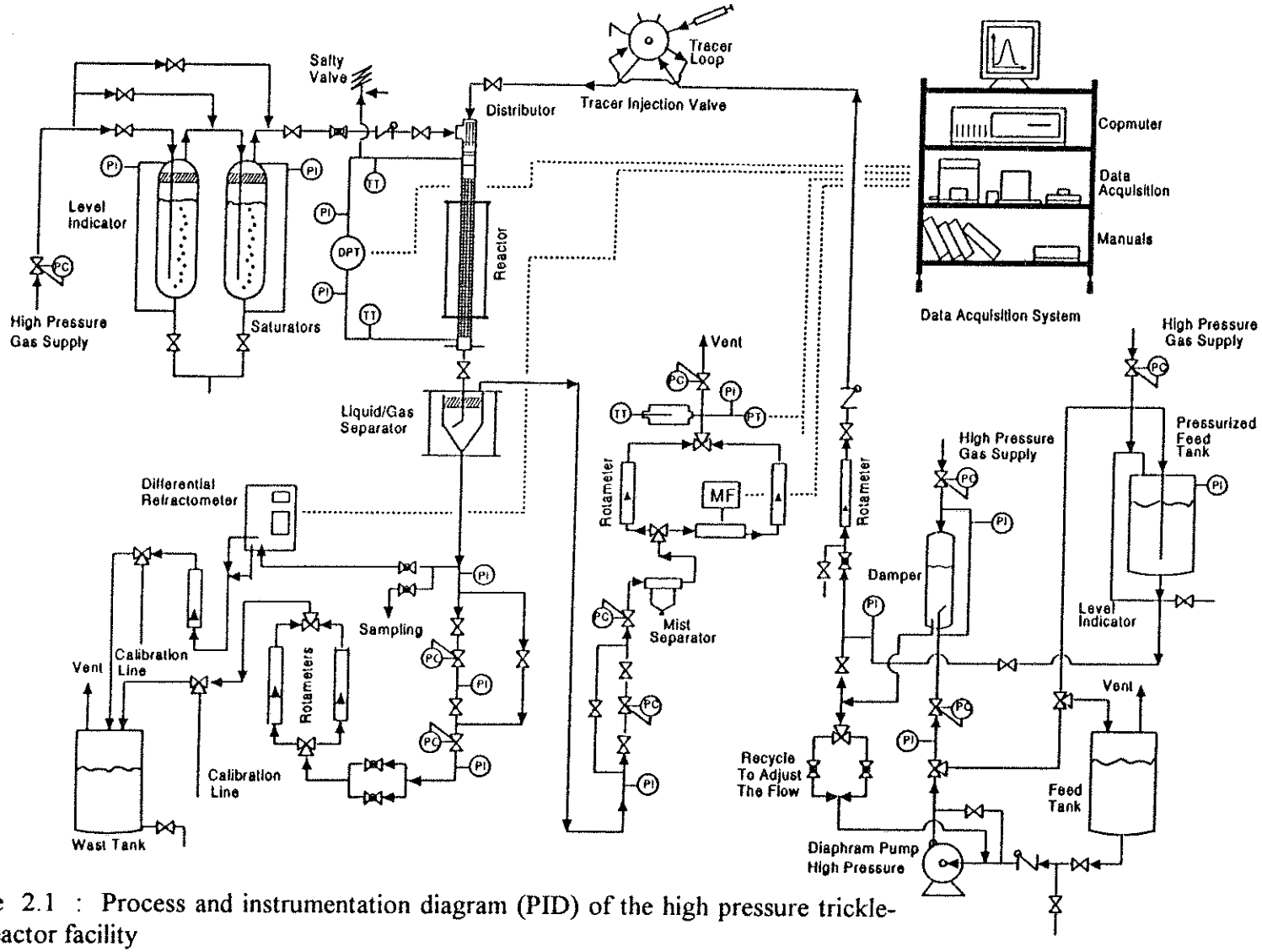

Figure 2.1 : Process and instrumentation diagram (PID) of the high pressure trickle-bed reactor facility

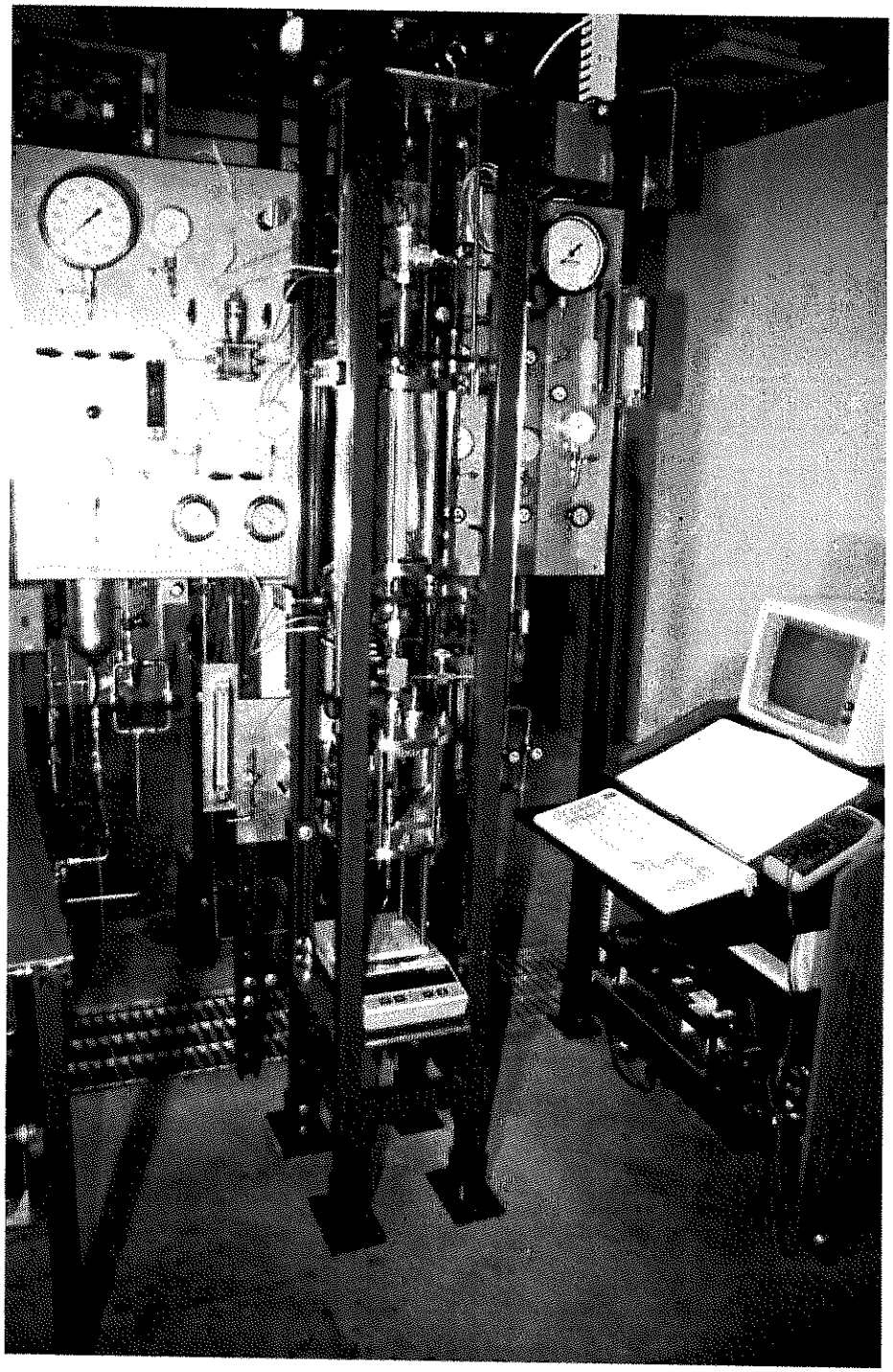

Figure 2.2: (a) Front view of the high pressure trickle-bed reactor facility

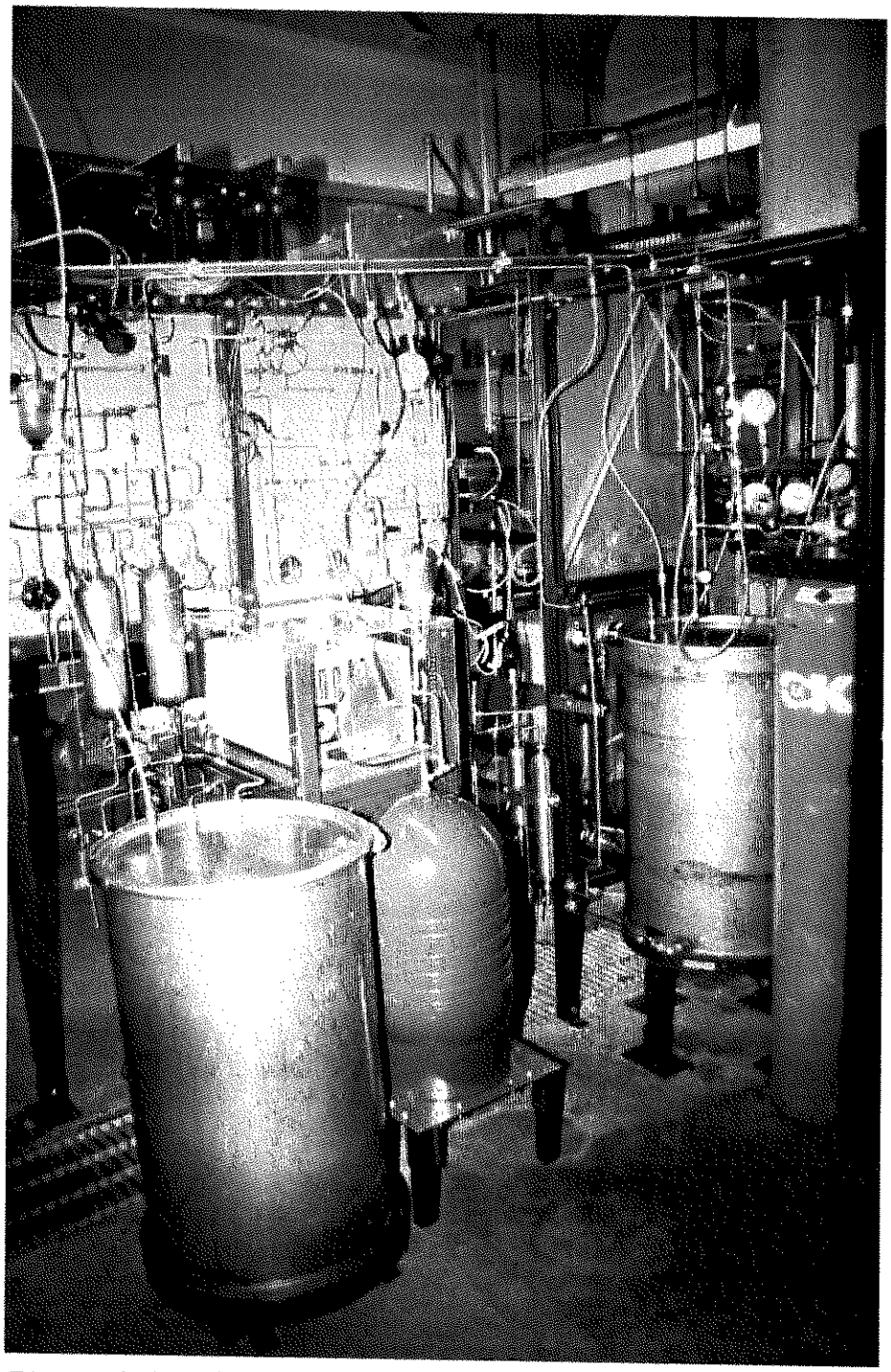

Figure 2.2: (b) Rear view of the high pressure trickle-bed reactor facility

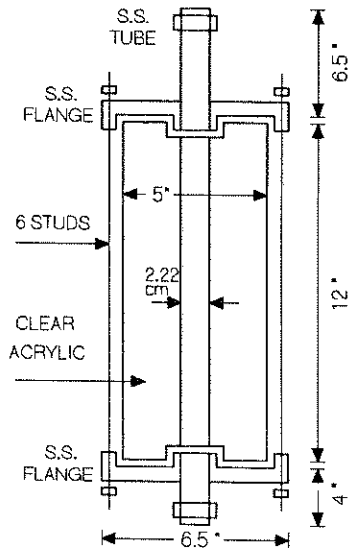

Figure 2.3 : Schematic diagram of 1 inch trickle-bed reactor with acrylic window

One end of each of these was welded to a 6.5 inch (16.51 cm) diameter stainless steel flange which is connected to the acrylic middle section, while the other end of both upper and lower stainless steel sections were fitted with a 1 inch swagelok nut and connected to the liquid/gas distributor and packing support, respectively. Both flanges were machined to accommodate two o-rings at the contact point between the flanges and the acrylic to prevent leakage. The middle section is constructed from a 5 inch (12.7 cm) outside diameter optically clear acrylic rod with a hole of diameter equal to that of stainless steel tubing (2.22 cm) machined along the rod length. The reactor's three sections are connected by six 3/8 inch (0.375 cm) threaded studs that tie each flange to the other.

Two acrylic plates, 1.27 cm thick and 22.86 cm x 22.86 cm in size, are used to attach the reactor to its support structure which consists of four vertical unitstrud channels mounted in the front of the facility's control and instrumentation panel. One

plate was connected to the reactor upper section flange, while the other was connected to the flange of the reactor lower section. This, along with the reactor's support structure, enables adjustment and maintenance of reactor verticality prior to each operation. It also permits mounting the reactor on four vertical linear motion systems each of which consists of two sliding blocks that move freely and vertically on a vertical rail. Each rail is mounted on a unitstrud channel. Four sliding blocks are connected to the upper acrylic plate while the other four are connected to the lower acrylic plate. Such a design allows free vertical movement of the reactor set-up while minimizing friction. In order to measure liquid holdup inside the reactor bed by the difference in weight of the wet bed over the weight of dry bed, which is one of the recommended methods, the reactor rests on a fixed load cell or electronic balance (Holub, 1990 ; Levec et al., 1986; Sato et al.,1973; Crine and Marchot, 1981). Because the weight of liquid holdup in such reactor size is very small compared to the total weight of the reactor set-up (less than 0.3% of the total weight), the reactor set-up was counterbalanced by five springs. One end of each spring was linked to a fixed plate fitted at the top of the structure, while the other end was linked to a moving plate which is connected by four 3/8 inch (0.375 cm) studs to the upper acrylic plate. This design permits adjusting the counterbalanced weight within the desired range. Unfortunately, the weighing method was found unsuitable for measuring the liquid holdup at high pressure operation because it indicates a larger weight than the weight of the liquid holdup. The additional weight is due to the dense gas imparting force on the bed.

The 1 inch (2.19 cm) stainless steel bed has two stainless steel support plates which are used to mount it properly into the reactor support structure of the facility. A 1 inch swagelok nut was fitted at each end of the reactor tube to connect it to the liquid/gas distributor and packing support.

The 3/4 inch (1.55 cm I.D.) and 1/2 inch (1.05 cm I.D.) stainless steel beds have a plate to mount them properly into the reactor support. 3/4 inch and 1/2 inch swagelok nuts were fitted at each end of the 3/4 and 1/2 inch reactor, respectively. Swagelok reduced connectors were used to connect these reactors to the 1 inch swagelok fitting of the liquid/gas distributor and packing support.

2.1.2 Liquid / Gas Distributor

The reactor's liquid/gas distributor (reactor head), as shown in Figure 2.4a and b, has been designed similar to the industrial type distributor to produce uniform liquid and gas distribution. It consists of 21 stainless steel tubes of 0.0625 inch I.D. (1.6mm) to distribute the liquid phase. The liquid is introduced to these tubes through a perforated plate. The gas phase enters the space surrounding the tubes that carry the liquid phase and leaves through the holes surrounding these tubes (0.14 inch (3.55 mm)) as well as other holes in between (0.030 inch (0.762 mm)). The bottom end of the distributor was welded to a 1 inch swagelok connector in which a 1/8 inch NPT threaded hole was machined. The hole is connected to the high pressure port of the Viatran differential pressure transducer (DPT), to a pressure indicator (PI), and to a pressure relief valve. It is also utilized to accommodate the 1/16 inch thermocouple (type K) to measure the temperature at the top of the reactor catalyst bed. The thermocouple was connected to Omega switch/display device. The pressure drop across the catalyst bed is measured by two different ranges of the differential pressure transducers (0-50 inch water column (w.c.) (0-1.8 psi) and 0-750 inch w.c. (0-27 psi)) which are mounted on the control and instrumentation panel. These differential pressure transducers are vented by a ventilation line. The pressure relief valve is set at 900 psig (6.3 MPa) and its output is connected to the facility ventilation line as well.

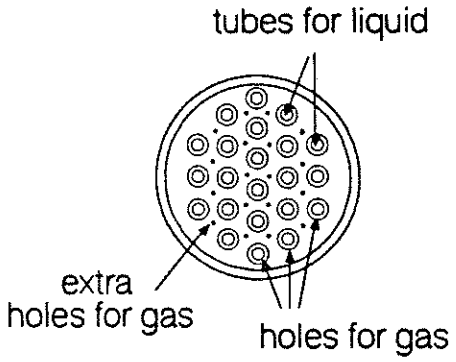

(b)

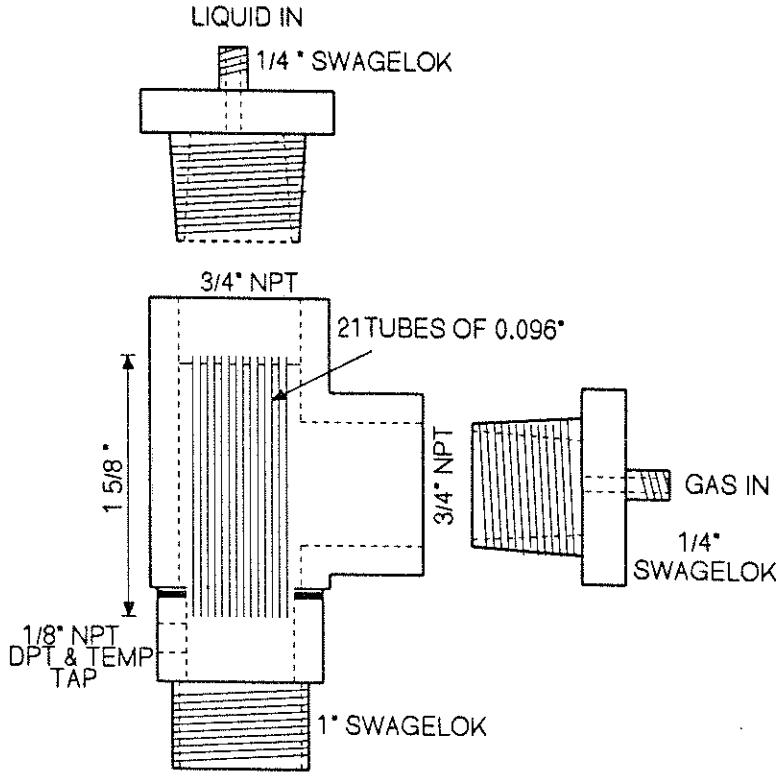

(a)

Figure 2.4 : Reactor's liquid / gas distributors. (a) Distributor for two phase flow operation. (b) Top view of the distributor's tubes and holes

Another small volume gas/liquid distributor has been designed and constructed as shown in Figure 2.4c to be used in tracer experiments for liquid-filled operation. This operation mode is required for the evaluation of external liquid-solid contacting efficiency as will be discussed later. A small volume distributor has been found in this work and El-Hisnawi (1981) to produce better tracer response curve in liquid-filled operation.

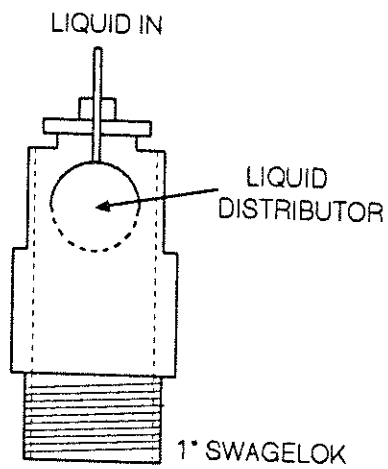

(c)

Figure 2.4 : Reactor's liquid / gas distributors. (c) Distributor for tracer liquid-filled operation

2.1.3 Packed Bed Support

The reactor's packing support (reactor bottom) as shown in Figure 2.5 , consists of a connector of a 1 inch swagelok fitting to a 3/4 inch NPT female thread. The packing support plate is mounted into the 1 inch swagelok fitting. This plate is a fine stainless steel wire mesh covered by a layer of glass wool. The other end is connected to a connector of 3/4 NPT male to 3/4 inch swagelok nut which ties into a 3/4 inch swagelok on/off valve. A 1/8 inch NPT thread hole is machined for the low pressure port of the differential pressure transducer (DPT), for a pressure indicator (PT), and also accommodates a 1/16 inch thermocouple (type K) to monitor the temperature at the bottom of the reactor catalyst bed. A 0.318 cm x 10.16 cm x 10.16 cm stainless steel plate was welded to the 3/4 inch NPT female thread part of the packing bed support. This plate is used to support the reactor set-up on a fixed load cell when such device is employed to measure liquid holdup.

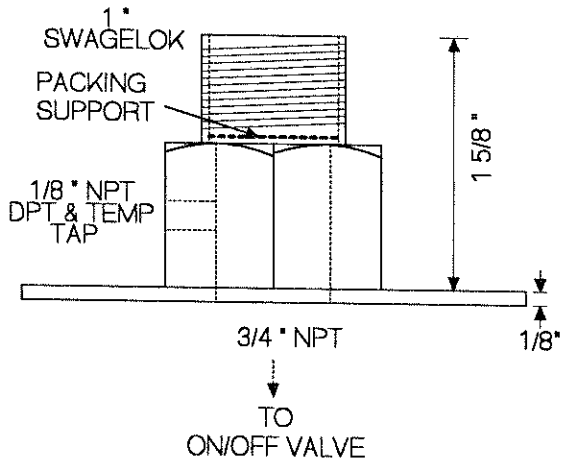

Figure 2.5 : Packed bed support

2.1.4 Gas / Liquid Separator

The gas/liquid separator has been designed and constructed from a 8 inch (20.32 cm) diameter optically clear acrylic rod which was machined as shown in Figure 2.6 . Its bottom was designed like a funnel in order to minimize the liquid volume in the bottom part of the separator as a part of the tracer experiment requirements where the volume of the externals to the packing bed need to be minimized. It was constructed from optically clear material in order to observe and control easily the liquid level at the bottom of the separator. This is very important to ensure that the gas phase does not flow to the tracer analytical unit, to maintain stable pressure drop , and to measure on line the liquid flow rate. The separator is connected to the reactor bottom's on/off valve, gas outlet stream and to the liquid outlet stream through two stainless steel flanges of 8.5 inch (21.59 cm) diameter . O-rings were mounted between the acrylic rod and the flanges to prevent leakage. Six studs of 3/8 inch (0.953 cm) are utilized to tie each flange to the other. The upper flange was welded to two of the 3/4 inch NPT thread female connectors. The upper end of the central female connector was connected to the 3/4 inch swagelok on/off valve through a connector with the 3/4 inch NPT male to 3/4 inch swagelok nut. This valve is connected to the reactor bottom to carry both gas and liquid stream to the separator. The other end of the central female connector was connected to a 3/4 inch pipe to carry both gas and liquid inside the separator toward the wall through the demister. The liquid moves down over the wall to the bottom of the separator, while the gas flows upward through the demister to the gas effluent stream. This arrangement helps in stabilizing the liquid level, particularly at high liquid flow rate, which also helps in stabilizing pressure drop and in maintaining manually a constant liquid level. A demister of stainless steel mesh is mounted in the upper part of the

separator around the central 3/4 inch pipe. The demister serves to trap the liquid mist from the effluent gas stream.

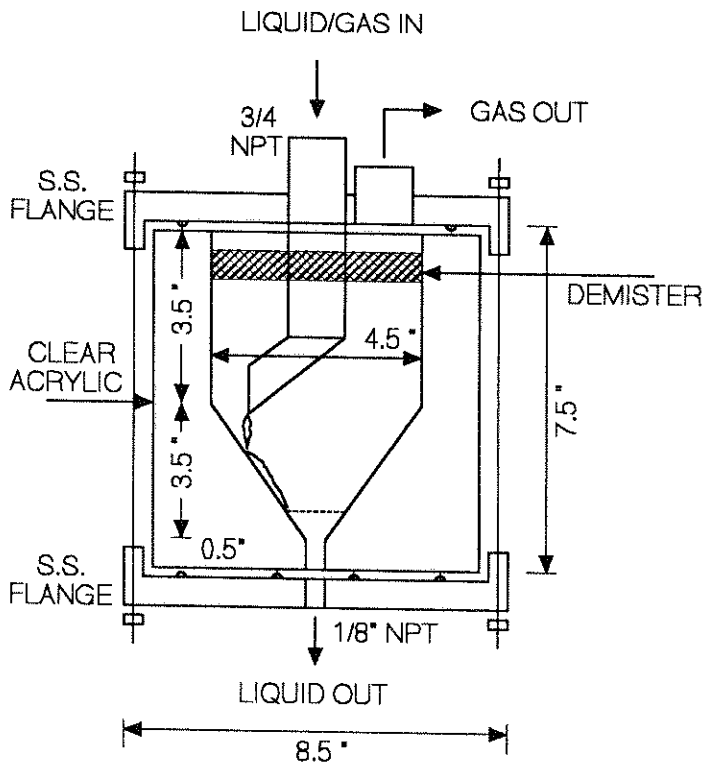

Figure 2.6 : Gas / liquid separator

A small volume gas/liquid separator (as first design chose), which is preferred for tracer experiments failed to produce good gas-liquid separation, particularly at high gas or liquid flow rates and at high pressure operation where the gas becomes more dense. Such separator was a 3/4 inch NPT thread tee connector. The gas was drawn through slots machined in a 1/4 inch tube, while the liquid flowed downwards similar to the sketch shown in Figure 1.1. The liquid level was detected by the Omega ultrasonic level detector surrounding a 1/2 inch pipe at the tee connector outlet.

2.2 LIQUID DELIVERY SYSTEM

Liquid phase is delivered to the reactor by two means. The first one is by a pressure tank (20 gallon, up to 1000 psig (7 MPa)) and the second by Calgon high pressure metering pump (up to 1000 psig) with the maximum capacity of 7 gal/h. The suction port of the pump is connected to a 30 gallon stainless steel atmospheric feed tank. The pump discharge is delivered either to the reactor, or to the atmospheric feed tank, or to the pressurized feed tank. The pump can be utilized to fill the high pressure feed tank with the desired liquid. Such a tank is pressurized independently by a high pressure gas cylinder, where the pressure can be adjusted by a high pressure regulator. The outlet liquid stream of the tank is then delivered to the reactor through a high pressure Brooks rotameter (up to 1000 psig), check valves and a tracer injection valve. The liquid flow rate can be adjusted and controlled by a needle valve mounted at the rotameter inlet. At the pump discharge line to the reactor a pressure regulator valve and a small pressurized tank of one liter capacity are mounted in order to adjust the desired operating pressure. Such a small pressurized tank is also utilized to damp the pump pulsing flow rate and to smooth the flow to the reactor if the pump is selected as means of liquid delivery. In this case , if low liquid flow rate is needed, part of the output of the small pressurized tank is recycled to the pump suction tube. The small pressurized tank is also pressurized independently by a high pressure gas cylinder. A 1/8 in swagelok on/off valve is mounted at the liquid entrance to the reactor liquid/gas distributor. This valve and the 3/4 inch swagelok on/off valve mounted at the outlet gas/liquid stream from the reactor bottom are used to measure the liquid holdup by drainage.This is achieved by closing both valves simultaneously and then draining the reactor bed which will be discussed in more detail later. The exit liquid stream from the gas/liquid separator is split into sampling and waste stream. The sampling line is also split into two

lines, one of them is passed to the on-line tracer analytical equipment, while the other stream is connected to a needle valve to collect samples manually. The waste stream is passed to two high pressure liquid regulators, to maintain reactor pressure, and to drop the liquid stream's pressure to atmospheric pressure. Upon leaving the pressure regulators, the liquid flows to either a low or high range rotameter. The outlet of both rotameters is either collected in a 30 gallon stainless steel atmospheric waste tank or passed to a on line calibration line. The bubbles in the liquid exit stream make the actual reading of the float position on the rotameter scale extremely difficult due to the movement of the float caused by bubbles. Consequently, relying solely on the rotameter's calibration curve gives inaccurate measurement of the flow rate. Therefore, a on line liquid flow rate measurement, on both the waste and sampling liquid streams is performed manually through the calibration line.

The collected liquid waste in the waste tank can be pumped using the high pressure pump either to the atmospheric or pressurized feed tank if the waste liquid can be reused. The feed and waste tanks vent lines are connected to the facility ventilation line. Pressure indicators, are mounted at different points in the liquid delivery system to monitor the system's pressure. Some of the system's valves, pressure regulators and indicators, and liquid rotameters are mounted on the facility control and instrumentation panel.

2.3 GAS DELIVERY SYSTEM

The gas delivery system consists of high pressure gas cylinders. The pressure is adjusted by a pressure regulator. The gas is allowed to pass through two high pressure saturators (bubblers). The gas feed is saturated with liquid to prevent evaporation in the reactor catalyst bed. A 1/4 inch swagelok on/off valve is mounted on the gas entrance to

the reactor liquid/gas distributor. This valve is closed once reactor liquid input stream valve and reactor outlet stream valve are closed during liquid holdup measurements by draining method. The gas outlet stream from the gas/liquid separator passes through two pressure regulators, which maintain the pressure inside the reactor and drop the gas stream pressure to the low pressure of the gas rotameters for which the rotameters were calibrated. Upon leaving the regulators, the gas flows to a low and high range Brooks gas rotameters. Another pressure regulator is mounted at the outlet of the rotameters. Both pressure regulators (at the rotameters inlet and outlet) are used to adjust and control the gas flow rate to the reactor and the outlet rotameter's calibration pressure of the employed rotameter. Hence, by measuring the pressure and the temperature at the outlet gas stream of the rotameter and utilizing its calibration curve at that pressure, the actual gas flow rate inside the reactor can be evaluated.

A mass flowmeter is also mounted on the outlet gas stream. It can be connected either in parallel or in series to the gas rotameters and is implemented to measure the outlet mass flow rate.

A thermocouple type K is used to measure the gas temperature at the rotameters outlet. It is mounted inside a small vessel, rather than inside the 1/4 inch tubing to prevent contacting its tip to the stainless steel wall. Both an accurate pressure indicator and pressure transducer are used to measure the gas pressure at the rotameters outlet. The gas outlet stream from the exit rotameter pressure regulator is connected to the facility ventilation line. The facility is vented by the ventilation line outside the laboratory to the atmosphere by a large capacity ventilator. Pressure indicators, are mounted at different points in the gas delivery system to monitor the system's pressure. Some of the system's valves, pressure regulators and indicators, and gas rotameters are mounted on the facility control and instrumentation panel.

2.4 TRACER TECHNIQUE SET-UP

Tracer technique has been chosen to evaluate the external liquid-solid contacting efficiency (details of the technique needed to measure this parameter will be provided later). It consists of injection valve and analytical equipment. The tracer is introduced in the liquid stream through a high pressure multiport Valco valve which is located close to the reactor and is mounted on the facility control and instrumentation panel. The injection valve can be equipped with a desired loop volume that is used to introduce an impulse concentration disturbance in the liquid stream. The analytical equipment used to analyze the tracer concentration in the liquid effluent stream is a Differential Refractometer (DR) (Water 410), which is on-line, and a Gas Chromatograph (GC) (GOW MAC 69-550). The sampling stream, which is split from the main liquid stream exiting the gas / liquid separator, is additionally split into two lines to be either passed continuously to the on line DR or to a needle valve to collect samples manually for the GC.

The Differential Refractometer has been used successfully at atmospheric pressure operation to measure on-line the tracer concentration of the reactor outlet liquid stream (El-Hisnawi, 1981; Mills,1978). It consists of two cells. One cell is the reference and it is filled with reference liquid. Through the other cell (called sampling cell) the sampling stream flow continuously. The difference in the refractive index which is proportional to the tracer concentration, is continuously measured relative to the reference cell. The Differential Refractometer gives a voltage output which is linearly proportional to the difference in the refractive index and hence to the tracer concentration. The Differential Refractometer cells can handle pressure up to 100 psig and are located at the last stage in the DR measurement process which is opened to the atmosphere. From the Differential Refractometer sampling cell, the liquid flows to the

rotameter which is mounted on the facility control and instrumentation panel to measure its flow rate, and then either to the atmospheric waste tank or to on line calibration line to measure the flow rate. Unfortunately, the Differential Refractometer failed to operate properly in two phase flow mode at high pressure operation . This is because at high pressure more gas is dissolved in the solvent , which produces continuous bubbles in the atmospheric sampling cell due to pressure drop in the DR 1/16 inch tubing (0.009 inch I.D.) and the cell itself. This makes the DR measurements meaningless. Also it was found that maintaining the DR backpressure below 100 psig did not solve the problem. The bubble formation in the sampling cell becomes more pronounced particularly if the solvent is reused frequently. However, the Differential Refractometer works properly with liquid filled operation (only liquid phase) when such operation is required for the external contacting efficiency measurements as will be discussed later. Therefore, in two phase flow operation samples were collected manually through the needle sampling valve in suitable intervals. A Gas Chromatograph is utilized to measure the tracer concentration in these samples taken from the reactor outlet liquid stream.

As already mentioned external volume to the reactor bed should be as small as possible in order to prevent distortion of the tracer signal which should represent the reactor bed. Therefore, the lines, fittings and valves are selected to give minimum external volume to the bed. For this reason, the bottom part of the gas/liquid separator was designed in a funnel shape. The external liquid volume is about 15% of the liquid volume in the packed bed and this is described in more detail in the subsequent chapters.

In order to be able to evaluate the moments of the tracer response of the bed only, the trickle bed reactor set-up is designed to be flexible so that the packed bed compartment can be removed and the reactor head connected to the reactor bottom (i.e liquid/gas distributor connected to packing support). This enables the measurement of the tracer response of the externals only. By subtracting the moments of the external

system from the moments of the total system (the bed and the externals), the bed moments can be evaluated. For this purpose, a shortest possible 1 inch O.D. stainless steel tube (2.5 inch (6.35 cm)long) with 1 inch swagelok nuts on each side is used to connect the swagelok fitting of the reactor head to that of the reactor bottom. In order to account for the contribution of this short tube in the response signal of the total system (external and the bed), the same length has been added to the reactor packing bed compartment making the total length of 22.5 inch (57.15 cm) as mentioned before.

For the purpose of the DR calibration and washing , a separate high pressure unit has been built and connected to the DR which consists of two small pressurized tanks (one tank for known mass fraction sample, and the other for pure solvent).

2.5 DATA ACQUISITION SYSTEM

A portable and flexible data acquisition system set-up has been designed and constructed. It was designed to be flexible for further future addition and for other different applications. The hardware for this system is summarized in Table 2.1, while the instruments and the equipment connected to the data acquisition are summarized in Table 2.2. Figure 2.7 shows the schematic diagram of the data acquisition system. The software which is required to obtain the data from the hardware consists of library subroutines called PCLAB library. Many programs in Basic have been written to utilize PCLAB subroutine "ADC.VALUE" in obtaining the desired data. The programs are user friendly and can be easily modified to collect different data for different applications if necessary. Appendix 7.1 shows a program to perform sampling (discrete measurements) as an example. All programs are available in a computer disk at Chemical Reaction Engineering Laboratory (CREL).

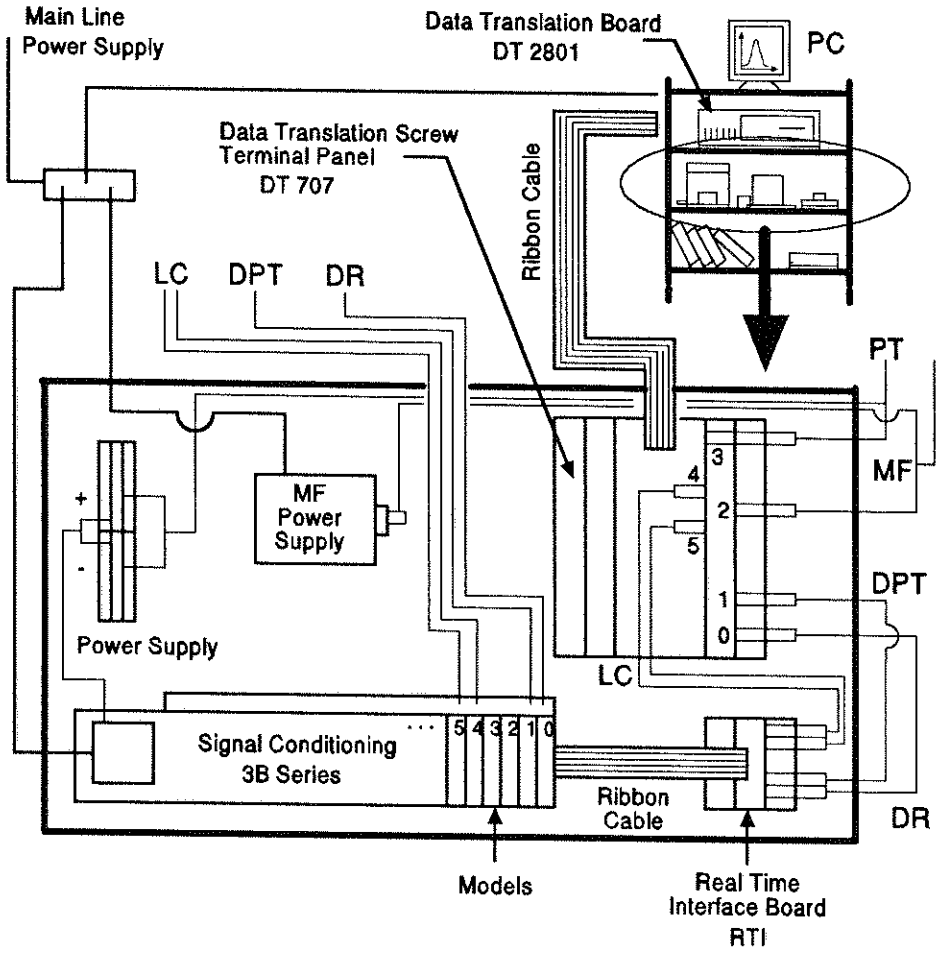

Figure 2.7 : Schematic diagram of the data acquisition system

Table 2.1 : Hardware for the data acquisition system

Hardware	Description
Personal Computer (PC)	IBM personal computer with 8088 microprocessor.
Data Translation A/D Board (DT 2801)	It is mounted inside the PC. It converts the analog signal into a digital one and vice versa. It is set to convert 0-10 volt DC into 0-4095 digits. It consists of 16 channels.
Data Translation Screw Terminal Panel (DT 707)	It provides convenient screw terminals which represent 16 channels for all user connections to the DT 2801 board. This includes an analog I/O, digital I/O, external clock, and external trigger connections . It is connected to the DT 2081 by a special ribbon cable.
Signal Conditioning System (3B Series)	It is Analog Devices Series 3B. It consists of 16 channels. These channels are designed in such a way that a plug in card or module can be purchased to meet the signal conditioning requirements of each input. Any input to this devise (e.g. mV, mA) is converted proportionally into 0-10 volt output signal or 4-20 mA output signal. The desired output signal is 0-10 volt since it is compatible with the DT 2801. The device also provides a power supply to various instruments at regulated ±15 volt DC at 800 mA and unregulated ± 24 volt DC at 350 mA. The output voltage signal is carried in a special ribbon cable which is not compatible either with the DT 707 or with the DT 2801.Therefore the next hardware (RTI) must be utilized.
Real Time Interface Board (RTI)	It is Analog Devices RTI board. It provides 16 channel terminal screws connections. It is used as an intermediate interface to transmit the signal output of the signal conditioning system, 3B to DT 707 and then to DT 2801.

Table 2.2 : Instruments connected to the data acquisition system

Instrument	Description
Differential Refractometer (DR)	Waters 410 Differential Refractometer is used. It gives output in voltage (mV to 10 volt DC, depending on its preset sensitivity). For the used sensitivity, the output is in millivolt. Therefore, a 3B30 analog device model is used with the signal conditioning system, 3B, to convert mV to 0-10 volt DC. Two custom board are available one to convert 0-281 mV to 0-10 volt DC while the other to convert 0-600 mV to 0-10 volt DC. The choice between them is based on the tracer concentration. It is excited by a regular power supply line (120 volt AC). The measured difference in the refractive index is proportional to its voltage output which is proportional to the solute concentration. The DR is connected to channel 0 .
Differential Pressure Transducer (DPT)	Viatran 374 wet/wet high pressure (up to 1000 psig) DPT is used. It gives signal of 4-20 mA. Hence, a 3B12 analog device model is utilized with the signal conditioning system,3B, to convert the signal into a 0-10 volt DC range. It is excited by regulating 15 volt DC supplied by the signal conditioning system , 3B. It is connected to channel 1.
Mass Flowmeter (MF)	Kurz 560-6 gas mass flowmeter is used. Its range is from 0-5 lpm. It gives an output signal of 0-5 volt DC, therefore, its signal is connected directly to DT 707. It is excited by a separate power supply of 24 volt DC and is connected to channel 2.
Pressure Transducer (PT)	Omega P-181 pressure transducer is used. Its range is from 0-30 psig. It gives an output signal of 1-5 volt DC. Therefore its signal does not need conditioning and is connected directly to DT 707. It is excited by regulating 15 volt DC supplied from the signal conditioning system, 3B and is connected to channel 3.
Load Cell (LC)	Omega load cells are connected. Their ranges are 0-50 lb and 0-500 lb. They give an output of 2 mV per volt excitation. Therefore, a 3B18 analog device model is used with the signal conditioning system,3B, to convert their signal ranges into 0-10 volt DC. The load cell of 0-50 lb is excited by 3.33 volt DC, while the one of 0-500 lb is excited by 10 volt DC. These excitation voltages are supplied from the 3B18 model by setting it on the desired excitation voltage. Load cell of 0-50 lb is connected to channel 4, while the one of 0-500 lb is connected to channel 5.

3. EFFECT OF HIGH PRESSURE ON PRESSURE DROP AND LIQUID HOLDUP

3.1 BACKGROUND

Pressure drop and liquid holdup are important hydrodynamics parameters for design and scale-up. They affect other important design and scale-up parameters such as degree of wetting, gas-liquid interfacial area, mass and heat transfer, catalyst loading, mean residence time of the liquid phase, axial dispersion, the capacity of the reactor to take up the heat generated in highly exothermic reactions without thermal runaway occurring, required feed pressure, etc.. There is a strong relationship between liquid holdup and pressure drop in a trickle-bed reactor. Pressure drop represents the energy dissipated due to fluid flow through the reactor bed. Obviously, the greater the liquid holdup in a particular bed the more resistance there is to fluid flow which produces a larger pressure drop across the reactor bed (i.e. more energy dissipated).

The total liquid holdup in a porous packed bed consists of internal liquid holdup and external liquid holdup. The internal liquid holdup (ε_{Li}) fills the pores of the catalyst due to the capillary forces. Therefore, it is equal to the total catalyst pore volume per reactor bed volume. The external liquid holdup (ε_L) is the liquid volume which partially occupies the void volume of the packed bed per reactor bed volume. An alternative definition, sometimes referred to as the liquid saturation (β_L or ω_L), is the external liquid volume per reactor void volume ($\beta_L = \varepsilon_L / \varepsilon_B$), where ε_B is the bed porosity. For reactor design and scale-up the external liquid holdup is the one to be considered. It is divided into dynamic liquid holdup (ε_{Ld}) and static liquid holdup (ε_{Ls}). The dynamic liquid holdup represents the moving portion of the liquid while the static liquid holdup represents the liquid situated around the contacting points of the particles and is

independent of the gas flow, liquid flow and liquid viscosity (Wammes et al. , 1991 ; Charpentier et al., 1968 ; Shulman et al., 1955). In this entire text the word liquid holdup refers to the total external liquid holdup .

A vast number of investigations on pressure drop and liquid holdup has been reported in the literature. Most of them were performed at atmospheric pressure while the operation of interest is high pressure . The models developed to predict pressure drop and liquid holdup were formulated either by relating them together (i.e. each one is depending on the other) or by predicting them independently. Due to the complexity of the flow field in trickle-bed reactors and insufficient information available to describe the bed pore structure, fundamental models are still exceedingly difficult and as yet no such models have been successfully accomplished. Hence, empirical and phenomenological approaches have been utilized. In the empirical approach, the experimental data are correlated based on some grouping of variables. Often such correlations are only reliable for the type of systems tested. This implies that extrapolation to systems with different physical properties or operating conditions including pressure not covered by the original correlations is not justified unless first experimentally tested. Using such empirical approach , the data were correlated :

(i) Based on Lockart-Martinelli (1949) parameter ($\chi = \{(\Delta P/Z)_L /(\Delta P/Z)_G\}^{0.5}$) (Ellman et al.,1988, 1990 ; Larachi et al., 1990, 1991 ; Larkins et al., 1961 ; Charpentier et al., 1968, 1971 ; Sato et al., 1973 ; Midoux et al., 1976 ; Morsi et al., 1982, 1984 ; Weekman and Myers, 1964 ; Rao et al., 1983a ; Tosun, 1984 ; Reiss, 1976 ; etc.).

(ii) In terms of the measurable operating variable and fluid and packing properties, or dimensionless groups that combine them such as Reynolds number, Galileo number, Weber number, etc. (Wammes, 1990 ; Wammes et al., 1990, 1991 ; Turpin and Huntington,1967; Specchia and Baldi, 1977 ; Clements and Schmidt, 1980 ; Matsuura et al., 1976 ; Talmor, 1977 ; Hofmann, 1978 ; Kan and Greenfield, 1979 ; Patil and

Sharma, 1981; Blok et al., 1983 ; Reynier and Charpentier, 1971 ; Crine and L'Homme, 1982, etc.).

(iii) Modified forms of Ergun equation to account for the existence of the other flowing phase based on empirical considerations. The original Ergun equation (Ergun,1952) was developed to predict pressure drop for single phase flow in packed-bed (Sweeney, 1967; Hutton and Leung, 1974 ; Specchia and Baldi, 1977 ; Rao et al., 1983, 1985 ; Saez and Carbonell, 1985 ; Saez et al., 1986 ; Levec et al., 1986).

The phenomenological (or mechanistic) approach relies on building a simpler physical picture (a conceptual model) of the phenomena involved. Based on the simplified geometry all pertinent equations are derived using the appropriate conservation laws and required accepted constitutive forms. Such phenomenological approach is often very useful and the developed relationships can safely be employed on systems of very different physical properties and operating conditions as long as the conditions for the validity of the model are not violated. Phenomenological models are more powerful than the empirical correlations but their region of validity must be carefully specified and quantified (Saez and Carbonell, 1985 ; Saez et al., 1986 ; Levec et al., 1986 ; Melli and Scriven, 1991 ; Holub, 1990 ; Holub et al.,1992).

Holub (1990) and Holub et al. (1992) developed a simple phenomenological model to predict pressure drop and liquid holdup for the trickle flow regime. Holub (1990) represented the actual bed void space in a trickle bed reactor as a single, inclined flat-walled slit. The liquid flows as a film over the wall of the slit, while the gas flows in the center. Such model was tested for experimental data obtained only at atmospheric pressure and showed better agreement with the experimental data than previous atmospheric models and correlations. Unfortunately, Holub's model (1990) was neither tested at high pressure operation nor were its predictions examined at high pressure. Saez and Carbonell (1985) introduced the relative permeability concept in correlating

pressure drop and holdup in the trickle flow regime. It was found that the concept has no theoretical basis in the treatment of inertial regime and the relative permeability for the inertial and viscous regime are not the same (Levec et al., 1986). Attempts by Saez et al. (1986) to justify the use of relative permeability based on representing the two phase trickling flow in trickle flow regime as an array of parallel conduits of circular cross section were not fully successful. The correlation fails to match the data well (Holub, 1990 ; Levec et al., 1986). Melli and Scriven (1991) represented the "void space" in trickle-bed reactor as a collection of enlargements, or pore bodies connected by passages where the flow route map network (the macroscale (bed scale) and the microscale (particle scale)) were connected by means of a statistical network theory. Such approach does not allow ready quantification to large beds used in practice.

Recently few investigators reported data on pressure drop and liquid holdup obtained at high pressure operation in the trickle flow regime (Wammes, 1990 ; Wammes and Wasterterp, 1990; Wammes et al., 1990, 1991 ; Larachi et al., 1991; Ellman, 1988 ; Ellman et al., 1988 ; Ellman et al., 1990). It was observed that high pressure operation affects significantly the pressure drop and liquid holdup. In all these investigations the data was correlated based on a fully empirical approach with no mechanistic description of the effect of high pressure on pressure drop and liquid holdup. Table 3.1 shows Holub's model (1990) as well as the recent proposed correlations and models for pressure drop and liquid holdup that were developed based on high pressure data. The survey of the correlations and models for pressure drop and liquid holdup that were established based on atmospheric data can be found in many texts and articles (Sai and Varma, 1987; Holub, 1990 ; Ellman, 1988 ; Wammes, 1990 ; Dudukovic' and Mills, 1986 ; Ramachandran and Chaudhari, 1983 ; Shah, 1979 ; Zhukova et al., 1990 ; ect.)

As mentioned earlier, Holub's phenomenological model (1990) for trickle-flow regime is of interest to be studied further to establish a mechanistic description of the effect of high pressure on pressure drop and liquid holdup and to compare its validity at high pressure operation to that of the recently reported correlations.

Table 3.1 : Recent correlations for pressure drop and liquid holdup based on data obtained at high pressure and Holub's (1990) model

Author	Packing type	d_p(cm)	d_r(cm)	ε_B	Pressure	Approach
Holub , 1990	glass beads	0.3	7.95	0.375	atm	phenomenological
	extrudate	0.16x0.32	2.54	0.335		
	sphere alumina	0.32	12.22	0.45		

$$\psi_L = \left(\frac{\varepsilon_B}{\varepsilon_L}\right)^3 \left[\frac{E_1 \mathrm{Re}_L}{Ga_L} + \frac{E_2 \mathrm{Re}_L^2}{Ga_L}\right] \quad ; \quad \psi_G = \left(\frac{\varepsilon_B}{\varepsilon_B - \varepsilon_L}\right)^3 \left[\frac{E_1 \mathrm{Re}_G}{Ga_G} + \frac{E_2 \mathrm{Re}_G^2}{Ga_G}\right]$$

$$\psi_L = 1 + \frac{\rho_G}{\rho_L}(\psi_G - 1) \quad ; \quad \psi_\alpha = \frac{\Delta P/Z}{\rho_\alpha g} + 1 \quad , \quad \alpha = L \text{ or } G$$

Wammes et al., 1991	glass beads	0.3	5.1	0.39	up to 7.5 MPa	empirical
	Cyl. Alumina	0.32x0.33		0.41		

$$\beta_d = 3.8\left(\frac{\rho_L U_L d_p}{\mu_L}\right)^{0.55} \left[\frac{d_p^3 \rho_L^2 g}{\mu_L^2}\left(1 + \frac{\Delta P/Z}{\rho_L g}\right)\right]^{-0.42} \left(\frac{6(1-\varepsilon_B)d_p}{\varepsilon_B}\right)^{0.65}$$

$$\frac{\Delta P}{0.5\rho_G U_G^2}\left(\frac{d_p}{Z}\right) = 155\left[\frac{\rho_G U_G d_p \varepsilon_B}{\mu_G(1-\varepsilon_B)}\right]^{-0.37} \left[\frac{1-\varepsilon_B}{\varepsilon_B(1-\beta_t)}\right]$$

Table 3.1 continued

Author	Packing type	d_p(cm)	d_r(cm)	ε_B	Pressure	Approach
Larachi et al. , 1991	glass beads	0.14-0.2	5	---	up to 12 MPa	empirical

$$\beta_t = 1 - 10^{-\Gamma} \quad ; \quad \Gamma = 1.22 \; \frac{We_L^{0.15}}{X_G^{0.15}\,\mathrm{Re}_L^{0.2}}$$

$$\frac{(\Delta P/Z)\, d_h \rho_G}{2\, G^2} = \frac{1}{\left\{(\mathrm{Re}_L\, We_L)^{0.25}\; X_G\right\}^{1.5}} \left[31.3 + \frac{17.3}{\left\{(\mathrm{Re}_L\, We_L)^{0.25}\; X_G\right\}^{0.5}} \right]$$

$$X_G = \frac{G}{L}\sqrt{\frac{\rho_L}{\rho_G}} \quad ; \quad \mathrm{Re}_L = \frac{\rho_L U_L d_p}{\mu_L} \quad ; \quad We_L = \frac{L^2 d_p}{\rho_L \sigma_L} \quad ; \quad d_h = \left[\frac{16\, \varepsilon_B^3}{9\, \pi (1-\varepsilon_B)^2} \right]^{0.33} d_p$$

Ellman et al., 1988 , 1990	sphere & cylinder	0.116-0.3	2.3 - 10.0	0.27-0.49	ut to 10 MPa	empirical

$$\beta_d = 10^k \quad ; \quad k = 0.001 - \frac{0.42}{\left[X_L^{0.5}\, \mathrm{Re}_L^{-0.3} \left(\frac{a_s\, d_h}{(1-\varepsilon_B)} \right)^{0.3} \right]^{0.48}}$$

$$\frac{(\Delta P/Z)\, d_h\, \rho_G}{2\, G^2} = 200\,(X_G\, \delta_2)^{-1.2} + 85\,(X_G\, \delta_2)^{-0.5}$$

$$\delta_2 = \frac{\mathrm{Re}_L^2}{\left(0.001 + \mathrm{Re}_L^{1.5}\right)} \quad ; \quad X_G = \frac{G}{L}\sqrt{\frac{\rho_L}{\rho_G}} \quad ; \quad X_L = \frac{1}{X_G} \quad ; \quad \mathrm{Re}_L = \frac{\rho_L U_L d_p}{\mu_L} \quad ;$$

$$a_s = \frac{6(1-\varepsilon_B)}{d_p} \quad ; \quad We_L = \frac{L^2 d_p}{\rho_L \sigma_L} \quad ; \quad We_G = \frac{G^2 d_p}{\rho_G \sigma_L} \quad ; \quad d_h = \left[\frac{16\, \varepsilon_B^3}{9\, \pi (1-\varepsilon_B)^2} \right]^{0.33} d_p$$

3.2 HOLUB'S PHENOMENOLOGICAL MODEL

In trickle-flow regime the liquid flows as films or rivulets over the catalyst bed, while the gas flows as continuous phase through the remaining voids as depicted in Figure 3.1.

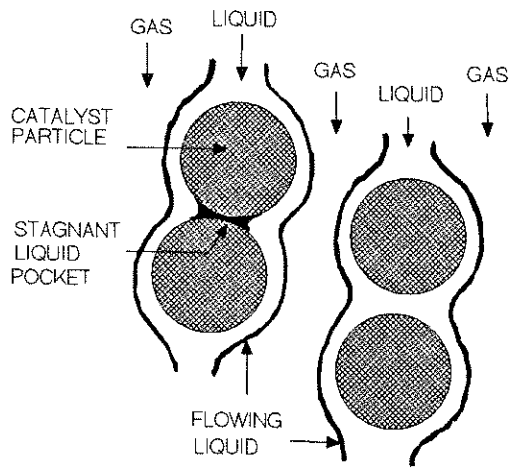

Figure 3.1 : Trickle-flow regime of fully wetted particles

Holub (1990) developed a simple phenomenological model for gas-liquid flow in trickle flow regime (low interaction regime). In such model, the complex geometry of the actual void space in a packed bed of particles is represented as a single, flat-walled slit of average half width, W , half wall thickness, S_D , and angle of inclination , θ , to the vertical axis as shown in Figure 3.2 . The liquid is assumed to completely wet the wall with a film of uniform thickness , δ, while the gas flows in the central core. This is clearly a very simple representation of the actual complex void geometry.

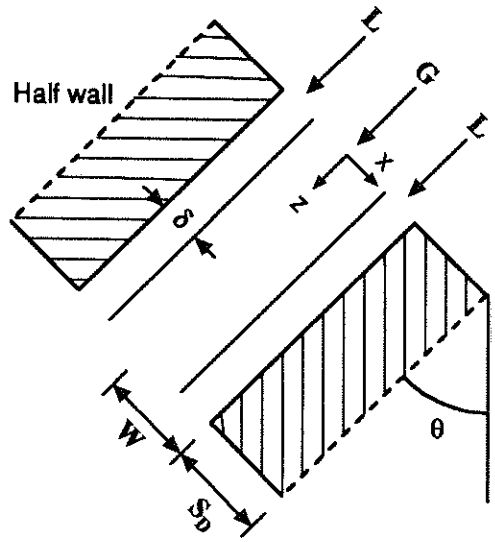

Figure 3.2 : Slit model representation of the geometry of a single pore in the bed (Holub, 1990)

The slit parameters are related to that of the actual trickle-bed by the following assumptions (Holub, 1990 ; Holub et al., 1992) :

(i) The void to solid and liquid to solid volumetric ratios are assumed to be the same in the slit and the bed.

(ii) The solid surface area per unit solid volume is the same in the two geometries (i.e. the slit and the bed).

(iii) The average slit inclination is related to the bed tortuosity (T).

(iv) The phase superficial velocities are the same in the slit and the actual bed.

These assumptions lead to the following relationships:

$$\frac{W}{S_D} = \frac{\varepsilon_B}{1-\varepsilon_B} \quad ; \quad \frac{\delta}{S_D} = \frac{\varepsilon_L}{1-\varepsilon_B} \quad ; \quad S_D = \frac{d_p}{6} \tag{3.1}$$

$$Cos\,\theta \;= T \quad ; \quad V_L = \left(\frac{U_L}{\varepsilon_L}\right)T \quad ; \quad V_G = \left(\frac{U_G}{\varepsilon_B}\right)T \tag{3.2}$$

By using these relationships , two phase flow momentum balance equations in the slit model are mapped to the actual bed model which yields the following dimensionless equations for the trickle flow regime in the form of modified Ergun equations (more details can be found in Holub, 1990) :

$$\psi_L = \left(\frac{\varepsilon_B}{\varepsilon_L}\right)^3 \left[\frac{E_1 \mathrm{Re}_L}{Ga_L} + \frac{E_2 \mathrm{Re}_L^2}{Ga_L}\right] \tag{3.3}$$

$$\psi_G = \left(\frac{\varepsilon_B}{\varepsilon_B - \varepsilon_L}\right)^3 \left[\frac{E_1 \mathrm{Re}_G}{Ga_G} + \frac{E_2 \mathrm{Re}_G^2}{Ga_G}\right] \tag{3.4}$$

By equating the dimensional pressure gradient ($\Delta P/Z$) in each phase, leads to the following relationship between ψ_L and ψ_G:

$$\psi_L = 1 + \frac{\rho_G}{\rho_L}\left(\psi_G - 1\right) \tag{3.5}$$

Equation 3.5 represents an implicit relationship for liquid holdup . The dimensionless variables of equations 3.3, 3.4 and 3.5 are defined as follows :

$$\psi_\alpha = \frac{\Delta P/Z}{\rho_\alpha g} + 1 \tag{3.6}$$

$$Ga_\alpha = \frac{g d_p^3 \varepsilon_B^3 \rho_\alpha^2}{\mu_\alpha^2 (1-\varepsilon_B)^3} \tag{3.7}$$

$$\mathrm{Re}_\alpha = \frac{U_\alpha d_p \rho_\alpha}{\mu_\alpha (1-\varepsilon_B)} \tag{3.8}$$

where α = L or G for liquid and gas respectively.

E_1 and E_2 are the Ergun constants which characterize the bed ($E_1 = 72T^2, E_2 = 6Tf_{wall\ cat.}$) and are not two phase flow parameters. Therefore, they are determined from single phase flow experiments in the bed of interest (e.g. gas phase flow in dry bed). The use of "standard Ergun constants" was found to lead to high errors (Holub, 1990 ; Dudukovic' et. al., 1991 ; MacDonald et. al.,1979).

Equation (3.3), (3.4) and (3.5) form a closed system for determining the pressure drop and liquid holdup. By substituting equations (3.3) and (3.4) into equation (3.5), a nonlinear implicit equation for liquid holdup is obtained which can be readily solved numerically by Newton-Raphson method with only a few iterations. Knowing the liquid holdup, pressure drop can be evaluated by equation (3.3) or (3.4).

The validity of the model predictions was confirmed at atmospheric pressure operation. No attempt has been made to test it at operating condition of interest (high pressure operation). Figure 3.3 shows the comparison of the Holub's model prediction and the atmospheric experimental data (Holub, 1990; Holub et al.,1992).

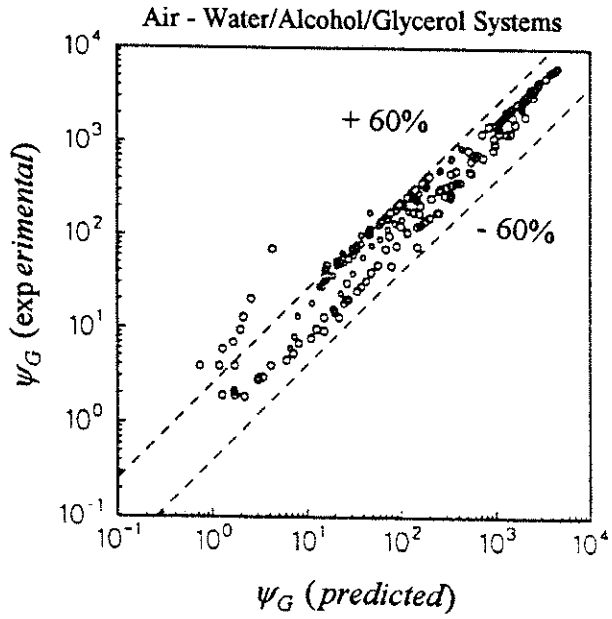

(a)

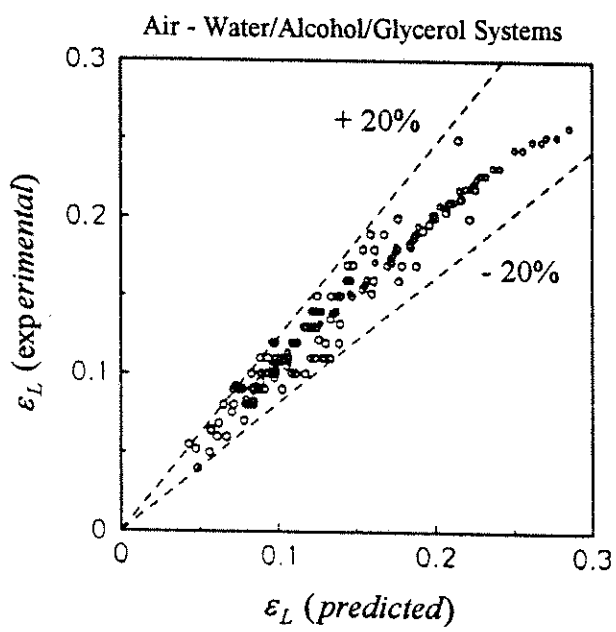

(b)

Figure 3.3 : Comparison of Holub's model (1990) and data for dimensionless gas phase pressure drop (ψ_G) and liquid holdup (ε_L)

3.3 PHENOMENOLOGICAL ANALYSIS OF THE EFFECT OF REACTOR PRESSURE AND GAS FLOW RATE ON PRESSURE DROP AND LIQUID HOLDUP

The influence of reactor pressure and gas flow rate on pressure drop and external liquid holdup in the trickle flow regime are explained phenomenologically based on the slit model of Holub (1990) shown in Figure 3.2.

The energy dissipation in a gas-liquid cocurrent downflow packed bed reactor is due to the frictional losses at the packing surface and the driving forces acting on the liquid flow. The driving forces consist of the pressure gradient and the gravitational force. The pressure gradient depends on the velocity and on the density of the flowing fluids. Higher liquid/gas superficial velocity and/or density produce a higher pressure gradient while higher liquid density increases the gravitational force. Since the gas density depends on the gas pressure, increasing the reactor pressure makes the gas more dense. Therefore, the effect of the gas phase on the pressure drop can be separated into the effect of the superficial gas velocity and of the reactor pressure. Accordingly, an increase in the reactor pressure (at constant superficial gas and liquid velocities for a given liquid and gas phase) results in a high pressure drop over the packed bed due to the increase in the gas phase density. Increasing the superficial gas velocity at high pressure, yields much higher pressure drop across the reactor bed.

Based on Holub's (1990) slit model and equation (3.3), the dependence of liquid holdup on the pressure drop is described by the following equation :

$$\varepsilon_L = \varepsilon_B \left[\frac{E_1 \mathrm{Re}_L + E_2 \mathrm{Re}_L^2}{Ga_L \left(1 + \frac{\Delta P/Z}{\rho_L g} \right)} \right]^{1/3} \tag{3.9}$$

where, the term $(\Delta P/Z)/(\rho_L\ g)$ is the dimensionless pressure drop which represents the ratio of the pressure drop to the gravitational forces.

In general, as liquid superficial flow rate increases, pressure drop increases as discussed above. The increase in the denominator of equation (3.9), due to the increase in $(\Delta P/Z)/(\rho_L\ g)$, is smaller than the increase in the numerator due to the increase in Re_L and Re_L^2. Therefore, liquid holdup always increases as liquid flow rate increases. When higher liquid density is utilized, dimensional pressure drop and gravitational force increase. In this case, the dimensionless pressure drop , $(\Delta P/Z)/(\rho_L\ g)$, may decrease. Therefore, liquid holdup is affected both by $(\Delta P/Z)/(\rho_L\ g)$ and liquid physical properties (density and viscosity) which are accounted for in Re_L and Ga_L . The effect of bed characteristics on pressure drop and liquid holdup are considered in the Ergun constant , bed voidage, and Galileo number.

According to equation (3.9), five cases can be deduced for a given packed bed. These cases describe the effect of reactor pressure and gas flow rate on liquid holdup as well as on the dimensionless pressure drop (Al-Dahhan, 1991).

Case 1 : (No gas flow)

Without gas flow, $U_G = 0$, the ratio $(\Delta P/Z)/(\rho_L\ g)$ is zero , The gravitational force is the only driving force. Hence liquid holdup is maximal.

Case 2 : (Low pressure, low gas superficial velocity)

At atmospheric to low pressure and at low gas superficial velocity, the pressure drop is negligible in comparison to the gravitational force. Therefore, the dimensionless pressure drop , $(\Delta P/Z)/(\rho_L\, g)$, is small and changes only slightly and can be neglected. Hence, the reactor pressure influence on liquid holdup is negligible.

Case 3 : (Low pressure , high gas superficial velocity)

At atmospheric pressure to low pressure and at high gas superficial velocity, the pressure gradient increases in comparison to the gravitational force. Thus the ratio, $(\Delta P/Z)/(\rho_L\, g)$, is larger which causes a decrease in the liquid holdup. Now, the gas phase superficial velocity influences liquid holdup. Moreover, the increase in pressure drop at high range of liquid flow rate is larger than that of **Case 2**. Hence, the quantitative difference between the numerator and the denominator of equation (3.9) at higher range of liquid flow rate is greater than that at low range of liquid flow rate. The effect of gas velocity in this case is more noticeable at high liquid flow rate than that at low flow rate.

Case 4 : (High pressure , low gas superficial velocity)

At elevated pressure, the gas density increases. As a result the pressure drop increases. Thus the ratio , $(\Delta P/Z)/(\rho_L\, g)$, increases which causes a decrease in liquid holdup. Since the effect of gas velocity on pressure drop is greater than that of gas density (Ergun, 1952), the influence of elevated pressure at low gas velocity is less than that of **Case 3** at both low and high liquid flow rates.

Case 5 : (High pressure , high superficial gas velocity)

At elevated pressure and high gas superficial velocity, the pressure drop increases significantly due to both gas density and superficial velocity. As a result, the dimensionless pressure drop , $(\Delta P/Z)/(\rho_L\, g)$, increases significantly and hence liquid holdup decreases considerably. Therefore, the effect of gas flow rate on pressure drop and liquid holdup is more pronounced at elevated pressure. Moreover, the effects of high pressure and high gas velocity at high liquid flow rate on pressure drop and liquid holdup are significantly greater than that at low liquid flow rate. In general, the effect in this case is noticeably larger than that in all cases above.

3.4 EXPERIMENTAL INVESTIGATION

A detailed description of the experimental installation used in this study has been presented in Chapter 2.

3.4.1 Pressure Drop and Liquid Holdup Measurements

Pressure drop across the catalyst bed is measured by high pressure differential pressure transducers, DPT, which are connected to the top and the bottom of the bed. Two different ranges of DPT are utilized: low range (0-50 inch water column, w.c. (1.8 psi)) and high range (0-750 w.c. (27 psi)) . The data acquisition system as well as accurate Fluke multimeter are employed to measure and monitor pressure drop as discussed in Section 2.5.

Liquid holdup within a packed bed has been measured by various experimental methods as discussed in Table 3.2 (Ellman et al., 1990; Holub, 1990; Wammes, 1990 ; Crine and Marchot, 1981; Schwartz et al.,1976; Schwartz, 1975; Charpentier, 1968).

Table 3.2 : Experimental methods used to measure liquid holdup in packed-beds

Method	Description
Collecting (draining) method	By simultaneously shutting off the inlet and outlet streams and then draining the reactor, draining holdup can be measured. The remaining holdup in the bed is measured by weighing the reactor after being drained and subtracting the weight of the dry reactor bed. This holdup consists of external static and capillary (inside the pores) holdups (Wammes, 1990; Larkins et al., 1961)
Weighing method	By weighing the dry reactor and subtracting this weight from the weight of the reactor in two phase flow operation , the total liquid holdup (external and internal) is obtained. This method is recommended and utilized at atmospheric pressure where it gives direct measurements of liquid holdup without perturbing the experimental system (Shulman et al., 1955; Holub, 1990; Levec et al.,1986; Sato et al, 1973; Crine and Marchot, 1981). In this work it was found that this method is not suitable and not recommended at high pressure operation.
Tracer method	By injecting a tracer (impulse or pulse) in the inlet liquid stream , the mean residence time (first moment ,μ_1, which is equal to $((V_r/Q_L)\varepsilon_{Lt})$ can be determined. Hence, liquid holdup can be evaluated (El-Hisnawi, 1981 ; Larachi, et al., 1991) . Alternatively, tracer method may be carried out using decreasing step injections of tracer (Schubert et al., 1986).
Scattering technique	By exposing the liquid to a beam of x-ray or γ-ray and measuring the attenuation of the beam due to the presence of the liquid, the total liquid holdup could be determined (Jones and Zuber,1975).
Conductivity method	By measuring the apparent electrical conductivity across the bed in the presence of a conductive liquid, liquid holdup can be evaluated. This conductivity is a function of the amount of liquid held between the two electrodes (Basic',1992 ; Ellman et al.,1990).
Optical method	By introducing an optical probe in the packing, the local liquid holdup can be measured (Hewitt, 1978).
Volume method	By measuring the volume of liquid outside the bed when a known quantity of liquid circulates in a closed circuit through the reactor (Charpentier et al., 1968).

The experimental facility described in chapter 2 was designed to measure liquid holdup by draining, weighing and tracer methods. All of these methods have been utilized in this study. The weighing method was found unsuitable and is not recommended at high pressure operation. It indicates a larger weight than the weight of the liquid within the bed. The additional weight is due to the dense gas imparting a force on the bed. The experimental liquid holdup data presented here were measured by the draining method, while in certain experiments, both draining and tracer methods are employed.

Prior to each two phase flow experiment, the packed bed after being extensively prewetted by soaking the bed and leaving it over night soaked, is operated first in the high interaction regime (pulsing and/or bubble flow regimes) at high liquid mass velocities and then the mass velocities are reduced to the desired level at which pressure drop and liquid holdup are measured. This procedure, besides assuming a uniform liquid/gas distribution, minimizes liquid maldistribution and prevents hysteresis effects in measured pressure drop (Dudukovic' et al., 1991; Kan and Greenfield, 1979; Levec et al., 1988). During each experiment, the operating procedure described in Appendix 7.2 is followed. However, the liquid level in the gas/liquid separator must be maintained constant to stabilize the pressure drop and to measure on line the mass liquid flow rate by collecting the liquid outlet stream from the calibration line over the stable period of the reactor operation. The operation is assumed to be stable when the reactor pressure, pressure drop and the gas and liquid throughput do not change for at least 5 minutes.

Pressure drop data is collected by the data acquisition system where the average measurements is computed at the end of sampling time. Liquid holdup is determined by draining (collecting) method : the on/off valves at the reactor liquid inlet stream and the reactor outlet are closed simultaneously followed by closing the on/off valve of gas inlet stream. After the gas/liquid separator is emptied, the reactor outlet valve is opened so

that the liquid trickles out of the reactor. By collecting and weighing the liquid, draining holdup ,ε_{Ld}, is determined (sometimes named dynamic holdup which is not accurate since part of the remaining external liquid which contributes to the dynamic holdup portion is not accounted for). The time of draining is at least 10 minutes. The remaining liquid holdup in the bed consists of liquid external to the particles, ε_{Ls}, (sometimes called static holdup although part of it would contribute as a dynamic holdup) and internal holdup (inside the pores of the particles ,$\varepsilon_{Li} = (1-\varepsilon_B)\,\varepsilon_p$, (also called capillary holdup)) in case of porous catalysts. It was found that the remaining holdup after draining (i.e. ε_{Ls}) for a given bed and liquid phase is independent of the operating conditions. It was measured by performing at least three separate experiments at different operating conditions (reactor pressure and gas/liquid flow rates) following the same draining procedure. In these experiments , after the reactor is drained, then weighed and the dry bed weight is subtracted, the remaining holdup (ε_{Ls}+ε_{Li}) is determined. The external remaining holdup (ε_{Ls}) is evaluated by subtracting the internal voidage of porous particles (ε_{Li}) . The total external holdup, ε_L, is :

$$\varepsilon_L = \varepsilon_{Ls} + \varepsilon_{Ld} \tag{3.10}$$

In certain experiments, the tracer method was also implemented in addition to the draining method. In the tracer method the total liquid holdup , ε_{Lt}, is determined from the mean residence time, first moment (μ_1), where total external liquid holdup can be evaluated as follows :

$$\mu_1 = (V_r/Q_L)\,\varepsilon_{Lt} \tag{3.11}$$

$$\varepsilon_L = \varepsilon_{Lt} - \varepsilon_{Li} \tag{3.12}$$

A detailed description of this technique is covered in the following chapter.

Pressure drop and liquid holdup data were reproducible within a relative error of 5%.

3.4.2 Operating Conditions Investigated

The flow conditions for the collected pressure drop and liquid holdup data were selected in the trickle flow regime. Figure 3.4 shows the region that is covered experimentally on the flow map of Fukushima and Kusaka (1977) to demonstrate that all data are in trickle flow regime. Visual observation through the acrylic window and by stable and steady pressure drop measurements also indicate that the operating regime is trickle flow.

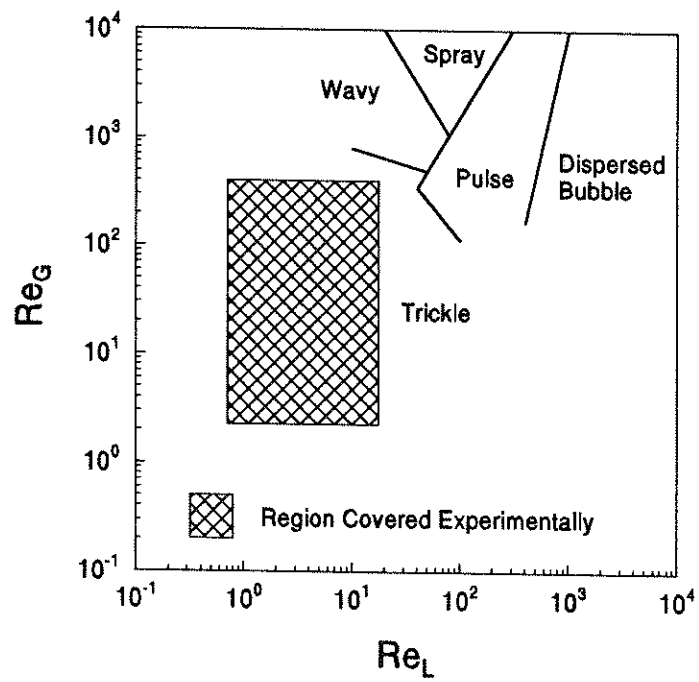

Figure 3.4 : Region of trickle flow regime covered experimentally in this study (flow map based on Fukushima and Kusaka (1977))

The range of reactor pressure, liquid and gas superficial velocities covered to investigate the effect of high pressure and gas flow rate on pressure drop and liquid holdup are presented in Table 3.3. The physical properties of the gas-liquid system are listed in Table 3.4 , while the packing bed characteristics utilized in this investigation are illustrated in Table 3.5.

Table 3.3 : Range of covered operating conditions

Condition	Covered Range
Reactor pressure , MPa Psig	$0.31 \leq P \leq 5.0$ $30 \leq P \leq 700$
Gas superficial velocity , cm/s	$1 \leq U_G \leq 11.7$
Gas superficial mass velocity, kg / m^2 s	$6.64 \times 10^{-3} \leq G \leq 4.03$
Liquid superficial flow rate , ml/min	$15 \leq Q_L \leq 93$
Liquid superficial mass flow rate, kg / m^2 s	$0.42 \leq L \leq 4.1$
Temperature, K	≈ 298

Table 3.4 : Physical properties of liquid-gas systems at 298 K and 1 atm

System	Density kg / m^3	Viscosity $N.s/m^2$	Surface tension N/m
Liquid Phase			
Water	1000	1.0×10^{-3}	72×10^{-3}
Hexane	663	3.07×10^{-4}	18.4×10^{-3}
Gas Phase			
Nitrogen	1.15	1.78×10^{-5}	---
Helium	0.166	1.97×10^{-5}	---

Table 3.5 : Packed bed characteristics

Reactor / Packing	Characteristics
Reactor	
Acrylic window reactor	d_r = 2.22 cm ; Length = 57.23 cm
Stainless steel reactor	d_r = 2.19 cm ; Length = 57.31 cm
Packing	
Glass Beads - stainless steel reactor	Type : nonporous sphere ; d_p= 0.114 cm ; d_r/d_p= 20 ; Bed length (Z) = 51.71 cm ; ε_B = 0.392
Silica shell - acrylic window reactor	Type : Porous sphere ; d_p = 0.152 cm d_r/d_p= 14.6 ; Bed length (Z) = 51.63 cm ; ε_B = 0.412 ; ε_p=0.697
0.5% Pd / Alumina-stainless steel reactor	Type : Porous extrudate; size = (0.157 x 4.3) cm; $(d_p)_{eq}$ = 0.199 cm ; d_r/d_p= 11 ; Bed height (Z) = 51.61 ;ε_B = 0.355; ε_p= 0.599

3.4.3 Results and Data Analysis

The influence of reactor pressure and gas flow rate on pressure drop and liquid holdup are investigated experimentally for different operating conditions, different bed characteristics and different liquid-gas systems. Figures 3.5 - 3.18 illustrate the experimental observations. Based on the phenomenological analysis (Section 3.3) , pressure drop data are presented in terms of the dimensionless pressure drop, $(\Delta P / Z)/(\rho_L\, g)$. The effects described phenomenologically in Section 3.3 match well the experimental observations and clearly reveal the various mechanistic cases (case 1 - 5).

The cases which are deduced from the phenomenological analysis (Section 3.3) are shown experimentally in Figures 3.5-3.10 for hexane-water / nitrogen-helium in glass beads, extrudate and spherical particle beds. In case of trickle flow without gas flow (case 1), the pressure gradient is zero and liquid holdup is maximal as shown in Figure 3.8. At low pressure and low superficial gas flow rate (case 2), the dimensionless pressure drop increases slightly while the liquid holdup decreases a little. As gas flow rate increases (case 3), the dimensionless pressure drop increases and liquid holdup decreases. At high pressure operation and low gas velocity (case 4), pressure drop increases slightly and liquid holdup decreases insignificantly over that of low pressure (case 2) for a given gas phase. The effect of case 3 on pressure drop and liquid holdup is larger than that of high pressure and low gas velocity (case 4). At high pressure and high gas velocity (case 5), the dimensionless pressure drop increases significantly and liquid holdup decreases considerably. The effect of the operating conditions in this case is obviously much larger than in other cases. This also indicates that the effect of gas flow rate is more pronounced at elevated pressure. Figures 3.6 , 3.9, and 3.11-3.13 confirm such observations. Figure 3.6 illustrates that pressure drop and liquid holdup at

2.13 MPa (295 psig) and superficial gas velocity equal to 8.75 cm/s are about the same of that at 1.55 MPa (210 psig) and gas velocity equal to 11.7 cm/s for hexane/helium system and a glass beads bed. For hexane/nitrogen system and extrudate bed, Figure 3.9 shows also that the pressure drop and liquid holdup are about the same for the conditions of 4.93 MPa (700 psig), U_G = 7.2 cm/s and 3.55 MPa (500 psig), U_G = 8.75 cm/s . Figures 3.11-3.13 show that at constant gas superficial velocity for a given system, pressure drop increases and liquid holdup decreases as reactor pressure increases. It is clear from these experimental observations, that the effects of reactor pressure and gas flow rate at high pressure are noticeable and need to be considered at operating conditions of industrial interest. It is noteworthy to mention that it is an improper way to describe such effects by representing the data in terms of gas mass superficial velocity as Larachi et al. (1990) did. This is because two effects of gas density (reactor pressure) and gas flow rate are linked together while their separable contribution depends on the range of the pressure and the gas flow rate. For instance, in Figure 3.5 the gas mass superficial velocity in case 4 is higher than in case 3 but the effect on pressure drop and holdup in case 3 is larger than that of case 4.

To investigate the effect of gas density at constant superficial gas velocity, hexane-nitrogen/helium systems were used. Helium pressure about seven times higher than that of nitrogen yields helium density equal to nitrogen density. Figure 3.14 shows that both systems at the same gas density render about the same effect. This confirms that the effect of high pressure operation is due to the increase in the gas density.

All experimental data shows that pressure drop and liquid holdup increase with increasing liquid flow rate as usually observed under atmospheric pressure. The effects of liquid physical properties (density and viscosity) on the pressure drop and liquid holdup are demonstrated in Figures 3.15 and 3.16. As liquid density increases, the liquid

holdup and dimensional pressure drop, $\Delta P/Z$, increase, while the dimensionless pressure drop, $(\Delta P / Z)/(\rho_L\ g)$, decreases.

The effect of bed characteristics on pressure drop and liquid holdup is illustrated in Figures 3.17-3.18. It is obvious that the small catalyst size results in high pressure drop and liquid holdup. The effects of bed characteristics are accounted for by the Ergun constants, bed voidage, and Galileo numbers in equation (3.9).

Figure 3.19 compares the liquid holdup measured by draining and tracer methods. It reveals acceptable agreement between these methods and such comparison is similar to the comparison reported by Tukac and Hanika (1992). Some of the liquid holdup obtained by tracer method is larger than that obtained by the draining method. This could be due to a systematic experimental error associated in measuring of liquid holdup by either method. It is suspected that the draining method may underestimate static holdup which is arrived at by subtraction of numbers similar in magnitude while the tracer method overestimates slightly external holdup. This combined effect would lead to the slight bias of larger holdups predicted by tracer method in comparison to the draining method. The above hypotheses for the causes of the discrepancy have not been proven.

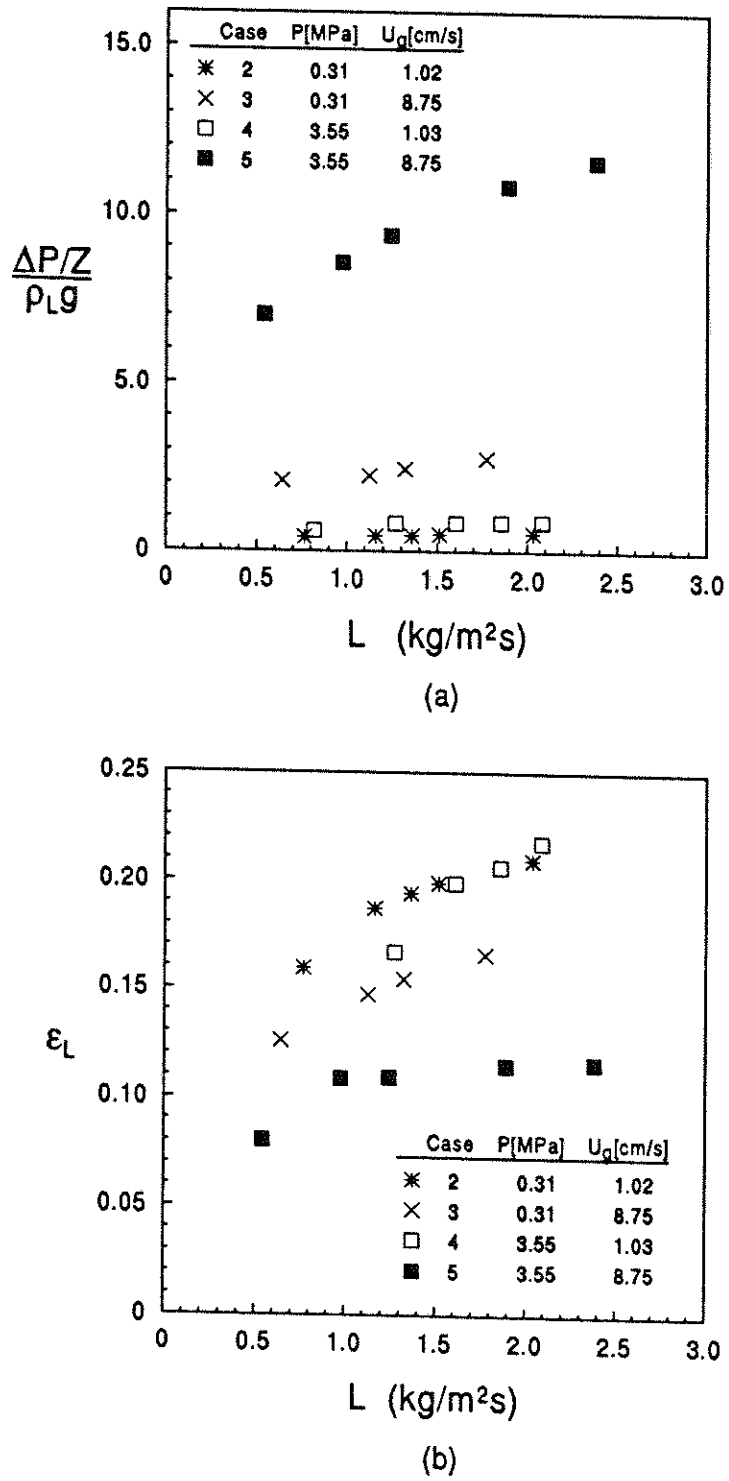

Figure 3.5 : Effect of reactor pressure and gas flow rate on pressure drop and liquid holdup. System : hexane/nitrogen; nonporous spherical glass beads ; $d_r/d_p = 20$

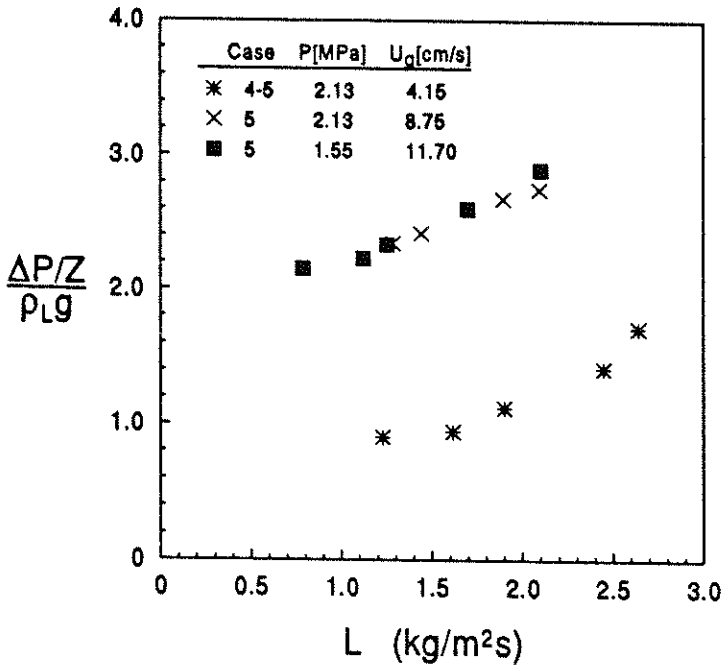

(a)

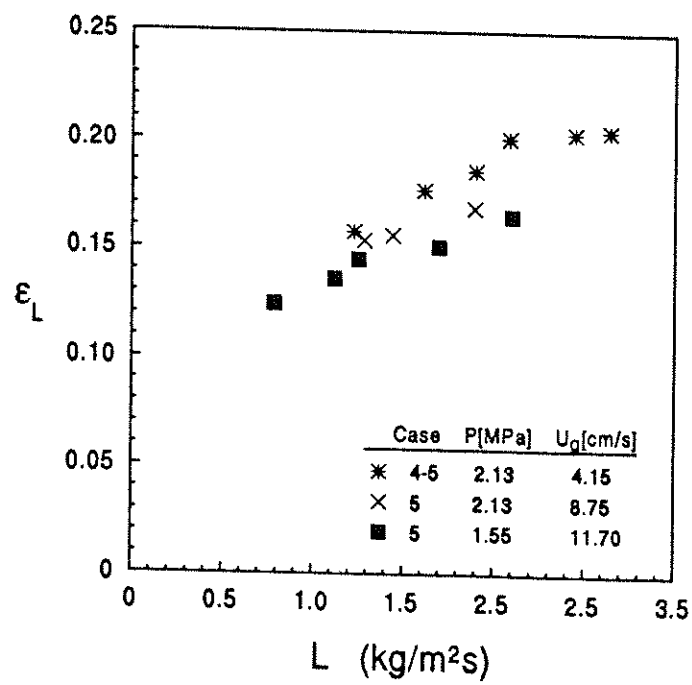

(b)

Figure 3.6 : Effect of reactor pressure and gas flow rate on pressure drop and liquid holdup. System : hexane/helium; nonporous spherical glass beads ; $d_r/d_p = 20$

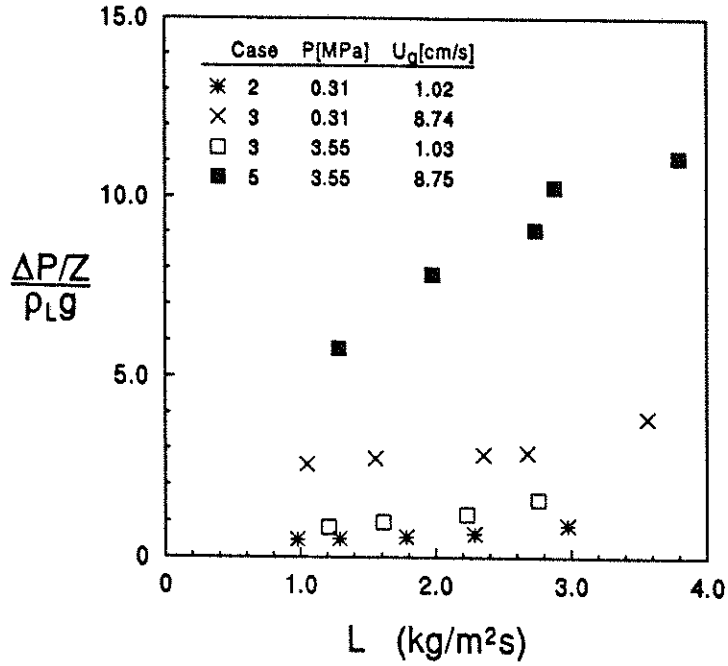

(a)

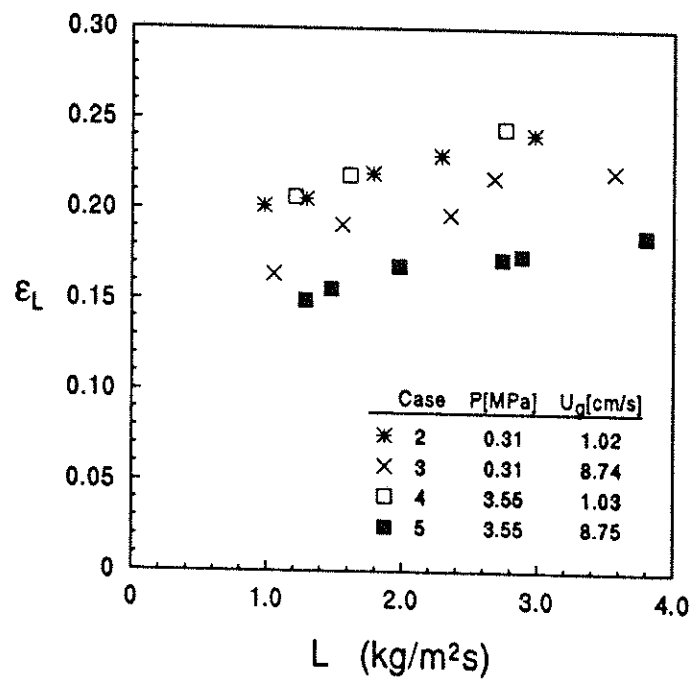

(b)

Figure 3.7 : Effect of reactor pressure and gas flow rate on pressure drop and liquid holdup. System : water/nitrogen; nonporous spherical glass beads ; $d_r/d_p = 20$

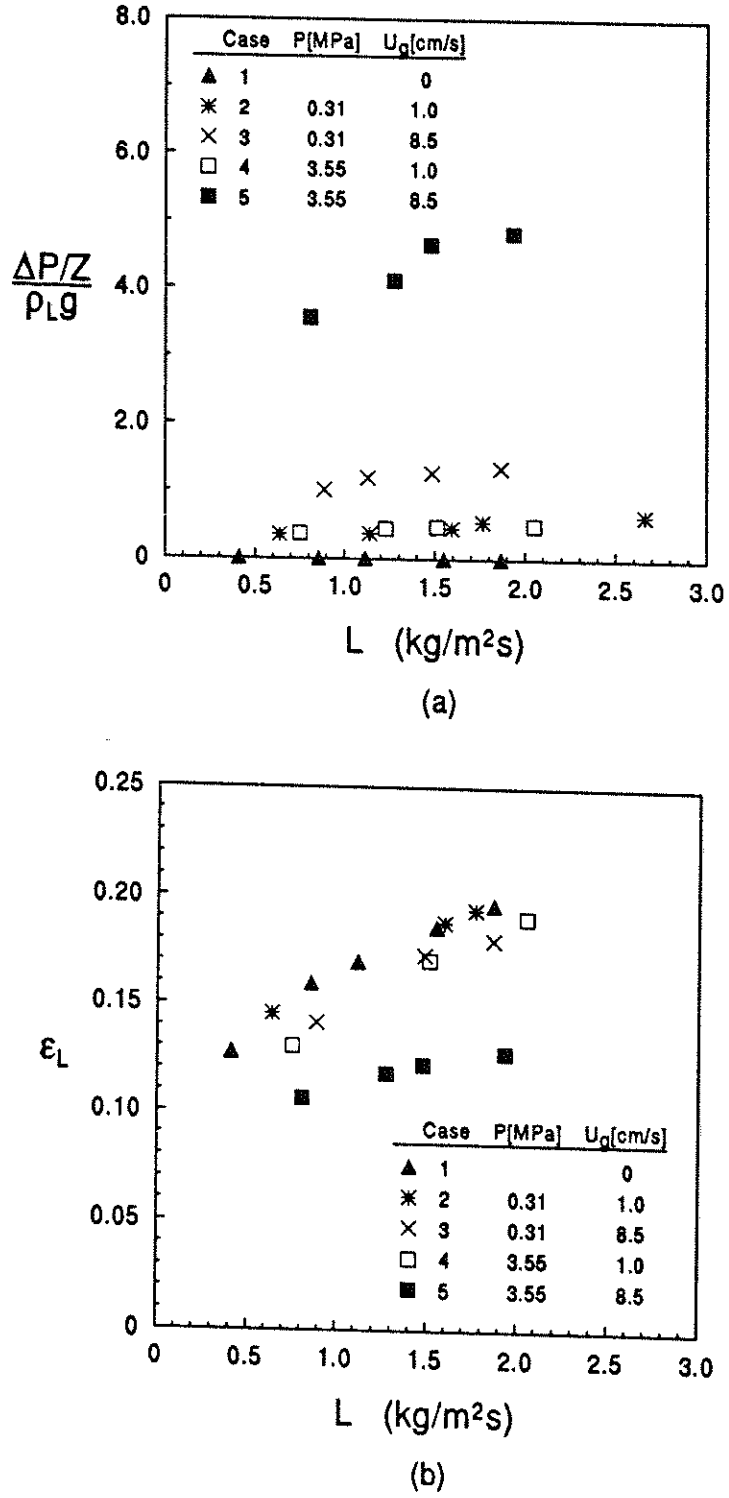

Figure 3.8 : Effect of reactor pressure and gas flow rate on pressure drop and liquid holdup. System : hexane/nitrogen; porous spherical silica shell ; $d_r/d_p = 14.6$

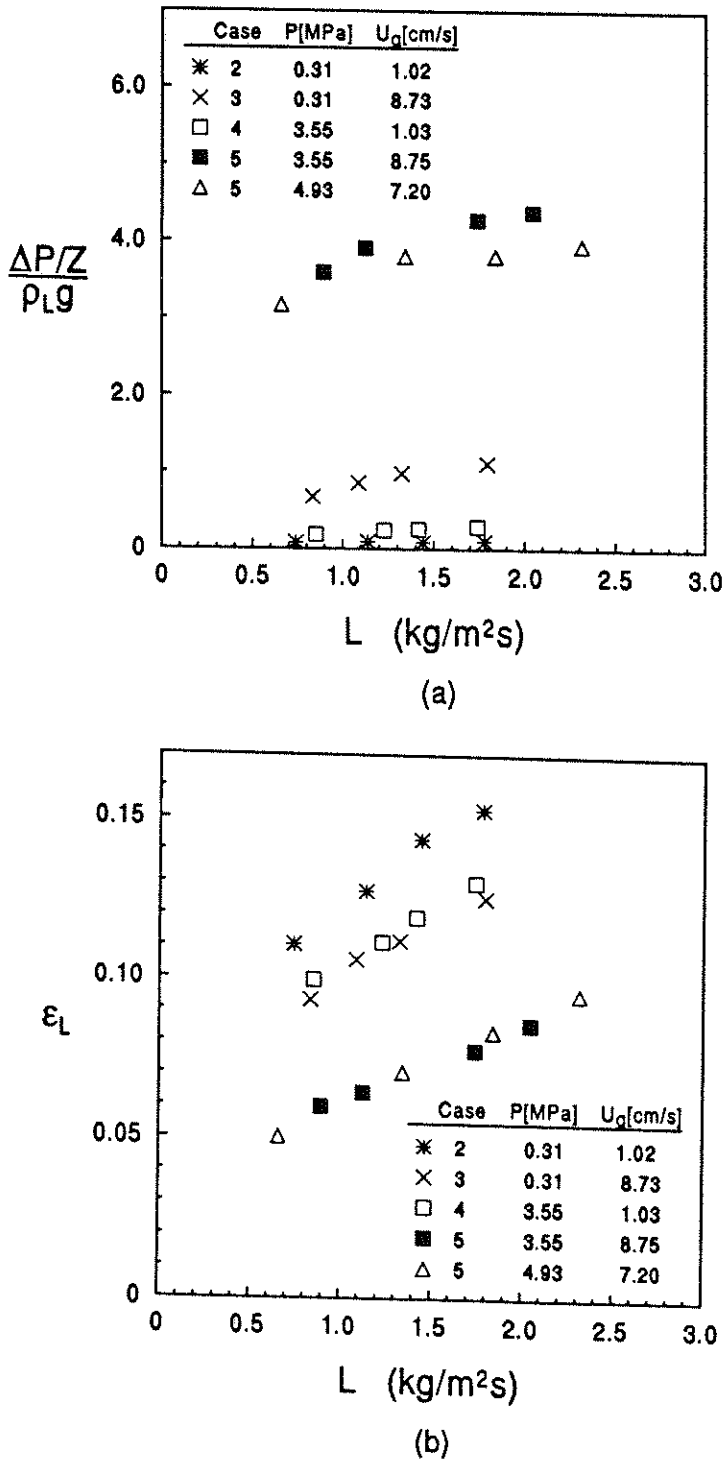

Figure 3.9 : Effect of reactor pressure and gas flow rate on pressure drop and liquid holdup. System : hexane/nitrogen; porous extrudate of 0.5 % Pd on alumina ; $d_r/d_p = 11$

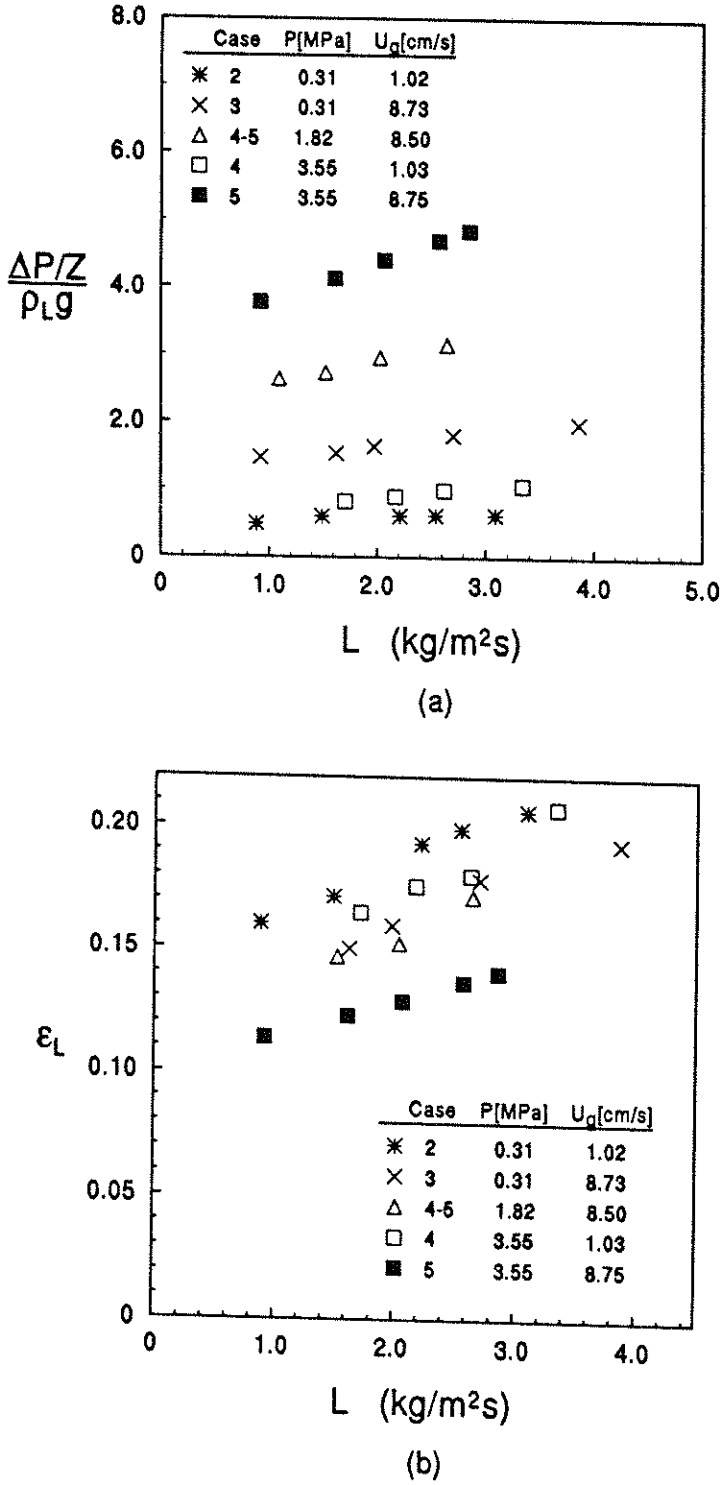

Figure 3.10 : Effect of reactor pressure and gas flow rate on pressure drop and liquid holdup. System : water/nitrogen ; porous extrudate of 0.5 % Pd on alumina ; $d_r/d_p = 11$

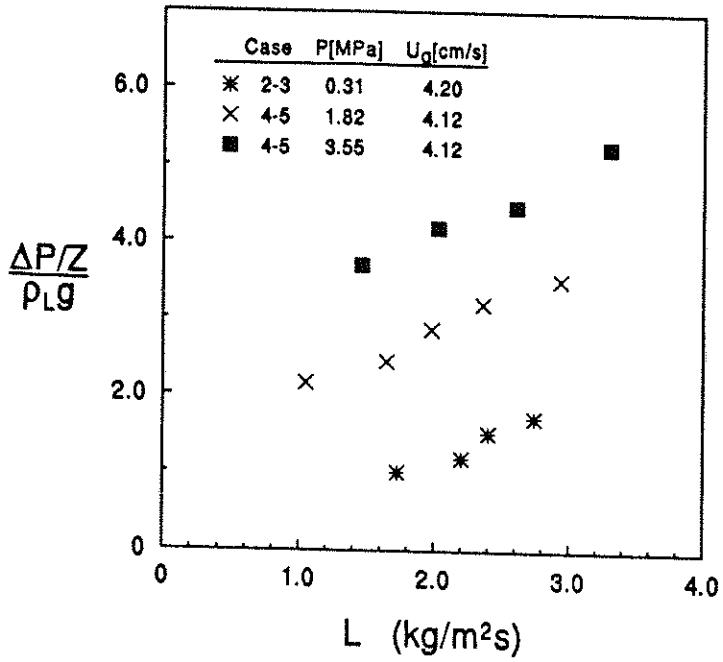

(a)

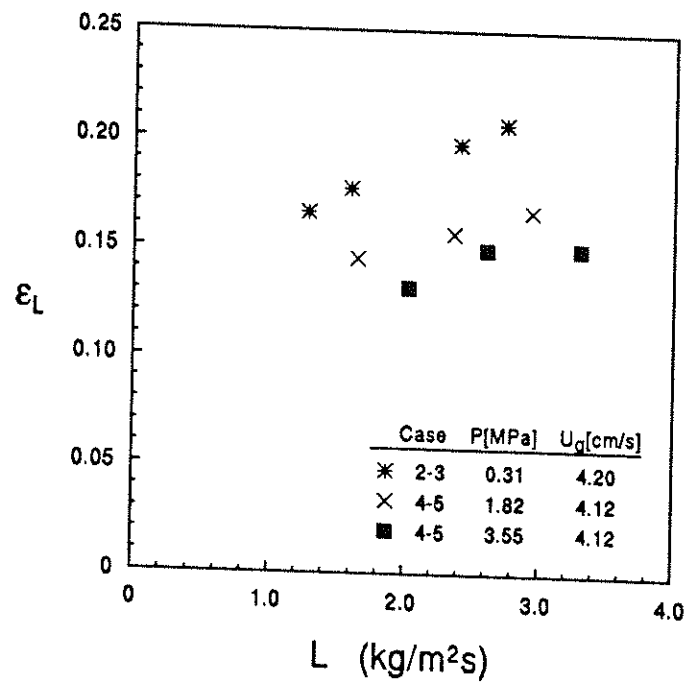

(b)

Figure 3.11 : Effect of reactor pressure on pressure drop and liquid holdup at $U_G \approx 4$ cm/s. System : hexane/nitrogen; nonporous spherical glass beads ; $d_r/d_p = 20$

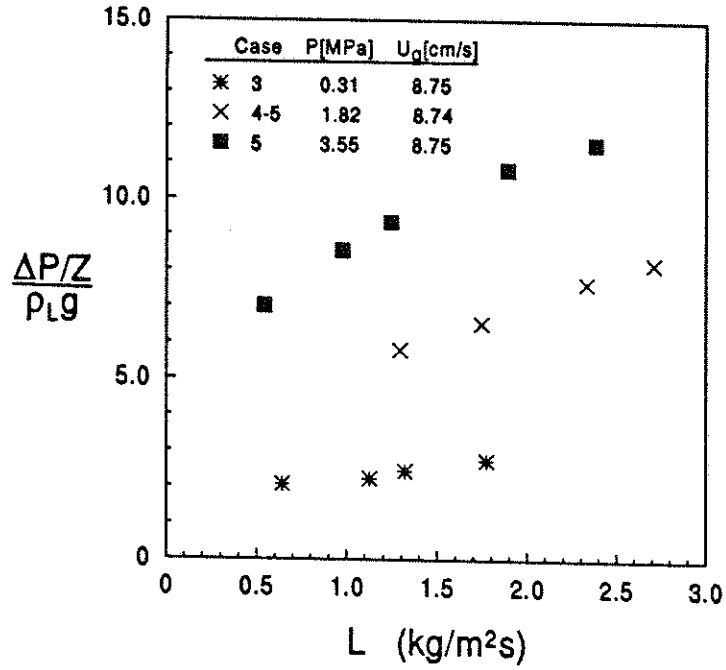

(a)

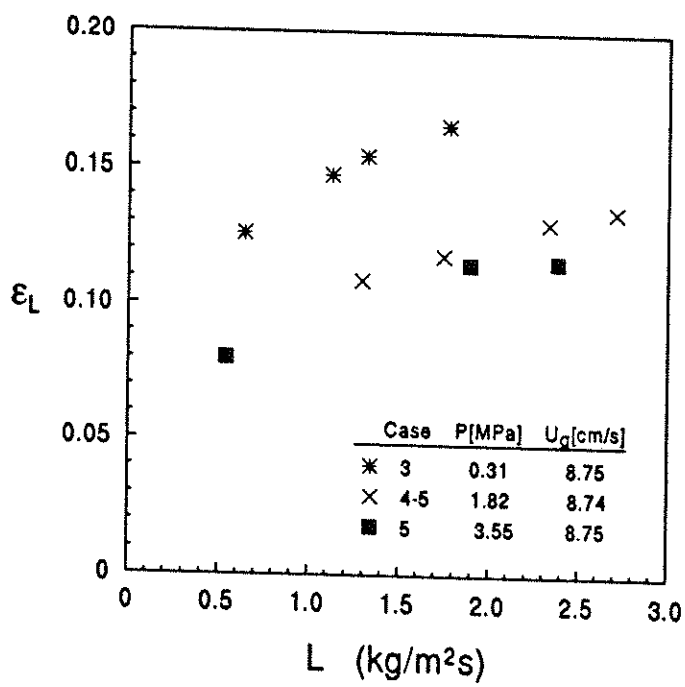

(b)

Figure 3.12 : Effect of reactor pressure on pressure drop and liquid holdup at $U_G \approx$ 8.75 cm/s. System : hexane/nitrogen; nonporous spherical glass beads ; $d_r/d_p = 20$

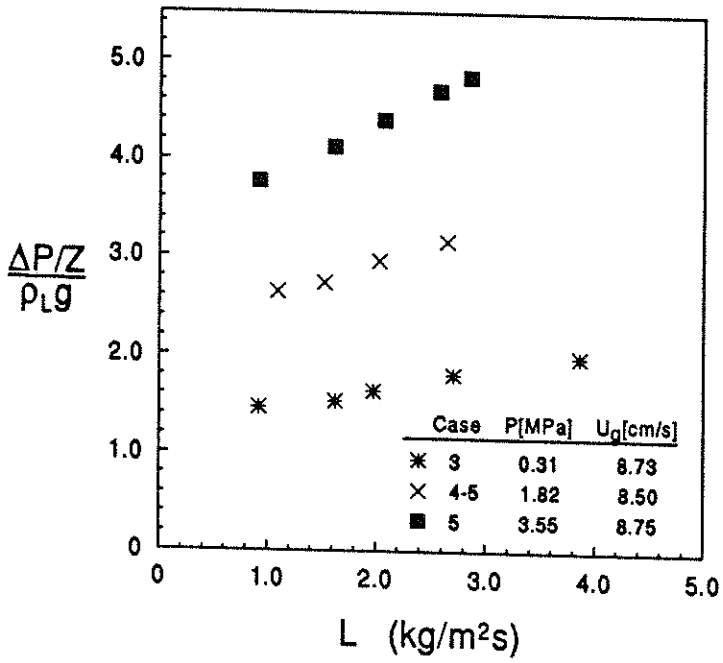

(a)

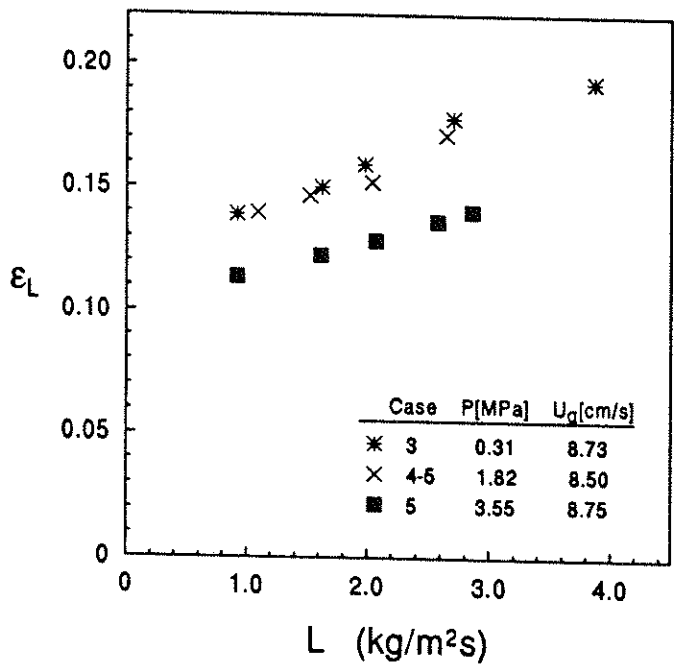

(b)

Figure 3.13 : Effect of reactor pressure on pressure drop and liquid holdup at $U_G \approx 8.75$ cm/s. System : water/nitrogen; porous extrudate of 0.5 % Pd on alumina; $d_r/d_p = 11$

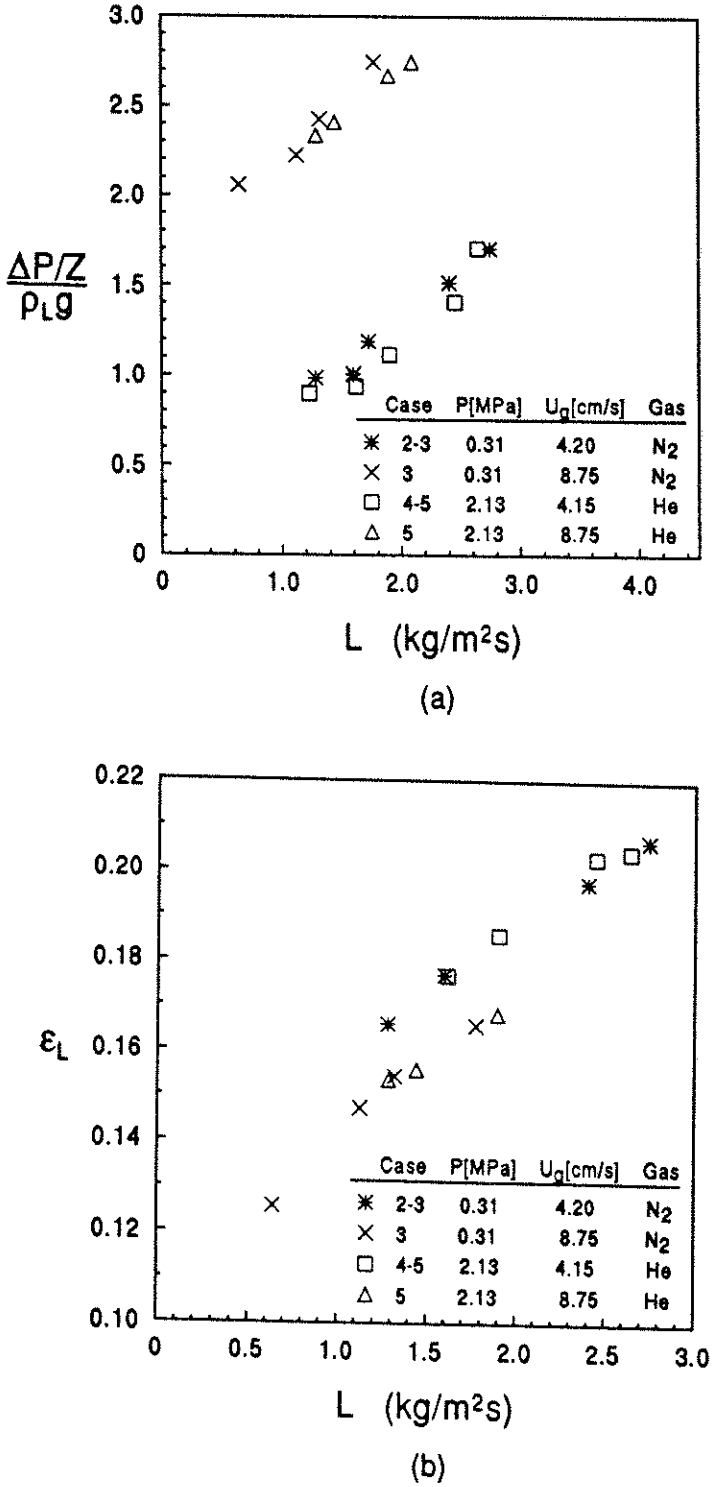

Figure 3.14 : Effect of gas density on pressure drop and liquid holdup. System: hexane/nitrogen and helium; nonporous spherical glass beads ; $d_r/d_p = 20$

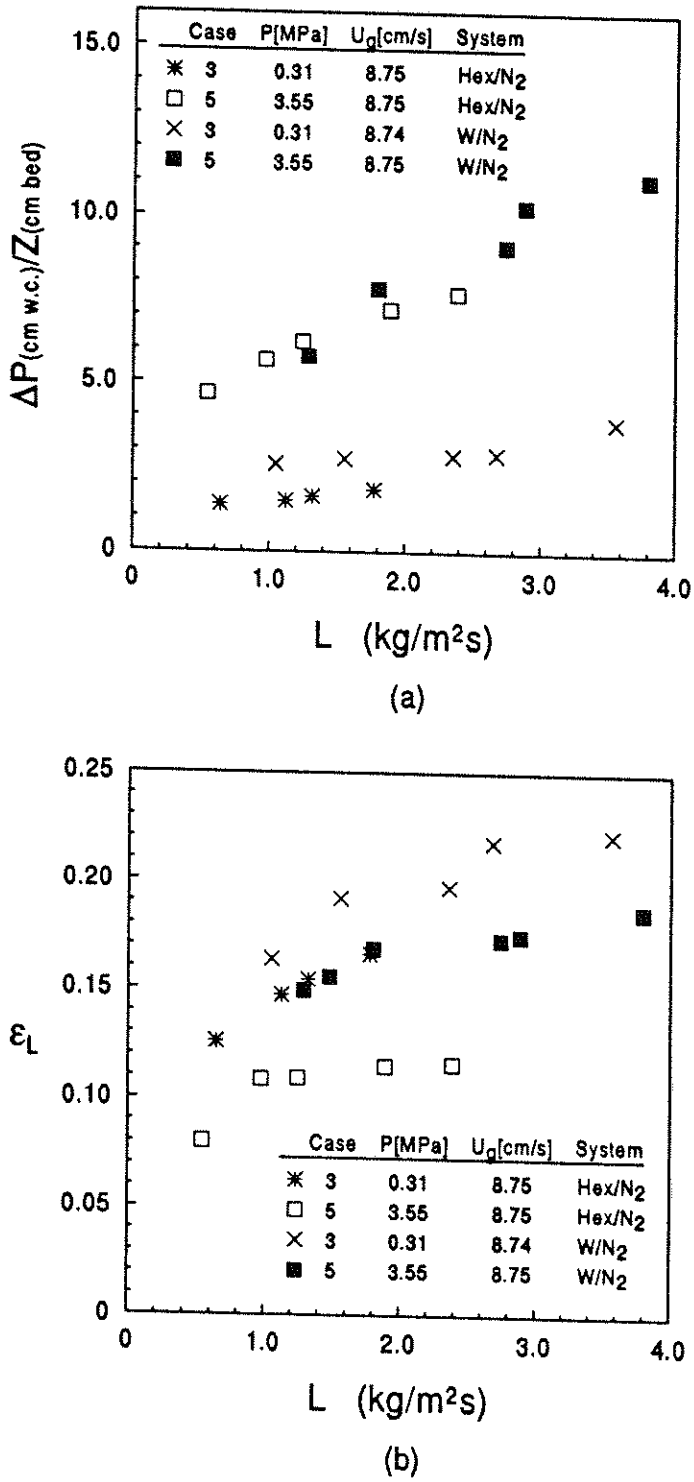

Figure 3.15 : Effect of liquid physical properties on pressure drop and liquid holdup. System: hexane/nitrogen and water/nitrogen; nonporous spherical glass beads;$d_r/d_p = 20$

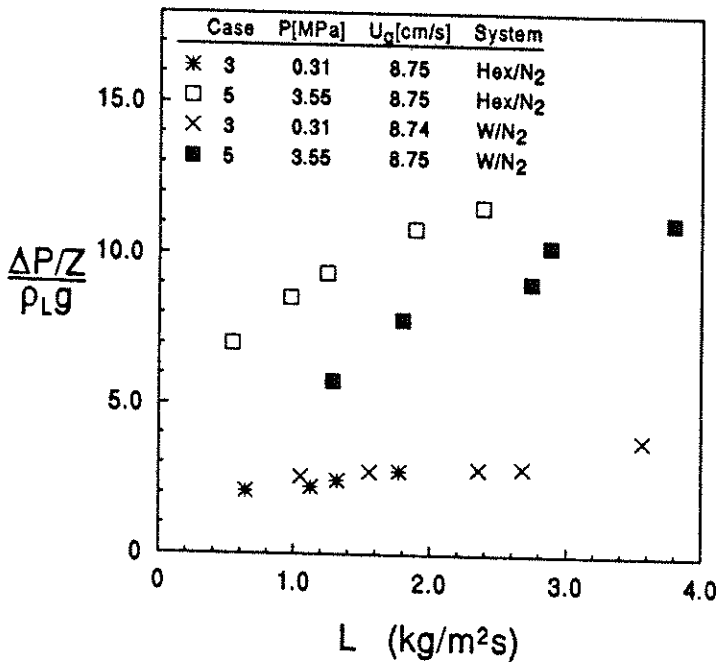

(c)

Figure 3.15 : Effect of liquid physical properties on pressure drop and liquid holdup. System: hexane/nitrogen and water/nitrogen; nonporous spherical glass beads; $d_r/d_p = 20$

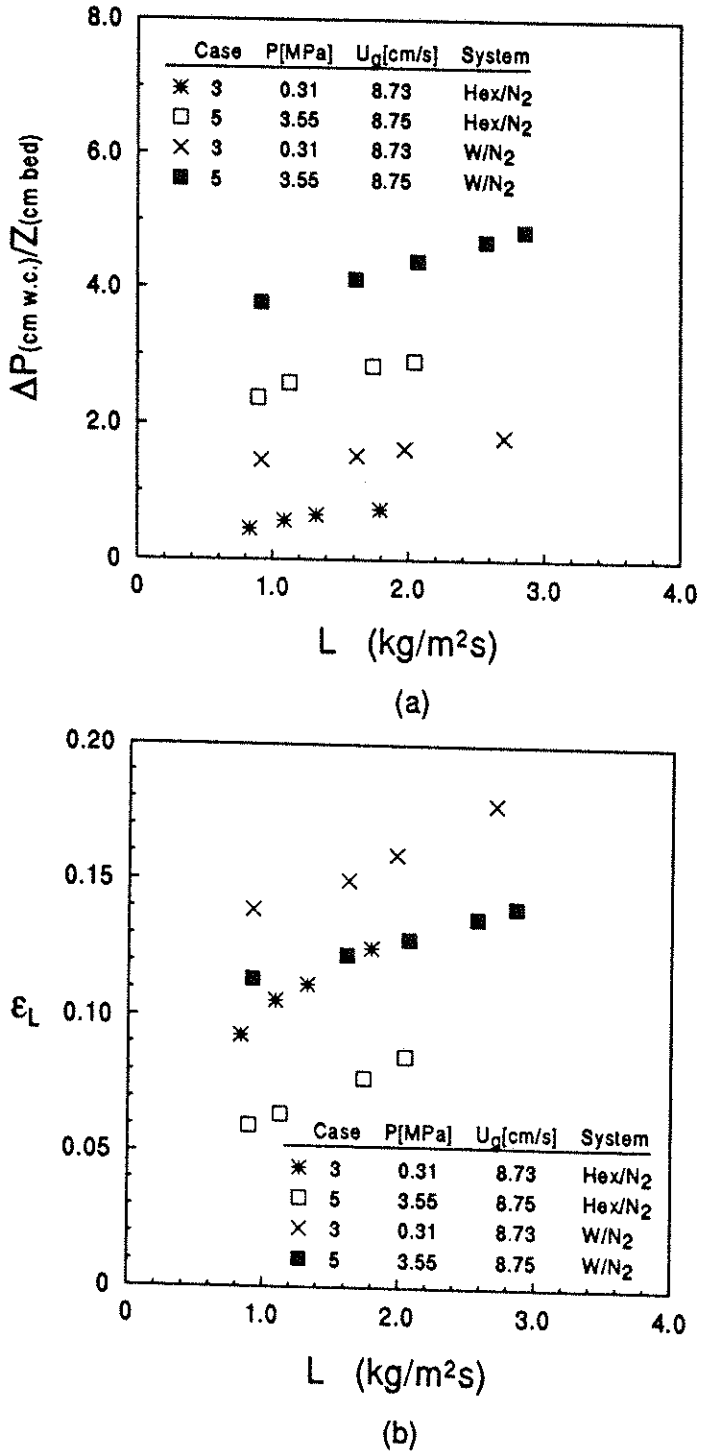

Figure 3.16 : Effect of liquid physical properties on pressure drop and liquid holdup. System: hexane/nitrogen and water/nitrogen; porous extrudate of 0.5 % Pd on alumina ; $d_r/d_p = 11$

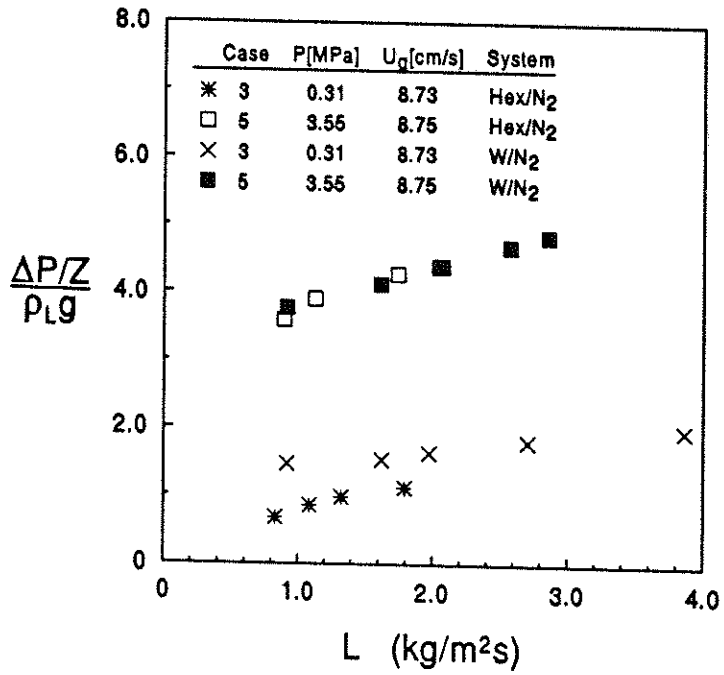

(c)

Figure 3.16 : Effect of liquid physical properties on pressure drop and liquid holdup. System: hexane/nitrogen and water/nitrogen; porous extrudate of 0.5 % Pd on alumina ; $d_r/d_p = 11$

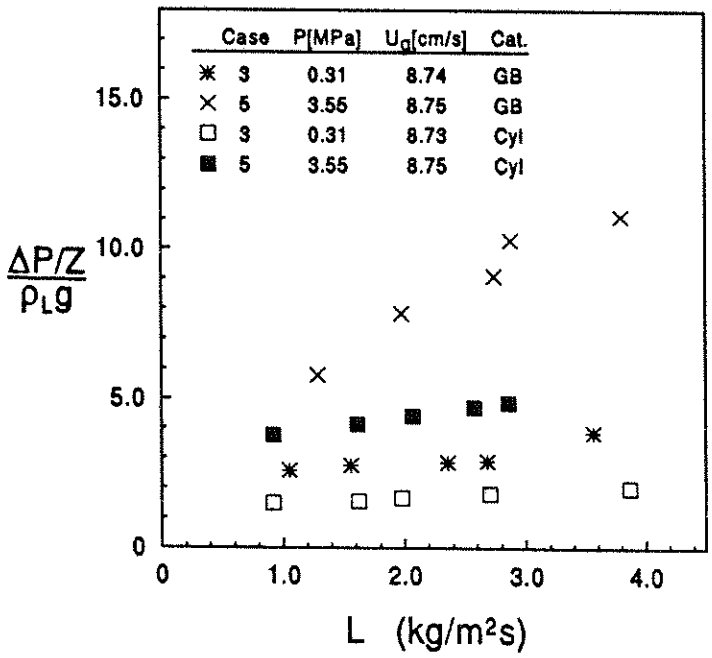

(a)

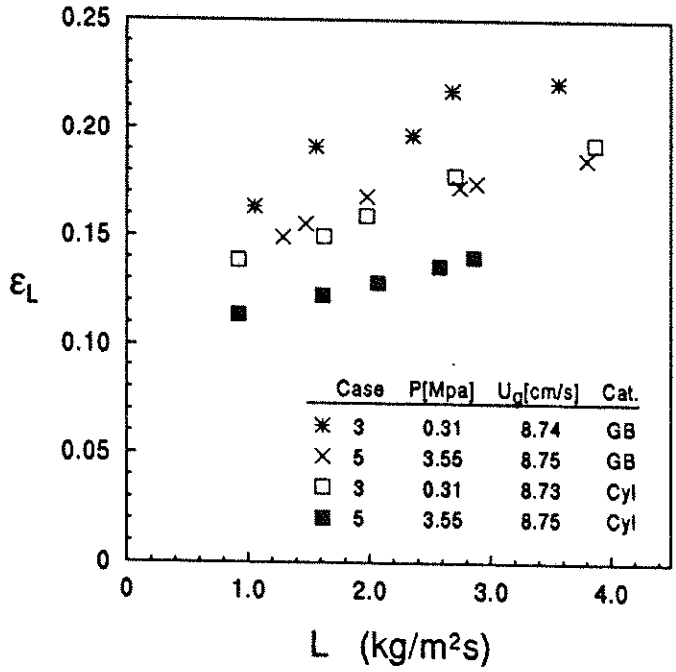

(b)

Figure 3.17 : Effect of bed characteristics on pressure drop and liquid holdup, System : water/nitrogen; GB: glass beads (d_p=0.114 cm); Cyl : extrudate ((d_p)eq=0.199 cm)

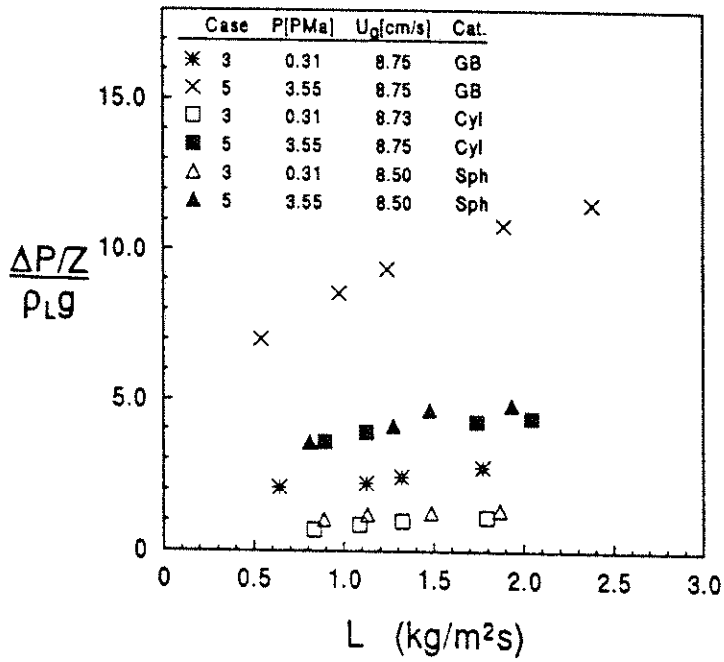

(a)

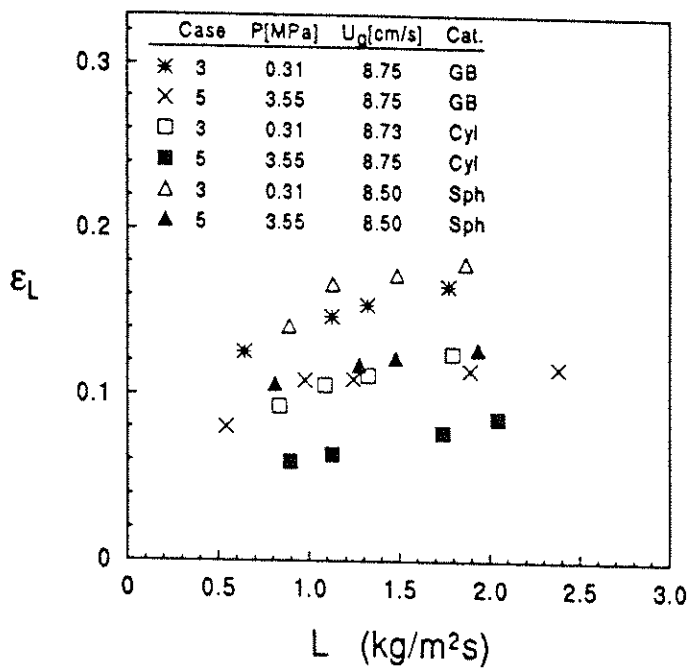

(b)

Figure 3.18 : Effect of bed characteristics on pressure drop and liquid holdup. System : hexane/nitrogen; GB: glass beads (d_p=0.114 cm); Cyl : extrudate ((d_p)eq=0.199 cm) Sph : spherical silica shell (d_p=0.152 cm)

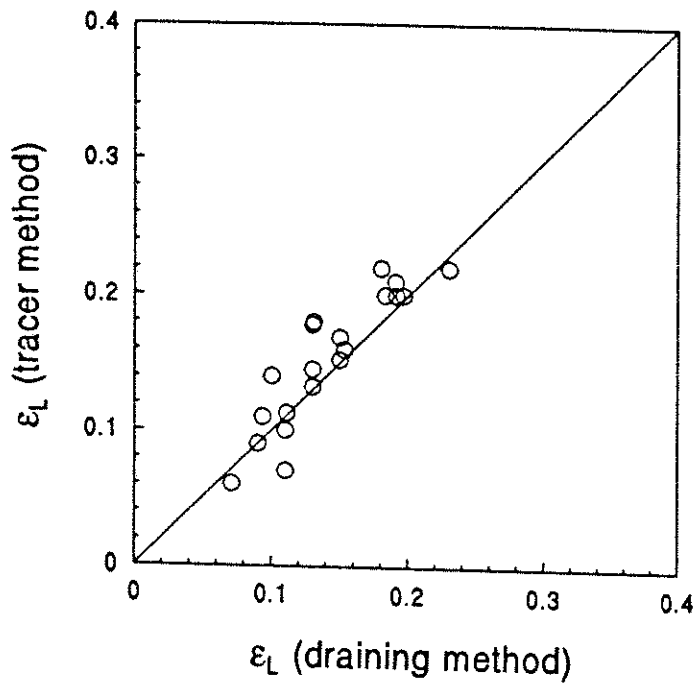

Figure 3.19 : Comparison between liquid holdup measured by draining and tracer methods

3.5 VALIDITY OF HOLUB'S MODEL (1990) AND OF OTHER RECENT CORRELATIONS

Holub's model (1990) has been justified at atmospheric pressure as shown in Figure 3.3 but was never tested at high pressure operation . The model requires the Ergun constants for each bed of interest to be measured by single phase flow pressure drop measurements. Since these constants represent the bed characteristics, they are reactor pressure independent as verified experimentally in this study. Hence, experiments with dry bed with gas phase flow only have been conducted at reactor pressure of 30 to 100 psig to measure Ergun constants, E_1 and E_2, for the bed characteristics shown in Table 3.5. The measured Ergun constants are listed in Table 3.6 which are within the magnitude experimentally determined by others (Macdonald et al.,1979; Holub, 1990). It was found that the best estimates of the Ergun constants can be obtained in the region when both viscous and inertial forces are important.

Table 3.6 : Measured Ergun constants

Packed bed	E_1	E_2
Spherical Silica Shell in acrylic window reactor dp= 0.152 cm;ε_B=0.412;d_r=2.22cm	260.2	2.48
Spherical Glass Beads in stainless steel reactor dp= 0.114 cm;ε_B=0.392;d_r=2.19cm	334.1	3.23
Extrudate 0.5% Pd on alumina in stainless steel reactor dp= 0.199 cm;ε_B=0.355;d_r=2.19cm	218.0	1.89

The validity of Holub's model at high pressure operation and other recent correlations are tested by comparing their prediction and the experimental data obtained in this investigation. The mean relative error in prediction is utilized for the comparison which is evaluated as follows :

$$\hat{e}_{\phi} = \frac{1}{N}\sum_{i=1}^{N}\frac{\left|\phi_{predicted} - \phi_{experimental}\right|}{\phi_{experimental}} \tag{3.13}$$

Where ϕ is either dimensionless pressure drop or liquid holdup .

Table 3.7 shows the mean relative error in prediction of Holub's model. The model prediction of pressure drop and liquid holdup collected in a bed of $d_r/d_p = 20$ is better than in beds of $d_r/d_p = 11$ and 14.6. This is because in a bed of $d_r/d_p \geq 20$, the liquid phase is better distributed than in a bed of $d_r/d_p \leq 20$ where in the later bed wall effect, axial dispersion and liquid maldistribution are encountered (Dudukovic' and Mills, 1986)

Table 3.7 : Comparison of Holub's model (1990) prediction and high pressure data for pressure drop and liquid holdup

Bed Type	$\hat{e}_{(\Delta P/Z)/\rho_L g}$	$\hat{e}_{\varepsilon_L}$
Data collected in the bed of $d_r/d_p = 20$	29 %	6.8 %
Data collected in the bed of $d_r/d_p = 14.6$ and 11	55 %	14 %
All collected data ($d_r/d_p = 20$, 14.6 and 11)	40 %	9.7 %

The graphical comparison of the Holub's model prediction for pressure drop and liquid holdup at high pressure operation and the collected data in this investigation in the beds of d_r/d_p = 11, 14.6 and 20 (Figure 3.5-3.18) is shown in Figure 3.20. The data is bounded within the same error range reported by Holub et al. (1992) at atmospheric pressure (± 60% for pressure drop and ± 20% for liquid holdup). However the model prediction of pressure drop and liquid holdup improves for the bed of d_r/d_p = 20 as shown in Figure 3.21 . The data are bounded between ± 45% and ± 15% for pressure drop and holdup, respectively, as discussed above.

Moreover, Holub's model (1990) predicts properly the trend of the effects of reactor pressure, gas flow rate, liquid flow rate, physical properties, and bed characteristics that are demonstrated in Figures 3.5 - 3.18. As an example, Figure 3.22 illustrate the trend of Holub's model prediction versus some of the experimental observations. The model also predicts well the effect of gas density at constant superficial velocity as shown in Figure 3.23. The relative difference between the model prediction using nitrogen gas and helium gas is within 6 %. This is due to the difference in viscosity between these gases . This difference decreases as the pressure increases where the gas density effects dominate. Such small effect would be difficult to observe experimentally since the difference is within the experimental error.

Holub (1990), Holub et al. (1992) and Dudukovic' et al. (1991) compared in terms of mean relative error Holub's model prediction for pressure drop and liquid holdup with prediction of various models based on modified forms of Ergun equation (Saez and Carbondell, 1985; Specchia and Baldi , 1977) and based on empirical correlations (Larkins et al. , 1961; Turpin and Huntington, 1967 ; Midoux et al.; Ellman et al.,1988). Their comparisons reveal that Holub phenomenological model predictions are much better than that of these models. Therefore, only the recent correlations developed based on high pressure data (Table 3.1) are compared with Holub's model as

shown in Table 3.8. It is clear that Holub's model predicts pressure drop and liquid holdup at low to high pressure better than the recently developed empirical correlations. Larachi et. al. (1991) correlation predicts total liquid saturation, while Ellman et. al. (1988) predicts dynamic saturation where the static liquid saturation need to be evaluated from other correlations. Wammes et. al. (1991) holdup correlation relates dynamic liquid saturation to pressure drop , while pressure drop correlation relates pressure drop to total liquid saturation. In order to solve these equations simultaneously static liquid saturation is required which needs to be evaluated by other correlations. In Table 3.8, the measured experimental static saturation has been used in Ellman et. al. (1988) and Wammes et. al. (1991) correlations prediction.

Table 3.8 : Comparison of models to data

	Only high pressure data		All data of which 63% is high pressure	
Model	$\hat{e}_{(\Delta P/Z)/\rho_L g}$	$\hat{e}_{\varepsilon_L}$	$\hat{e}_{(\Delta P/Z)/\rho_L g}$	$\hat{e}_{\varepsilon_L}$
Holub's (1990)	41%	12%	40 %	9.7 %
Wammes et al. (1991)	85%	52%	88 %	41 %
Larachi et al. (1991)	64%	18%	89 %	14.5 %
Ellman et al. (1988, 1990)	59%	18%	65%	21.5 %

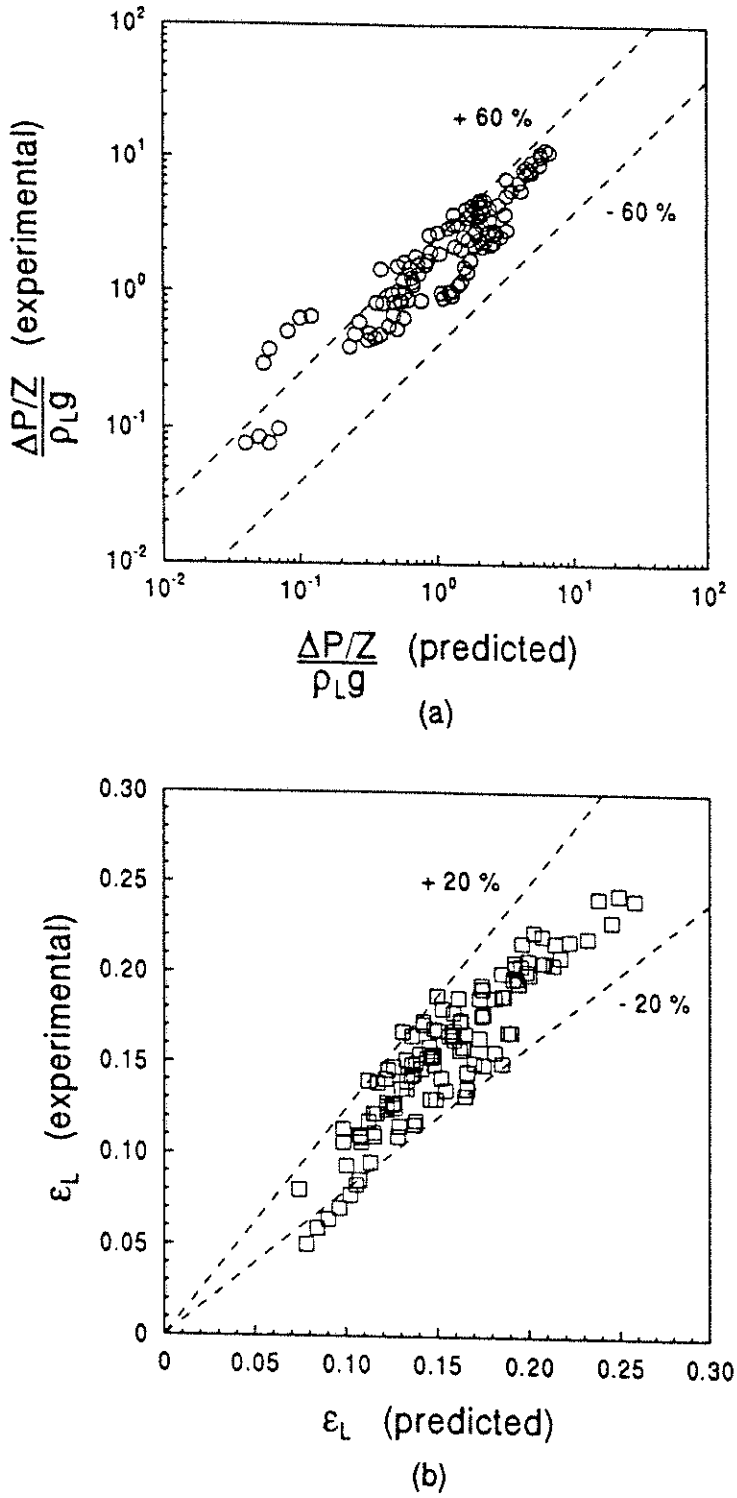

Figure 3.20 : Comparison of Holub's model (1990) prediction and high pressure data obtained in beds of d_r/d_p= 11, 14.6 and 20

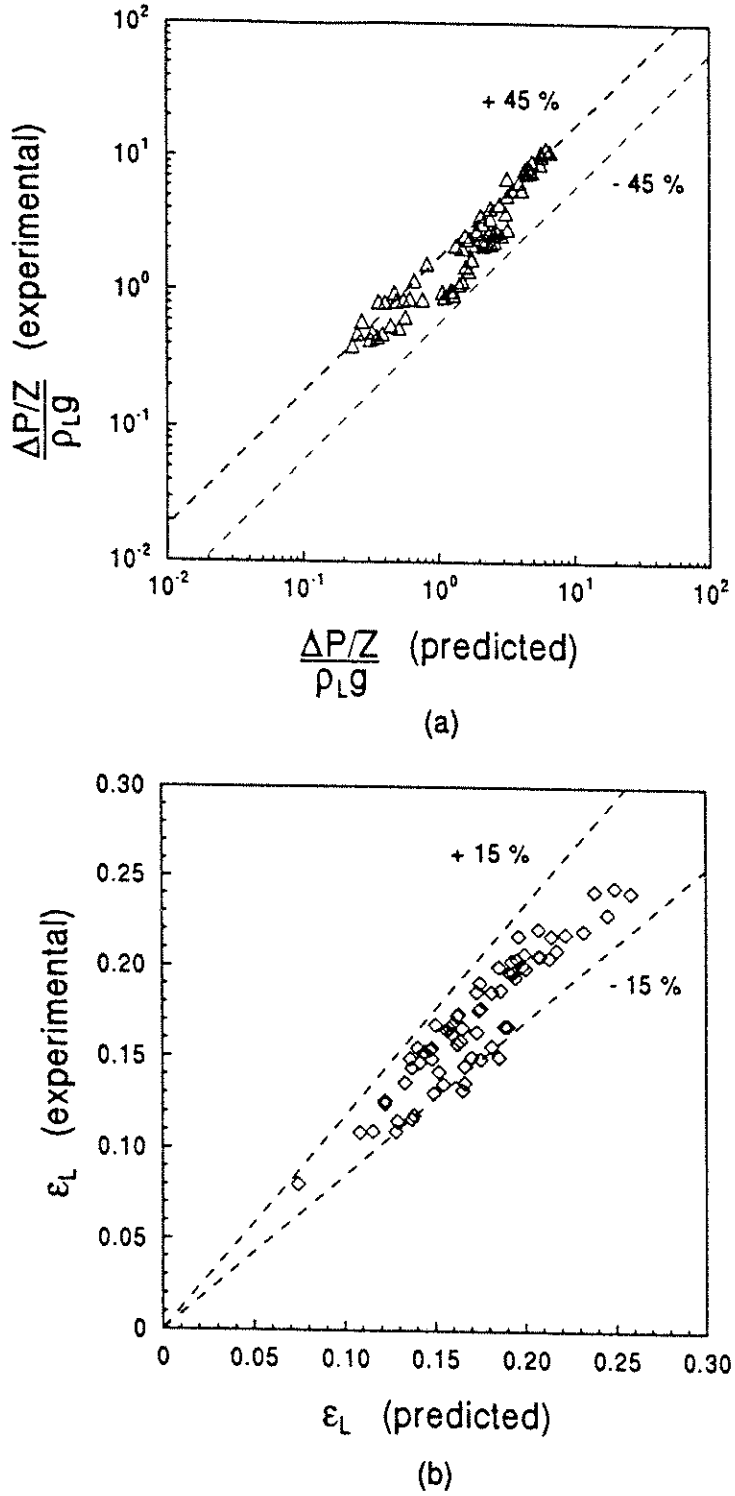

Figure 3.21 : Comparison of Holub's model (1990) prediction and high pressure data obtained in the bed of $d_r/d_p = 20$

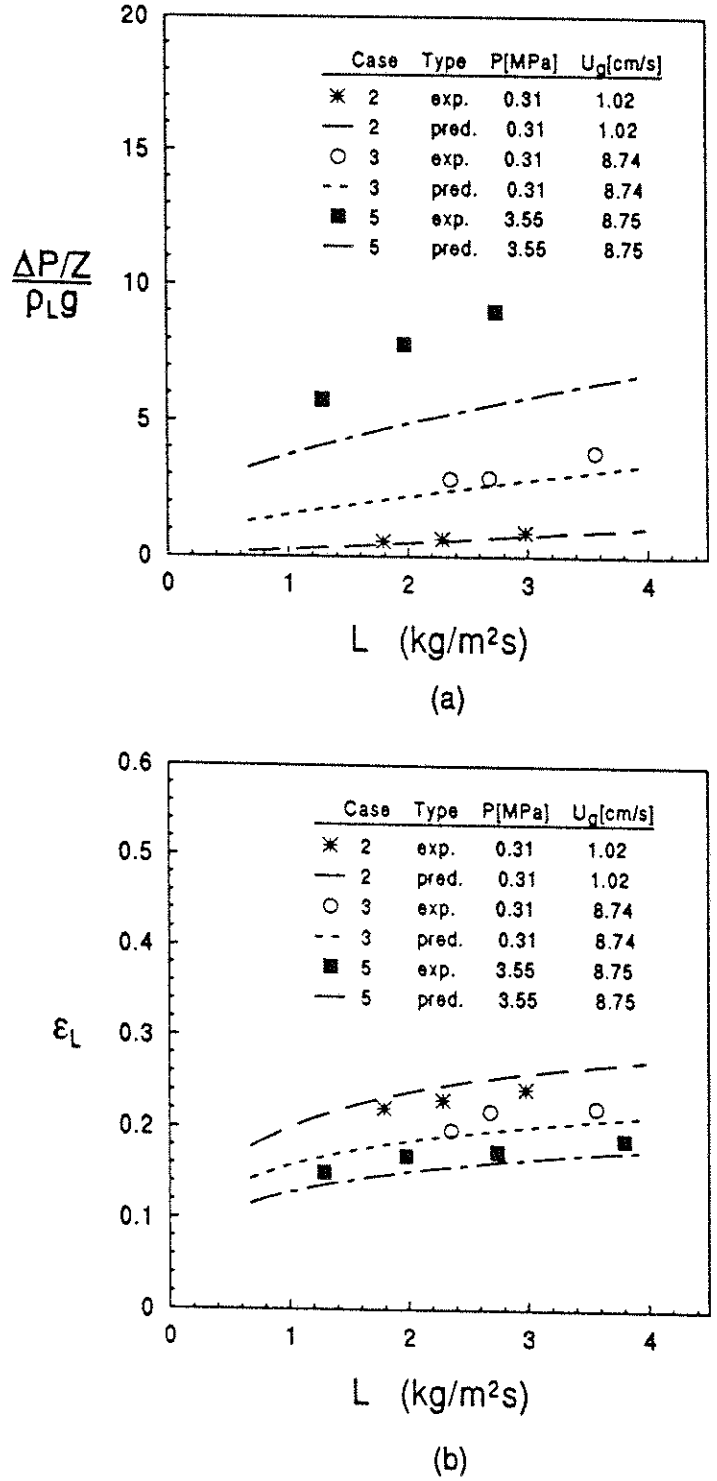

Figure 3.22 : Trend of Holub's model (1990) prediction versus the experimental observation. System: water/nitrogen; nonporous glass beads; $d_r/d_p = 20$

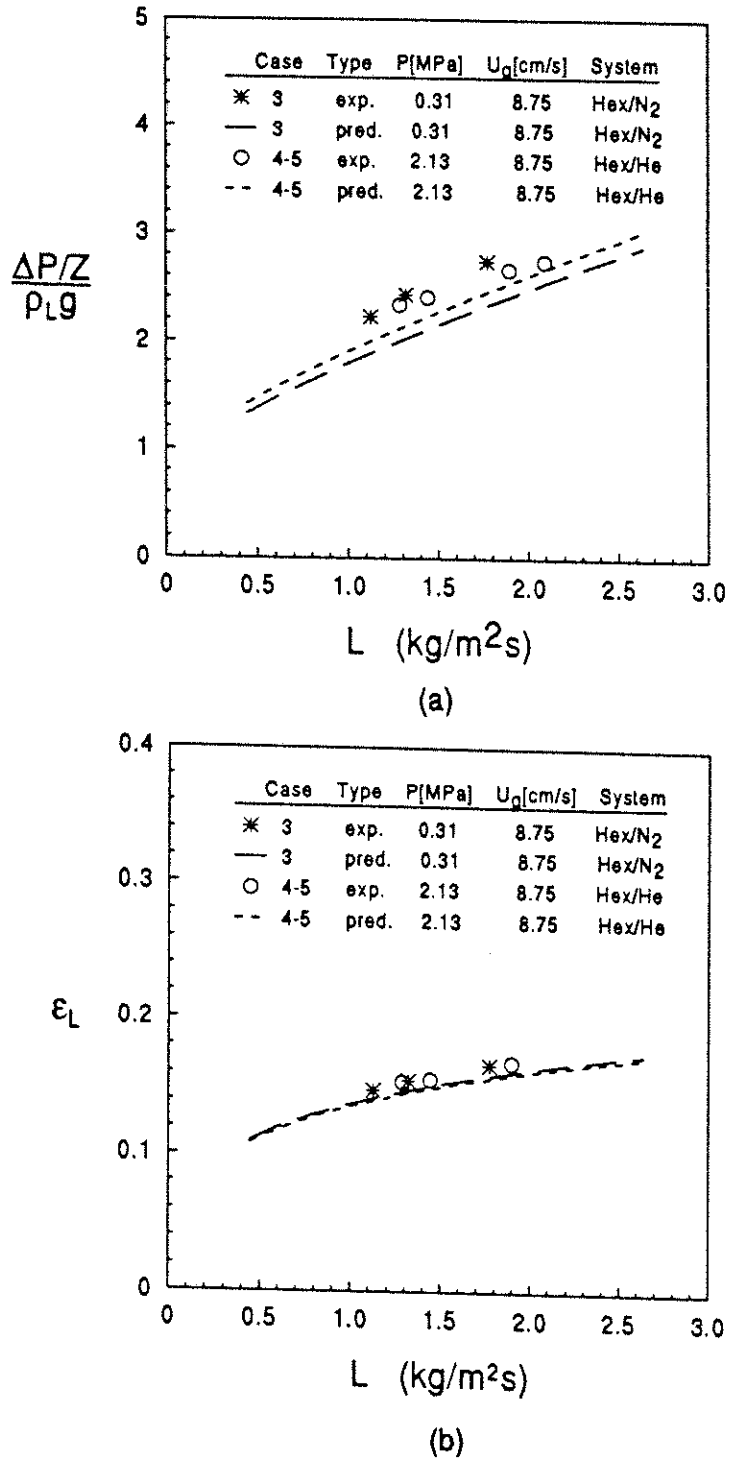

Figure 3.23 : Holub's model (1990) prediction of the effect of gas density on pressure drop and liquid holdup. System : hexane / nitrogen-helium ; nonporous glass beads; d_r/d_p=20

4. EFFECT OF HIGH PRESSURE ON EXTERNAL LIQUID-SOLID CONTACTING EFFICIENCY

4.1 BACKGROUND

External liquid-solid contacting efficiency is important design and scale up parameter. It is essential in determining the degree of catalyst utilization in trickle-bed reactors, since only wetted catalyst can contribute to the reaction in case of nonvolatile liquid reaction , and wetted and dry catalyst behave differently in case of volatile liquid reactions (Dudukovic' and Mills, 1986). Therefore, in order to predict trickle-bed reactor performance and model its behavior, it is necessary to know the contacting efficiency and the effectiveness factor of the resulting partly wetted catalyst. Contacting efficiency effect on reactor performance can be seen in terms of its effect on the apparent reaction rate. The reaction rate over incompletely wetted packing can be greater or smaller than the rate observed over completely wetted packing. This depends upon whether the limiting reactant is present only in the liquid phase or in both gas and liquid phases. If the limiting reactant is nonvolatile, such as occurs in many hydrogenation processes, then a decrease in the solid-liquid contacting reduces the surface for mass transfer between the liquid and solid material causing a decrease in the reaction rate. However, if the liquid reactants are volatile and significant heat effects are also present, then, a gas phase reaction can occur on the dry area of the catalyst and consequently a higher reaction rate is observed. Moreover, with partly wetted catalyst, a conventional concept of an effectiveness factor become useless, since the concentration of the reactants does not remain constant over the entire external surface of the catalyst particles (Zhukova et al., 1990; El-Hisnawi, 1981; Mills, 1978; Dudukovic' and Mills, 1986; Mills and Dudukovic', 1981,1982).

Wetting of the porous catalyst can be internal and external. Internal contacting efficiency is the fraction of internal pore volume in the particles that is filled with liquid, while external contacting efficiency is the fraction of particles external area wetted by the flowing liquid. For prewetted beds, internal contacting efficiency is equal to unity (fully wetted pores) due to the capillary effects particularly for systems with low adiabatic temperature rise ($\Delta T_{ad} < 10^{\circ}$) and nonvolatile liquid or when liquid volatilization does not exceed 10% of the feed (El-Hisnawi, 1981; Dudukovic' and Mills, 1986). Therefore, external contacting efficiency is of interest to be addressed in this investigation .

The phenomena of incomplete catalyst wetting in laboratory scale reactors is the result of the reactor hydrodynamics at low liquid velocities. External contacting efficiency increases monotonically with liquid mass velocity and is unity only at highest velocities (Dudukovic' and Mills, 1986). Therefore, in trickle flow regime of laboratory reactors, two regions are encountered: A partially externally wetted particles region ($\eta_{CE} < 1$) and a fully externally wetted particles region ($\eta_{CE} = 1$).

Many studies of external liquid-solid contacting efficiency have been reported in the literature as shown Table 4.1. Some deal with theoretical and experimental methods to evaluate it, while others deal with demonstrating its effect on the performance of trickle-bed reactors. Until 1975, most of the wetting efficiency studies and correlations were obtained for packed-bed absorption towers using nonporous particles of large diameters and liquid mass velocity considerably greater than in trickle-bed reactors (Mills,1978). All current investigations on contacting efficiency were performed at atmospheric pressure. Hence, all correlations that were proposed to predict the external contacting efficiency, have been developed based on atmospheric data and empirical approach. No study appeared in the literature which investigated the effect of high pressure (operating condition of interest) on the contacting efficiency. Moreover, no

phenomenological model is available which can lead to better understanding of particles wetting phenomena. Therefore, it is unknown whether high pressure operation affects contacting efficiency and whether the empirical correlation developed based on atmospheric data can be utilized for its prediction at operating conditions of interest (high pressure). El-Hisnawi (1981) and El-Hisnawi et al. (1982) correlated empirically the external contacting efficiency in terms of superficial Reynolds and Galileo numbers based on a wide data base obtained at atmospheric pressure by tracer technique. They included all known tracer method and chemical reaction method data on small porous particles. El-Hisnawi's correlation is the only one available for small porous packing characteristic of trickle-bed reactor which will be considered for comparison in this investigation.

Table 4.1 : External contacting efficiency review

Author	Packing	d_p (cm)	d_r (cm)	ε_B	Method & System	Pressure	Approach
Ring and Missen, 1991	sphere	0.217	2.5	0.412	Tracer Organic	10 MPa	-----
Comments : No correlation was developed.							
Lazzaroni etal.,1988	sphere	0.24-0.34	3.05	---	Colorimetric Aqueous	atm	----
Comments : No correlation was developed. Only contacting efficiency has been measured.							
Ruecker et al.,1987	extrudate	0.16	1.9	---	Chemical Organic	5.2 MPa	----
$\eta_{CE} = 1.0 + 0.14\,\psi - 1.17\,\psi^2$, where ψ is the vapor-to-feed molar ratio							

Table 4.1 continued

Author	Packing	d_p (cm)	d_r (cm)	ε_B	Method & System	Pressure	Approach
ElHisnawi 1981	extrudate	0.1 to 0.2	1.9	0.35-0.43	Tracer Organic	atm	empirical

$\eta_{CE} = 1.617 \ \mathrm{Re}_L^{0.1461} \ Ga_L^{-0.0711}$, where $\mathrm{Re}_L = \dfrac{L\, d_p}{\mu_L}$ and $Ga_L = \dfrac{d_p^3\, g\, \rho_L^2}{\mu_L^2}$ (Form A)

$\eta_{CE} = 1.021 \ \omega_d^{0.224}$, where ω_d is dynamic liquid saturation (Form B)

Mills and Dudukovic 1981	pellet	20-25 mesh	1.9	0.37	Tracer Organic	atm	empirical

$$\eta_{CE} = 1 - Exp\left[-0.63\,\mathrm{Re}_L^{-1/3}\, Fr_L^{0.842}\, We_L^{0.448}\left(\frac{a_t\, d_p^2}{\varepsilon_B^2}\right)^{1.086}\right]$$

$$\eta_{CE} = \tanh\left[0.731\,\mathrm{Re}_L^{-1/3}\, Fr_L^{0.708}\, We_L^{-0.346}\left(\frac{a_t\, d_p^2}{\varepsilon_B^2}\right)^{0.924}\right]$$

Puranik and Vogelpohl 1974	different shapes	0.1-0.37	---	---	Physical Chemical Aq.&Org.	atm	empirical

$$\eta_{CE} = \left[1.05\,\mathrm{Re}_L^{0.047}\, We_L^{0.135}\left(\frac{\sigma_C}{\sigma_L}\right)^{0.206}\right]$$

$$\eta_{CE} = \left[1.045\,\mathrm{Re}_L^{0.041}\, We_L^{0.133}\left(\frac{\sigma_c}{\sigma_L}\right)^{0.182}\right]$$

Table 4.1 continued

Author	Packing	d_p (cm)	d_r (cm)	ε_B	Method & System	Pressure	Approach
Krauze and Serwinski 1971	rashing ring	0.5-1.7	---	---	Colorimetric	atm	empirical
$\eta_{CE} = 0.655\, L^{0.36}$,*low* L							
$\eta_{CE} = 0.655\, L^{0.36}$, *low* L							
$\eta_{CE} = 0.585\, L^{0.17}$, *high* L							
Onda et al.,1967	rashing ring sphere saddle	0.82-0.51	---	---	Colorimetric	atm	empirical
$\eta_{CE} = 1 - Exp\left[-1.45\, \mathrm{Re}_L^{0.1}\, Fr_L^{-0.05}\, We_L^{0.2} \left(\frac{\sigma_c}{\sigma_L}\right)^{0.75}\right]$							
Shulman et al.,1955	rashing ring saddle	1.27 - 3.8	---	---	dissolution naph. in aqueous	atm	empirical
$\eta_{CE} = 0.24\left(\frac{L}{G}\right)^{0.25}$, *rashing ring*							
$\eta_{CE} = 0.35\left(\frac{L}{G}\right)^{0.25}$, *saddle*							

4.2 PHENOMENOLOGICAL MODEL AND ANALYSIS

The flow pattern of the flowing liquid and gas in the trickle flow regime (gas continuous flow regime) is described as liquid flow in form of films and/or rivulets over the catalyst surface with gas phase flow in the center core. Trickle flow regime consists of partially externally wetted region at low liquid velocity and completely externally wetted particles at higher liquid velocity, as illustrated in Figure 4.1.

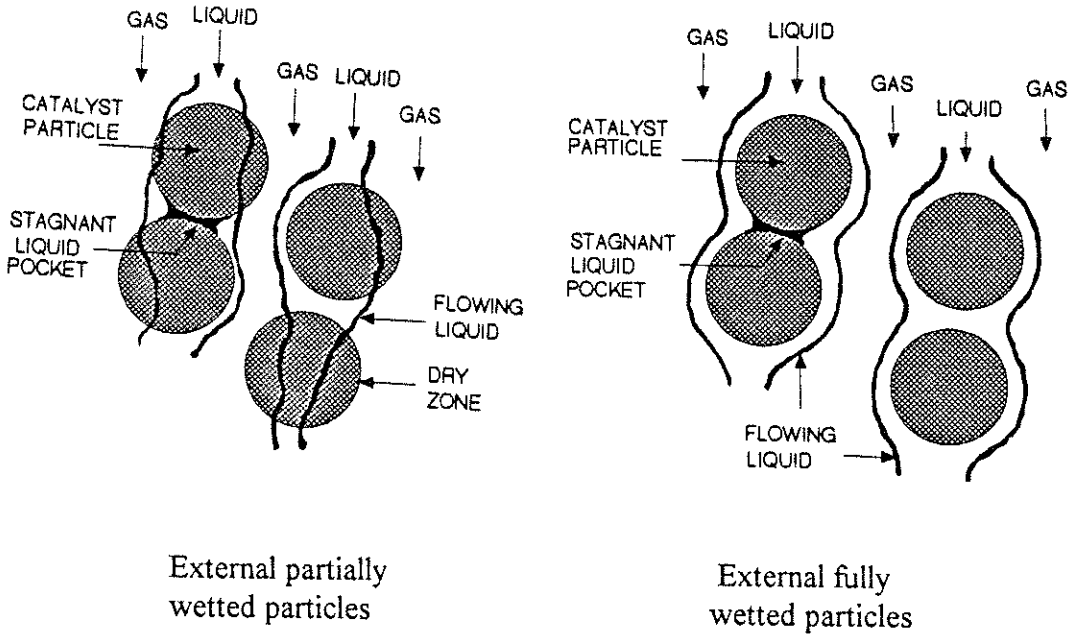

Figure 4.1 : Flow pattern of flowing liquid and gas in trickle flow regime for externally completely wetted and partially wetted particles

Due to the complexity of the flowing fluid field in trickle-bed reactors, a complete description of the hydrodynamics on the particle scale has not been yet accomplished. Such description is essential to understand the liquid-solid wetting phenomena. Accordingly, a phenomenological approach which relies on a simpler physical

representation of the phenomena is often useful and desirable in the absence of fundamental approaches. Based on Holub's (1990) simple representation of trickle flow regime (slit model) shown in Figure 3.2 , a phenomenological model and explanation of the effect of reactor pressure and gas flow rate on the external liquid-solid contacting efficiency can be developed.

It was found that the hydrodynamics of thin liquid films is directly related to processes that determine catalyst wetting (Dudukovic' and Mills, 1986). Hence,based on the slit model and assuming uniform porosity and liquid holdup over the packed bed, the mean thickness of the liquid film, δ , on the packing can be expressed as follows :

$$\delta = \left(\frac{total\ liquid\ holdup}{specific\ particles\ area\,(m^2_{particles}/m^3_{reactor})} \right) \tag{4.1}$$

$$\delta = \frac{\varepsilon_L}{\dfrac{6\,(1-\varepsilon_B)}{d_p}} \tag{4.2}$$

By substituting equation (3.9) into equation (4.2) and manipulating yield :

$$\delta = \left(\frac{d_p}{6}\right)\left(\frac{\varepsilon_B}{1-\varepsilon_B}\right)\left[\frac{E_1\,\mathrm{Re}_L + E_2\,\mathrm{Re}_L^2}{Ga_L\left(1+\dfrac{\Delta P/Z}{\rho_L\,g}\right)}\right]^{1/3} \tag{4.3}$$

Both liquid film thickness and liquid spreading determine liquid-solid contacting efficiency. Unfortunately, due to the complex geometry of the trickle-bed reactor, no fundamental model is available which quantitatively describes liquid spreading over external surface of porous packing in randomly packed beds to estimate liquid film thickness, film stability and wetting efficiency. Based on equation (4.3) the following mechanistic analysis can be deduced for a particular bed:

> *"As dimensionless pressure drop* $(\Delta P/Z)/\rho_L g$ *increases liquid holdup and liquid film thickness decreases. Hence, decreasing liquid film thickness and increasing the shear stress on the gas-liquid interface , by means of higher gas velocities or pressure , result in an improved spreading of the liquid film over the external packing area making them more wet . This causes the external liquid-solid contacting efficiency to increase. As liquid flow rate increases, both liquid holdup and pressure drop increase, which yield further improvement in the wetting efficiency"*

Recently Wammes (1990) and Larachi (1992) observed that at high pressure operation gas-liquid interfacial area increases. It becomes even larger as gas velocity increases.This confirms the spreading enhancement of the liquid over the external area of the catalyst which raises the contacting between gas-liquid and liquid-solid at conditions typical of industrial operations (high pressure).

In the absence of a fundamental relationship between the liquid film thickness and liquid-solid contacting efficiency , the following proportionality can be suggested based on the preceding discussion :

$$\eta_{CE} \propto \mathrm{Re}_L^n \left[\frac{1+\dfrac{\Delta P/Z}{\rho_L\, g}}{Ga_L} \right]^m \tag{4.4}$$

According to equation (4.4), and as discussed in chapter 3, the effect of reactor pressure and gas flow rate on liquid-solid contacting efficiency for a given bed and liquid phase can be described as follows :

Case 1 : (No gas flow)

Without gas flow, the contacting efficiency is minimal when the gravitational force, $\rho_L\, g$, is the only driving force for liquid flow.

Case 2 : (Low pressure , low gas superficial velocity)

At atmospheric to low pressure and at low gas superficial flow rate, the dimensionless pressure drop, $(\Delta P/Z)/\rho_L g$, is increased slightly (because of small increase in pressure drop) and liquid holdup is decreased a little compared to **case 1** of no gas flow. Hence, the contacting efficiency slightly increases, due to small improvement in liquid spreading over the catalyst particles. As liquid flow rate increases contacting efficiency increases due to the increase in both liquid holdup and pressure drop.

Case 3 : (Low pressure , high gas superficial velocity)

At atmospheric to low pressure and at high range of gas flow rates, dimensionless pressure drop increases and liquid holdup decreases compared to **case 2** (as demonstrated phenomenologically and experimentally in Chapter 3). This further improves the contacting efficiency by improving the spreading of the liquid over the catalyst particles. Moreover, the increase in pressure drop and liquid holdup at higher range of liquid flow rates further improves liquid-solid contacting efficiency.

Case 4 : (High pressure , low gas superficial velocity)

At high pressure and low gas flow rate, the gas density increases and the pressure gradient increases. It was found that such increase in pressure drop and decrease in liquid holdup compared to **case 2** is smaller than that of case 3 (Chapter 3). Therefore, contacting efficiency improves more than in **case 2** but less than in **case 3** due to improvement in liquid spreading over the catalyst particles in spite of reduced holdup. At higher liquid flow rates in this regime the wetting efficiency is enhanced by both increased liquid holdup and elevated pressure drop.

Case 5 : (High pressure , high gas superficial velocity)

At elevated pressure and high gas superficial velocity, the pressure drop increases significantly and liquid holdup decreases considerably compared to all previous cases (due to the effect of both gas density and velocity). The wetting of the particles improves noticeably because of further improvement in liquid spreading over the catalyst particles. This effect becomes significantly greater at high liquid flow rates when the dimensionless pressure drop increases considerably as well as liquid holdup.

According to the above analysis and based on equation (4.4), external liquid-solid contacting efficiency ,η_{CE} , should be best correlated in the following form

$$\eta_{CE} = c \ \mathrm{Re}_L^n \left[\frac{1 + \dfrac{\Delta P/Z}{\rho_L g}}{Ga_L} \right]^m \tag{4.5}$$

where c, m and n are evaluated by fitting the experimental data to equation (4.5). The effect of bed characteristics and physical properties are accounted for by the dimensionless pressure drop, Reynolds and Galileo numbers.

It is instructive to note that such a form without the $(1+ (\Delta P/Z)/\rho_L g)$ term and with Reynolds and Galileo numbers that did not include the bed voidage parameter as shown in Table 4.1 (Form A), was obtained at atmospheric pressure by El-Hisnawi (1981). The other form of El-Hisnawi's (1981) correlation (Form B, Table 4.1) which expresses contacting efficiency in terms of dynamic liquid saturation is not compatible with the phenomenological analysis discussed above.

4.3 EXPERIMENTAL INVESTIGATION

The details of the experimental facility used in this investigation have been discussed in Chapter 2.

4.3.1 External Liquid-Solid Contacting Efficiency Determination

Several experimental methods have been used to evaluate external liquid-solid contacting efficiency, η_{CE} , In general, they may be divided into two categories : (i) destructive methods and (ii) nondestructive methods. Destructive methods require a change in the nature of the bed or special choice of the flowing phase, or dismantling the bed. These methods have been mainly employed for evaluation of external contacting. Nondestructive methods rely on the dynamic tracer technique which is used also for evaluation of internal contacting and liquid holdup. Table 4.2 summarizes the methods used to determine contacting efficiency.

The tracer technique is chosen because it seems to be more promising in rapidly producing contacting information which is more representative of commercial processes than other destructive methods. It is also the only one that allows the determination of contacting efficiency in actual beds under operating conditions using catalyst packing and liquid of interests (Dudukovic′ and Mills, 1986; Van Klinken and Van Dongen, 1980). Sicardi et al. (1980) compared different experimental techniques and concluded that the best evaluation of the wetted areas of the catalyst is obtained by tracer methods.

Table 4.2 : Methods used to evaluate the external contacting efficiency

Method	Investigator	System Used
I - Destructive		
1 - Dissolution of nonreactive synthetic packing	* Shulman et al., 1955 * Lakota and Levec, 1990	Naphthalene in water
$\eta_{CE} = \left[\frac{(k_s a_{Ls})_{TF}}{(k_s a_{Ls})_{LF}}\right]$		
2 - Dissolution of synthetic packing with a reacting buffer solution	* Specchia et al., 1978	Phthalic anhydride in $KHCO_3$-K_2CO_3 solution
$(k_s a_s)_c = \sqrt{(k_s a_s)_p^2 + a_s^2 D k_1}$, where c and p represent chemical and physical coefficients.		
3 - Colorimetric	* Lazzaroni et al., 1988 * Onda et al., 1967 * Krauze and Serwinski, 1971	Direct measurement of the colored area
4 - Chemical reaction	* Satterfield, 1975 * Sedrik and Kenny, 1973 * Herskowitz, 1979	Hydrodesulfurizatio Hydrogenation, Ethanol Oxidation, SO_2 Oxidation
$\eta_{CE} = \frac{(k_{app})_{Trickle-Bed}}{(k_r)_{Complete\ wetting}}$		
$\bar{r}_r = f\,\bar{r}_L + (1-f)\,\bar{r}_G$, where $\bar{r}_r$ is overall reaction rate, $\bar{r}_L$ is wet area reaction rate, $\bar{r}_G$ is dry area reaction rate, f is fraction of wetting.		

Table 4.2 : continued

Method	Investigator	System Used
II - Nondestructive		
1. By measuring the volume of the stagnant liquid	* Wijffels et a., 1974	By expelling the stagnant pockets of solution by a known volume of liquid.
2. Tracer-based method	* Colombo et al., 1976 * Schwartz et al., 1976 * Mills, 1978 * Mills and Dudukovic', 1981, 1982 * El-Hisnawi, 1981	Adsorbing and nonadsorbing tracer in liquid hydrocarbons

$\eta_{CE} = \frac{(De)_{TF}}{(De)_{LF}}$, Introduced by Colombo (1976) which was found not to be recommended.

$\eta_{CE} = \sqrt{\frac{(De)_{TF}}{(De)_{LF}}}$, It is a recommended form (Ramachandran et al., 1987, 1986; Mills and Dudukovic', 1986)

Schwartz et al. (1976) and Colombo et al. (1976) introduced the tracer-based methods to evaluate both internal and external contacting efficiency. The evaluation of these parameters is based on the method of moments. Mills and Dudukovic' (1981,1982) and El-Hisnawi et al. (1981,1982) confirmed the validity of this method. In tracer-based methods, an impulse of nonabsorbent tracer is injected into the liquid at the inlet of trickle-bed reactor and the impulse response is monitored at the outlet. The first moment, μ_1 , the second moment, μ_2, and the variance, σ^2, of the normalized bed impulse response , E(t), are then calculated numerically, from their defining equations :

$$E(t) = \frac{C(t)}{\int_0^\infty C(t)\,dt} = \frac{R(t)}{\int_0^\infty R(t)\,dt} \tag{4.6}$$

where $C(t)$ is tracer concentration at time t, while $R(t)$ is a quantity proportional to it at time t.

$$\mu_1 = \int_0^\infty t\,E(t)\,dt \tag{4.7}$$

$$\mu_2 = \int_0^\infty t^2\,E(t)\,dt \tag{4.8}$$

$$\sigma^2 = \frac{\int_0^\infty (t-\mu_1)^2\,E(t)\,dt}{\int_0^\infty E(t)\,dt} = \mu_2 - \mu_1^2 \tag{4.9}$$

The calculated values of the first moment and variance can be utilized to evaluate liquid holdup and effective diffusivity of the tracer, respectively. Based on the central volume principle, the expressions needed to determine the effective diffusivity for two phase flow and liquid-filled operation modes, which are required to evaluate external contacting efficiency, were developed and reported by Mills (1978), El-Hisnawi (1981), Dudukovic' and Mills (1981,1986). Tables 4.3 and 4.4 summarize the first moments and variance expressions for extrudate and spherical porous catalysts for nonvolatile and nonadsorbing tracers. These expressions were developed based on the following assumptions: (1) isothermal trickle-bed reactor; (2) backmixing in the liquid phase is adequately described by the axial dispersion model; (3) nonvolatility of the liquid phase; (4) tracer is injected in the liquid phase only; (5) linear adsorption isotherm of the tracer in the catalyst pores; (6) complete internal wetting of the catalyst pores due to capillary effects. Mills (1978) and El-Hisnawi (1981) are referred to for detailed derivations of these expressions. However, in the tracer method (unsteady state behavior) it is not possible to define a characteristic length dimension for the catalyst particles such as equivalent diameter, which enables different porous particles shapes to be treated as

equivalent spheres as in the case of steady state behavior. This is because the volume of the particle as well as the accessibility of its interior are not rendered equivalent. Accordingly, the expression for the variance is expected to be different for different shapes of porous particles as shown in Tables 4.3 and 4.4 for cylindrical extrudates and spheres, respectively. Based on El-Hisnawi findings for cylindrical porous extrudates the assumption of considering them to be infinite cylinders (cylinder in which the diffusion throughout their ends are negligible as if their ends are sealed) is applied. Therefore, the expression for the moments for an infinite cylinder (which is much simpler than that for a finite cylinder) can be implemented to estimate liquid-solid contacting efficiency in the bed of porous extrudates as shown in Table 4.3 (El-Hisnawi, 1981). Moment expressions require liquid-solid mass transfer coefficient, k_s, and Peclet number, Pe_L, to be evaluated. In liquid-filled operation, it was found that the effect of k_s on σ^2 vanishes with an increase in liquid flow rate, while the effect of Pe_L is negligible at moderate to high liquid flow rate (El-Hisnawi, 1981). Hence, $(De)_{LF}$, can be evaluated at flow rate of interest without the use of any correlation for k_s and Pe_L. This can be achieved by estimating the dimensionless variance, σ_D^2 , at different flow rate. Plotting σ_D^2 versus volumetric flow rate yields a straight line . By utilizing the expression of the slope of such a line, shown in Tables 4.3 and 4.4, $(De)_{LF}$ for a particular bed of particles can be obtained. In two phase flow El-Hisnawi (1981) found that the effect of k_s and Pe_L is less pronounced compared to liquid-filled operation and can be neglected. Therefore, σ_D^2 expression can be simplified further (Tables 4.3 and 4.4) to evaluate $(De)_{TF}$ in two phase flow experiments.

Upon evaluating effective diffusivity, external contacting efficiency, η_{CE}, can then be estimated by comparing the effective diffusivity in two phase flow mode, $(De)_{TF}$, to that in liquid-filled mode, $(De)_{LF}$, as follows (Dudukovic' and Mills, 1986; Ramachandran et al., 1987, 1986; El-Hisnawi , 1981; Mills, 1978).

$$\eta_{CE} = \sqrt{\frac{(De)_{TF}}{(De)_{LF}}} \tag{4.10}$$

The obtained impulse response signal and hence the moments (μ_1 and σ^2) in both two phase flow and liquid-filled experiments represent together the packed bed and system externals to the bed (e.g. tubes, fittings, reactor head and bottom, connectors, valves,etc.). Therefore it is required to evaluate the moments of the bed only. This is achieved by performing liquid-filled and two phase flow experiments without the catalyst bed (i.e. only system externals) at various liquid flow rate. It was found that gas velocity and density (reactor pressure) has a negligible effect on the moments of the externals. Therefore, the first moment, μ_1, correlated linearly with the inverse of liquid volumetric flow rate based on central volume principle, while the variance is best correlated with the volumetric flow rate in power law form, $\sigma^2 \propto Q^{-c}$, (El-Hisnawi,1981). Hence, μ_1 and σ^2 of externals can be evaluated at the same liquid flow rates at which overall system experiments (bed and externals) are conducted. By subtracting the values of the moments of the externals from that of the overall system, the moments of only the packed bed can be determined (Dudukovic' and Felder , 1983 ; Levenspiel, 1986).

In liquid-filled mode smaller volume of reactor head than that of two phase flow is utilized, as shown in Figure 2.4c. This was found in this work, as well as by El-Hisnawi (1981), to produce a better response signal . Pressure drop and liquid holdup are measured as discussed in Chapter 3. The same experimental step by step procedure as discussed in Section 3.4.1 and Appendix 7.2 is followed.

Differential Refractometer (Water 410), DR, is used in liquid-filled operation to monitor the tracer concentration at the exit stream of the reactor. A tracer loop of (1 ml) volume is used which generates suitable response in the DR voltage signal to be within the range of the utilized signal conditioning module to convert (0-281 mV) into (0-10 V) as discussed in Section 2.5. As an example, Figure 4.2a illustrates a typical

DR voltage output, while Figure 4.2b displays the normalized impulse response curve, $E(t)$.

Unfortunately, DR did not operate properly with two phase flow mode at moderate to high pressure. This is because more gas is dissolved in the solvent at high pressure operation and the bubbles evolve in the DR sampling cell make its signal meaningless. Therefore Gas Chromatograph , GC, is utilized in two phase flow mode to measure heptane (tracer) concentration in hexane (solvent) at the reactor output. A GC column of 20% SP2100 / 0.1% Carbowax was used for hexane/heptane analysis. In this case samples are drawn manually from a fine needle valve in interval of (10 sec.) which increases to (20-30 sec.) in the tail region to ensure that the response returns back to the base line (for two phase flow experiments to evaluate the moments of externals, a 5 second sampling interval was utilized). 3 ml loop was found suitable for GC measurements. Separate experiments were conducted which verified that the same $E(t)$ curve was obtained with 1 ml and 3 ml loops. Figures 4.3a and 4.3b show the GC output and its $E(t)$curve, respectively. Computer programs have been developed to process the data, numerical computations, linear and nonlinear fitting, etc.. These programs are available in computer disk at Chemical Reaction Engineering Laboratory, CREL.

Table 4.3 : Expressions for the moments of infinite cylinder catalyst for a nonvolatile and nonadsorbing tracer (El-Hisnawi, 1981)

Theoretical Expressions

$$\sigma_D^2 = \frac{\sigma^2}{2\mu_1^2}$$

For porous catalyst ,

$\varepsilon_L = \varepsilon_{Lt} - \varepsilon_{Li}$; $\varepsilon_{Li} = f_i\left(1-\varepsilon_B\right)\varepsilon_p$, where $f_i = 1$ due to capillary effect ;

$\varepsilon_L = \varepsilon_{Ls} + \varepsilon_{Ld}$

I - Liquid-Filled Operation

$\varepsilon_L = \varepsilon_B$

$$\mu_1 = \frac{V_r\,\varepsilon_B}{Q_L}\left[1+\frac{S_{ex}\,r_p}{2V_p}\left(\frac{1-\varepsilon_B}{\varepsilon_B}\right)\varepsilon_p\right]$$

$$\sigma^2 = \mu_1^2\,\delta_0 + \frac{V_r}{Q_L}\,\varepsilon_P\,\frac{S_{ex}\,r_p}{2V_p}\left(1-\varepsilon_B\right)\frac{r_p^2\,\varepsilon_p}{4}\left[\frac{1}{(De)_{LF}}+\frac{4}{k_{Ls}\,r_p}\right]$$

where, $\delta_0 = 2\left[\frac{1}{Pe_L} - \frac{1}{Pe_L^2}\left(1-e^{-Pe_L}\right)\right]$

$$\sigma_D^2 = \frac{\delta_0}{2} + \frac{\left(\mu_1 - \frac{V_r\,\varepsilon_B}{Q_L}\right)\frac{r_p^2\,\varepsilon_p}{8}\left[\frac{1}{(De)_{LF}}+\frac{4}{k_{Ls}\,r_p}\right]}{\mu_1^2}$$

By substituting μ_1 into σ_D^2 expression results in a linear relationship between σ_D^2 and Q_L with slope equal to the following expression (k_{Ls} and Pe_L terms appears in the expression for the intercept):

$$slope = \frac{\frac{S_{ex}\,r_p}{2V_p}\left(\frac{1-\varepsilon_B}{\varepsilon_B}\right)\frac{r_p^2\,\varepsilon_p^2}{8\,(De)_{LF}}}{V_r\,\varepsilon_B\left[1+\frac{S_{ex}\,r_p}{2V_p}\left(\frac{1-\varepsilon_B}{\varepsilon_B}\right)\varepsilon_p\right]^2}$$

Table 4.3 : continued

Theoretical Expressions

II - Two phase flow operation

$$\mu_1 = \frac{V_r}{Q_L}\,\varepsilon_L$$

$$\mu_1 = \frac{V_r\,\varepsilon_L}{Q_L}\left[1 + \frac{S_{ex}\,r_p}{2V_p}\left(\frac{1-\varepsilon_B}{\varepsilon_L}\right)\,\varepsilon_p\right]$$

$$\sigma^2 = \mu_1^2\,\delta_0 + \frac{V_r}{Q_L}\,\varepsilon_P\,\frac{S_{ex}\,r_p}{2V_p}\,(1-\varepsilon_B)\,\frac{r_p^2\,\varepsilon_p}{4}\left[\frac{1}{(De)_{TF}} + \frac{4}{k_{Ls}\,r_p}\right]$$

$$\sigma_D^2 = \frac{\delta_0}{2} + \frac{\left(\mu_1 - \frac{V_r\,\varepsilon_L}{Q_L}\right)\frac{r_p^2\,\varepsilon_p}{8}\left[\frac{1}{(De)_{TF}} + \frac{4}{k_{Ls}\,r_p}\right]}{\mu_1^2}$$

By neglecting k_{Ls} and Pe_L , and substituting for μ_1 dimensionless variance expression becomes :

$$\sigma_D^2 = \frac{\left\{\left(\frac{V_r\,\varepsilon_L}{Q_L}\left[1 + \frac{S_{ex}\,r_p}{2V_p}\left(\frac{(1-\varepsilon_B)\,\varepsilon_p}{\varepsilon_L}\right)\right]\right) - \frac{V_r\,\varepsilon_L}{Q_L}\right\}\frac{r_p^2\,\varepsilon_p}{8\,(De)_{TF}}}{\left(\frac{V_r\,\varepsilon_L}{Q_L}\left[1 + \frac{S_{ex}\,r_p}{2V_p}\left(\frac{(1-\varepsilon_B)\,\varepsilon_p}{\varepsilon_L}\right)\right]\right)^2}$$

Table 4.4 : Expressions for the moments of spherical particles for a nonvolatile and nonadsorbing tracer (Mills and Dudukovic',1981)

Theoretical Expressions

$$\sigma_D^2 = \frac{\sigma^2}{2\mu_1^2}$$

For porous catalyst ,

$\varepsilon_L = \varepsilon_{Lt} - \varepsilon_{Li}$; $\varepsilon_{Li} = f_i\left(1-\varepsilon_B\right)\varepsilon_p$, where $f_i = 1$ due to capillary effect ;

$\varepsilon_L = \varepsilon_{Ls} + \varepsilon_{Ld}$

I - Liquid-Filled Operation

$$\varepsilon_L = \varepsilon_B$$

$$\sigma_D^2 = \frac{1}{Pe_L} + \frac{Q_L}{V_r\,\varepsilon_B}\,\frac{\delta_1}{\left(1+\delta_2\right)^2}$$

where , $\delta_1 = \delta_i + \delta_e$

$$\delta_i = \frac{\left(1-\varepsilon_B\right)\varepsilon_p}{\varepsilon_B}\;\frac{r_p^2\,\varepsilon_p}{15\,(De)_{LF}}$$

$$\delta_e = \frac{\left(1-\varepsilon_B\right)\varepsilon_p}{\varepsilon_B}\;\frac{r_p^2\,\varepsilon_p}{15}\;\frac{5}{k_{Ls}\,r_p}$$

$$\delta_2 = \frac{\left(1-\varepsilon_B\right)\varepsilon_p}{\varepsilon_B}$$

Plotting σ_D^2 versus Q_L yields a straight line with a slope equal to the following expression (k_{Ls} and Pe_L terms appears in the expression for the intercept) :

$$slope = \frac{\dfrac{\left(1-\varepsilon_B\right)\varepsilon_p^2}{\varepsilon_B}\;\dfrac{r_p^2}{15\,(De)_{LF}}}{V_r\,\varepsilon_B\left[1+\dfrac{\left(1-\varepsilon_B\right)\varepsilon_p}{\varepsilon_B}\right]^2}$$

Table 4.4 : continued

Theoretical Expressions

II - Two phase flow operation

$$\mu_1 = \frac{V_r}{Q_L}\,\varepsilon_L$$

$$\sigma_D^2 = \frac{1}{Pe_L} + \frac{Q_L}{V_r\,\varepsilon_L}\,\frac{\delta_1}{(1+\delta_2)^2}$$

where , $\delta_1 = \delta_i + \delta_e$

$$\delta_i = \frac{(1-\varepsilon_B)\,\varepsilon_p}{\varepsilon_L}\;\frac{r_p^2\,\varepsilon_p}{15\,(De)_{LF}}$$

$$\delta_e = \frac{(1-\varepsilon_B)\,\varepsilon_p}{\varepsilon_L}\;\frac{r_p^2\,\varepsilon_p}{15}\;\frac{5}{k_{Ls}\,r_p}$$

$$\delta_2 = \frac{(1-\varepsilon_B)\,\varepsilon_p}{\varepsilon_L}$$

By neglecting k_{Ls} and Pe_L , dimensionless variance expression becomes :

$$\sigma_D^2 = \frac{Q_L}{V_r\,\varepsilon_L}\;\frac{\dfrac{(1-\varepsilon_B)\,\varepsilon_p}{\varepsilon_L}\left(\dfrac{r_p^2\,\varepsilon_p}{15\,(De)_{TF}}\right)}{\left[1+\dfrac{(1-\varepsilon_B)\,\varepsilon_p}{\varepsilon_L}\right]^2}$$

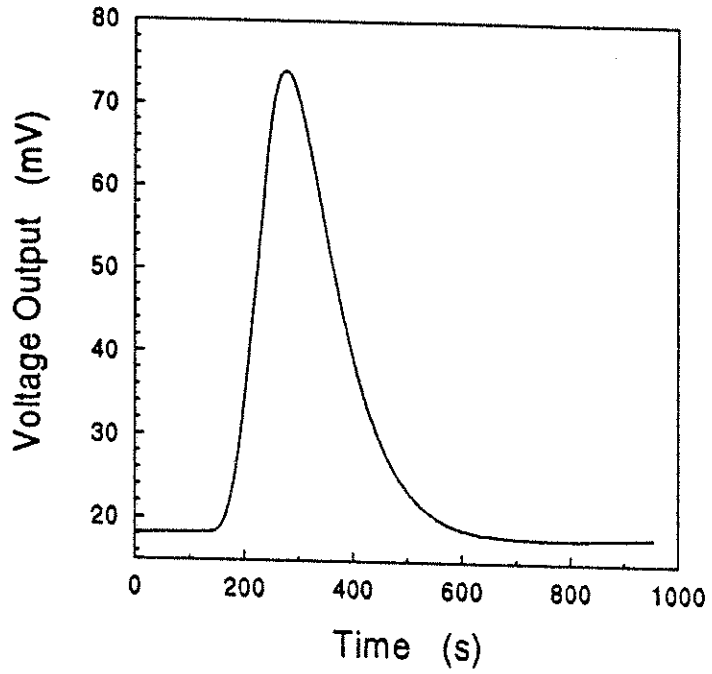

(a)

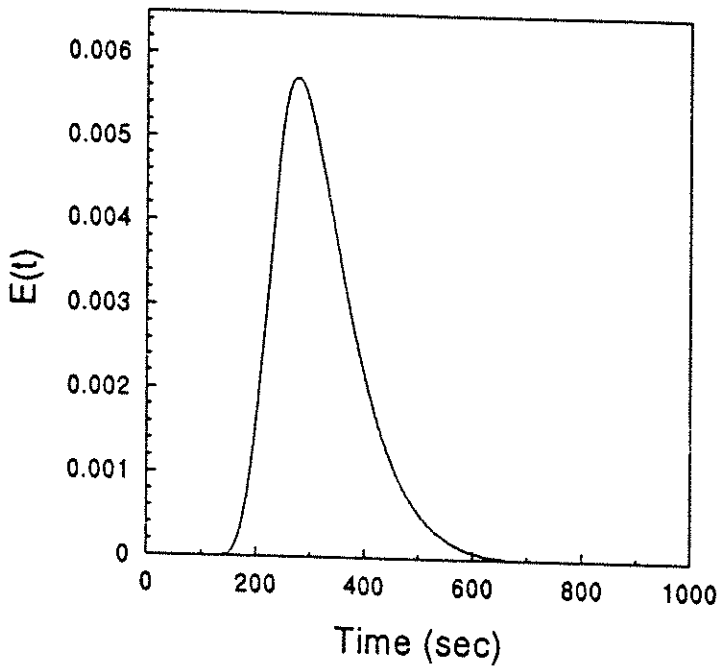

(b)

Figure 4.2 : (a) Typical differential refractometer voltage output in liquid-filled operation. Bed : silica shell sphere; L = 1.306 (kg/m^2 s). (b) Normalized curve E(t) of the response in (a)

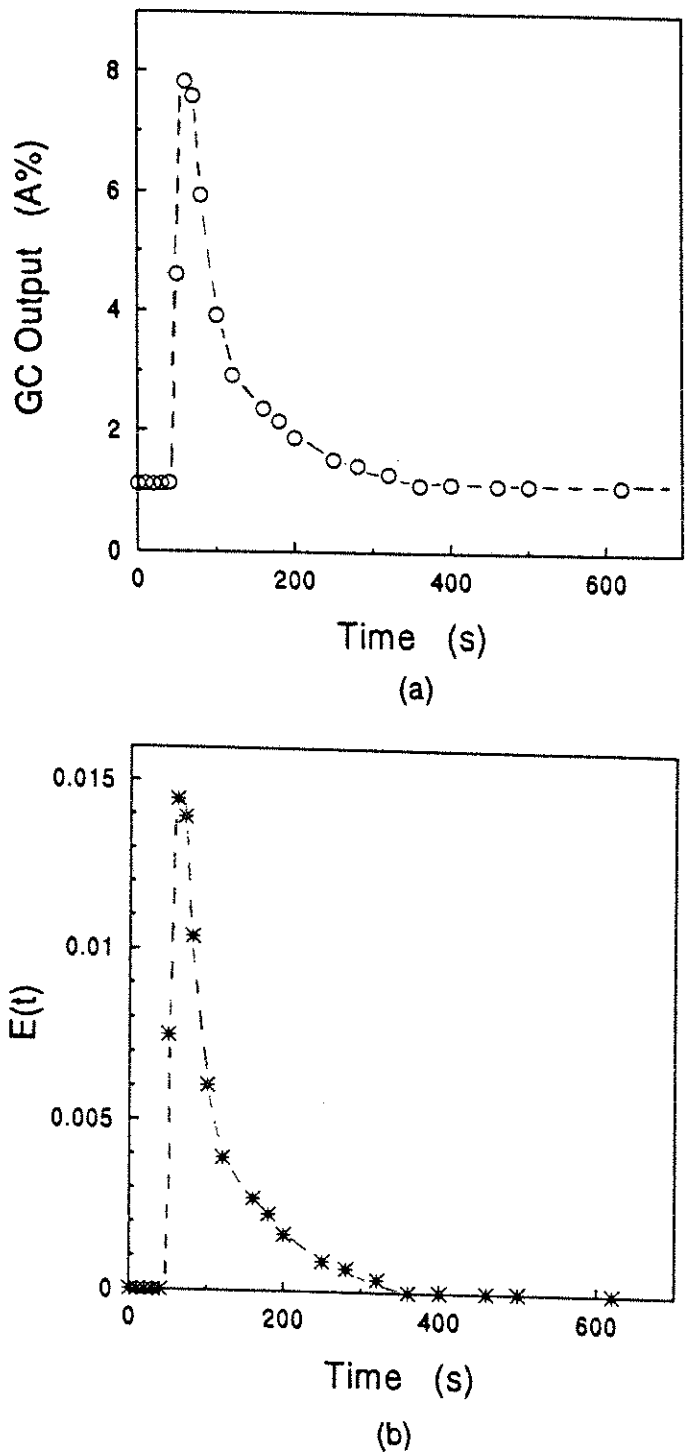

Figure 4.3 : (a) Typical GC output in two-phase flow operation. Pressure = 0.31 MPa (30 psig); U_G = 1 cm/s; L = 1.777 (kg/m^2 s). (b) Normalized curve E(t) of the response in (a)

4.3.2 Operating Conditions Investigated

Trickle flow regime is the flow condition of interest for external liquid-solid contacting efficiency investigation. The region of the experiments is within the trickle flow regime shown in Figure 3.4 on the flow map of Fukushima and Kusaka (1977). Visual observation through acrylic window and stable pressure drop measurements also confirm that the flow regime is trickle flow .

The selection of the system to be used in the this study is based on earlier studies by Mills (1978), El-Hisnawi (1981), Mills and Dudukovic' (1981), Schwartz et al. (1976) and Hanratty (1988). Thus, the hydrocarbon solvent is selected to be hexane. In order to remove traces of water , sulfur and other strongly adsorbing compounds, commercial grade hexane is passed over activated bed of F-1 porous alumina. This catalyst is activated at 140 C° in presence of dry nitrogen by using high temperature stainless steel packed bed reactor set-up (This set-up was rebuilt for such purpose). The selected tracer compound which gives the desired nonvolatile and nonadsorbing characteristics is high purity *n*-heptane . Nitrogen is used as the gas phase since it has low solubility in liquid hydrocarbons and is more dense, hence the effect of pressure is more pronounced. Physical properties of solvent hexane and nitrogen were listed previously in Table 3.4. The range of reactor pressure, liquid and gas superficial velocities covered in this investigation are listed in Table 4.5, while the packing bed characteristics utilized are shown in Table 4.6.

Table 4.5 : Range of covered operating conditions

Condition	Covered Range
Reactor pressure, MPa	$0.31 \leq P \leq 5.0$
Psig	$30 \leq P \leq 700$
Gas superficial velocity , cm/s	$1 \leq U_G \leq 8.75$
Gas superficial mass velocity, kg/m^2 s	$6.64 \times 10^{-3} \leq G \leq 4.03$
Liquid superficial flow rate, ml/min	$15 \leq Q_L \leq 93$
Liquid superficial mass flow rate, kg/m^2 s	$0.42 \leq L \leq 2.7$
Temperature , K	≈ 298

Table 4.6 : Packed bed characteristics

Reactor / Packing	Characteristics
<u>Reactor</u>	
Acrylic window reactor	d_r = 2.22 cm ; Length = 57.23 cm
Stainless steel reactor	d_r = 2.19 cm ; Length = 57.31 cm
<u>Packing</u>	
0.5% Pd on Alumina - Stainless steel reactor	Type : Porous extrudate; size = 0.157 cm x 4.3 cm; $(d_p)_{eq}$ = 0.199 cm ; d_r/d_p= 11; Bed length (Z) = 51.61cm ; ε_B= 0.355 ; ε_p= 0.599 ; ρ_p = 1.189 gm/cm^3
Silica Shell - Acrylic window reactor	Type : Porous sphere ; d_p= 0.152 cm; d_r/d_p= 14.6; Bed length (Z) = 51.63 cm ; ε_B = 0.412; ε_p= 0.697; ρ_p = 0.697 gm/cm^3

4.3.3 Results and Data Analysis

As discussed earlier, liquid-filled operation is required to determine the liquid-filled effective diffusivity, $(De)_{LF}$, of *n*-heptane tracer . Figure 4.4 illustrates the first absolute moment, μ_1, of extrudate and spherical particles bed versus the reciprocal liquid volumetric flow rate, Q_L^{-1}. The linear relationship indicate that the tracer-based method agrees with the central volume principle (Mills and Dudukovic', 1981; El-Hisnawi, 1981; Danckwerts, 1953). The experimental results for the variance for the extrudate and spherical catalyst are shown in Figure 4.5. In order to evaluate $(De)_{LF}$ of these particles according to Tables 4.3 and 4.4, the slope of the linear relationship between dimensionless variance , σ_D^2, and volumetric flow rate as presented in Figure 4.6 is calculated. Table 4.7 demonstrates the liquid-filled effective diffusivities , the fitted lines equation of Figures 4.4 - 4.6.

Table 4.7 : Liquid-filled effective diffusivities and the bed moments

Parameter	Extrudate Bed	Spherical Bed
$(De)_{LF}$, cm^2/s	17.49×10^{-6}	14.82×10^{-6}
μ_1 , s (Figure 4.4)	$\mu_1 = 154.476\ (1/Q_L)$	$\mu_1 = 170.5\ (1/Q_L)$
σ^2 , s^2 (Figure 4.5)	$\sigma^2 = 5566.677\ (Q_L)^{-1.0665}$	$\sigma^2 = 3675.82\ (Q_L)^{-1.4804}$
σ^2_D (Figure 4.6)	$\sigma^2_D = 0.09408\ Q_L + 0.013$	$\sigma^2_D = 0.055017\ Q_L + 0.017$

The two phase flow effective diffusivity ,$(De)_{TF}$, of *n*-heptane tracer was extracted from the dimensionless variance, σ_D^2 , of the response in each two phase flow experiment. The square root of the ratio of two phase flow effective diffusivity to liquid filled effective diffusivity was taken as a measure of the external liquid-solid contacting efficiency (equation 4.10)

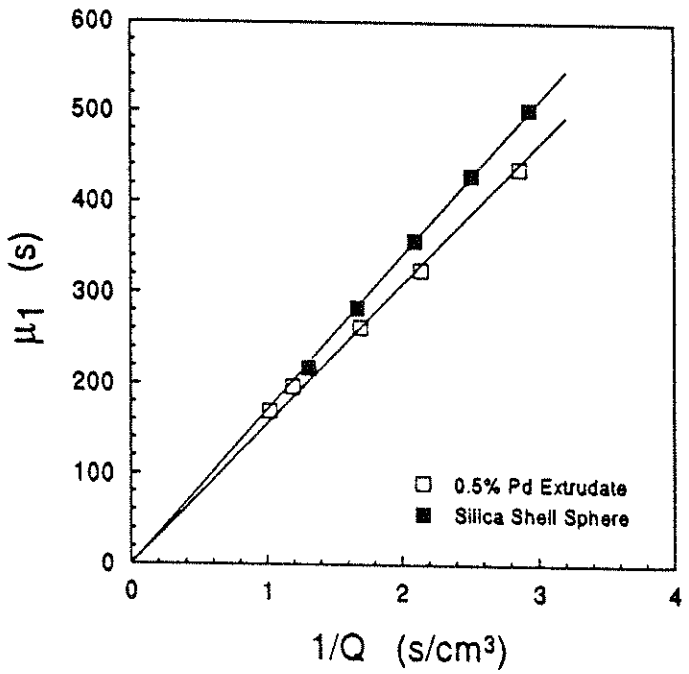

Figure 4.4 : Bed first moments for extrudate and spherical catalyst in liquid-filled operation

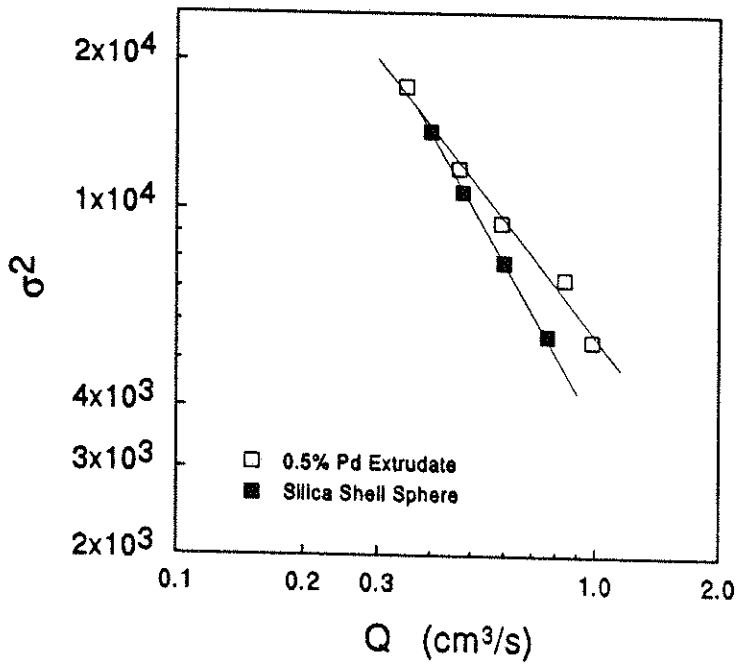

Figure 4.5 : Bed variance for extrudate and spherical catalyst in liquid-filled operation

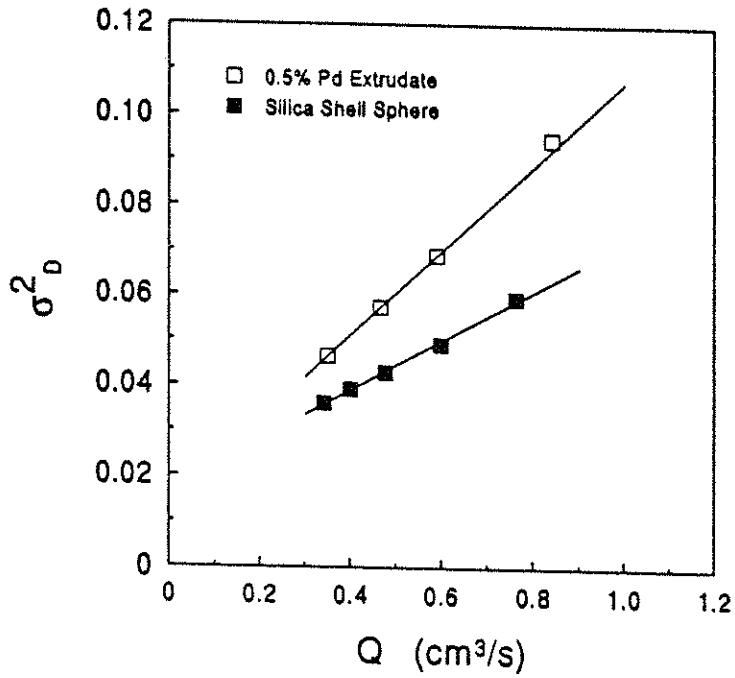

Figure 4.6 : Bed dimensionless variance for extrudate and spherical catalyst in liquid-filled operation

I. The Effect of High Pressure and Gas Flow Rate on Contacting Efficiency

The effect of reactor pressure and gas flow rate on liquid-solid contacting efficiency is consistent with the expectation deduced from the phenomenological analysis (Section 4.2). Examination of the results is presented in Figure 4.7 and 4.8 for extrudate and spherical catalyst, respectively, indicate that at low pressure and low gas superficial velocity, the effect of reactor pressure is small (case 2). As gas flow rate increases , the contacting efficiency increases (case 3) where the pressure drop increases (Figure 4.7b and 4.8b). But at elevated pressure and low gas flow rate (case 4), the pressure increases slightly. Therefore , the wetting efficiency increases only a little as a result. The effect of high pressure and high gas flow rate (case 5) is more pronounced on the contacting efficiency as well as on the pressure drop. In this case the contacting efficiency increases noticeably. Moreover, higher reactor pressure than that utilized in this study yields larger influence on liquid-solid contacting efficiency than that shown in Figures 4.7a and 4.8a. The contacting efficiency at 3.55 MPa (500 psig) and gas velocity equal to 8.75 cm/s is higher than that measured at 4.93 MPa (700 psig) and gas velocity equal to 7.2 cm/s because, the effect of gas flow is more pronounced on the contacting efficiency at high pressure as demonstrated in Figures 4.7a and 4.8a.. A comparison between different bed characteristics was examined as shown in Figure 4.9. The results indicate that the contacting efficiency in the spherical bed (d_p=0.152 cm) is larger than that in extrudate bed ($(d_p)_{eq}$=0.199 cm). This is consistent with pressure drop measurements which is larger in the spherical catalyst bed where the particles diameter is smaller than that of extrudate.

A comparison of the data for contacting efficiency obtained in this study at low pressure with some data obtained by El-Hisnawi (1981) at atmospheric pressure and the prediction of his correlation are shown in Figure 4.10. This comparison reveals that the

two data sets for about the same equivalent particles diameter and same solvent are close. However, El-Hisnawi's correlation, as shown in Table 4.1 (Form A), predicts higher values than both sets of data presented in Figure 4.10 but within the error margin of the correlation prediction. It is clear that this set of data has a higher slope with respect to Reynolds number than indicated by El-Hisnawi's correlation. However, El-Hisnawi's correlation correlates well other sets of data taken at atmospheric pressure so that all the data fall within the ± 10% margin (El-Hisnawi, 1981).

Accordingly, the data of this study confirm the mechanistic analysis which indicates that high pressure operation improves liquid-solid contacting efficiency. Although liquid holdup decreases at high pressure operation, contacting efficiency improves due to the improved spreading of the liquid film over more external particle surface. As liquid flow rate increases, liquid holdup and pressure drop increase. Hence, contacting efficiency improves further.

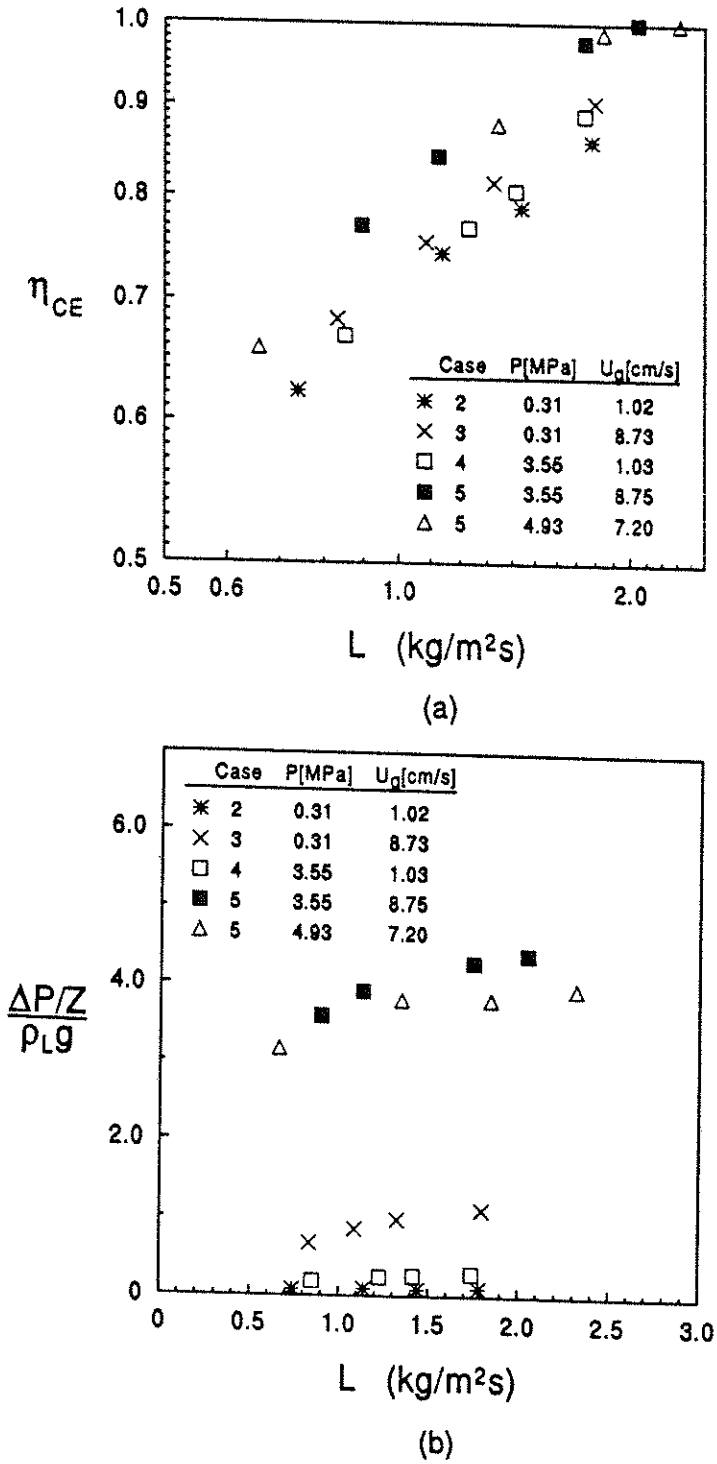

Figure 4.7 : Effect of high pressure and gas flow rate on liquid-solid contacting efficiency and pressure drop in extrudate bed. Solvent : hexane;tracer: heptane; gas : nitrogen; $(d_p)_{eq}$ (extrudate) = 0.199 cm

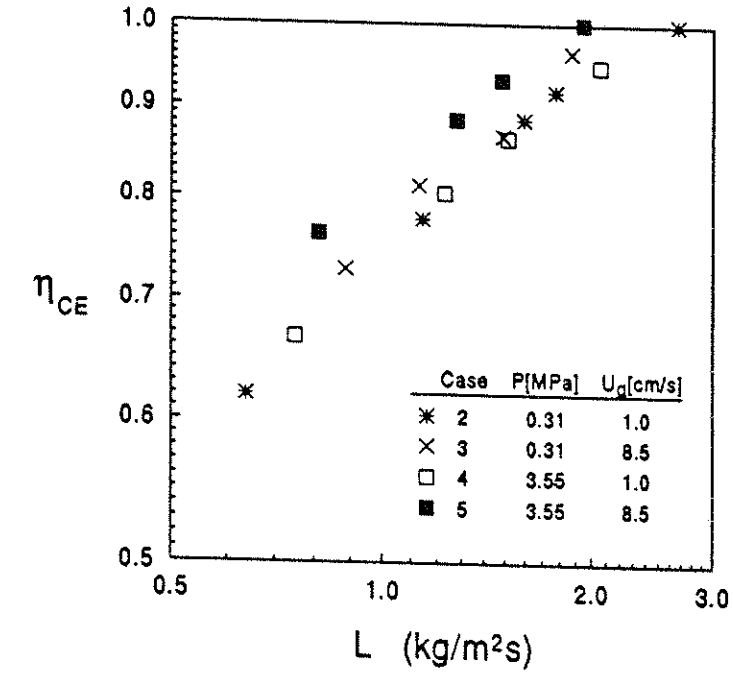

(a)

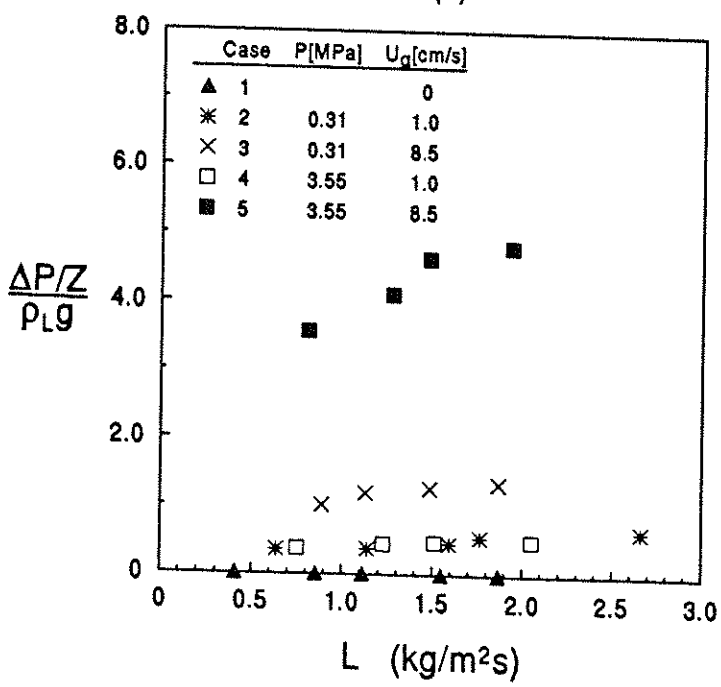

(b)

Figure 4.8 : Effect of high pressure and gas flow rate on liquid-solid contacting efficiency and pressure drop in spherical bed. Solvent : hexane; tracer: heptane; gas : nitrogen; d_p (sphere) = 0.152 cm

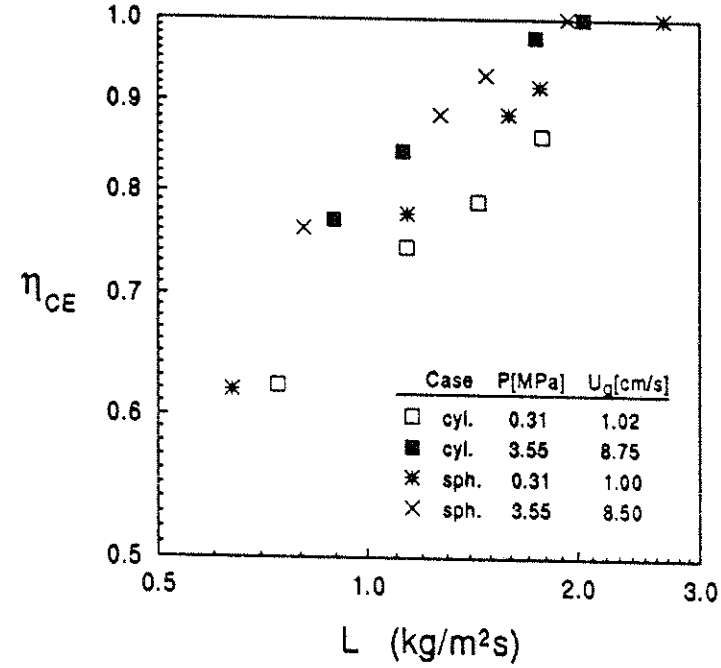

(a)

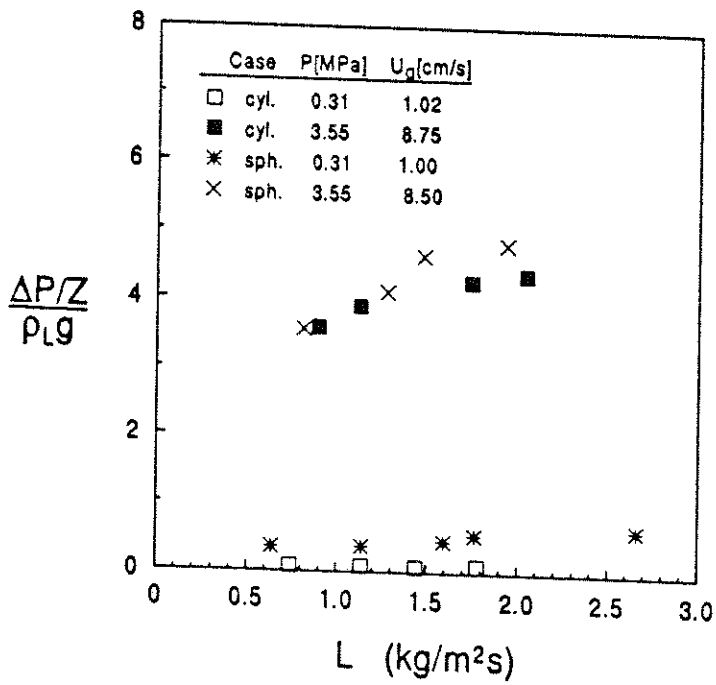

(b)

Figure 4.9 : Comparison between the contacting efficiency in extrudate and spherical beds. Solvent : hexane; tracer : heptane; gas : nitrogen; $(d_p)_{eq}$ (extrudate) = 0.199 cm; d_p (sphere) = 0.152 cm

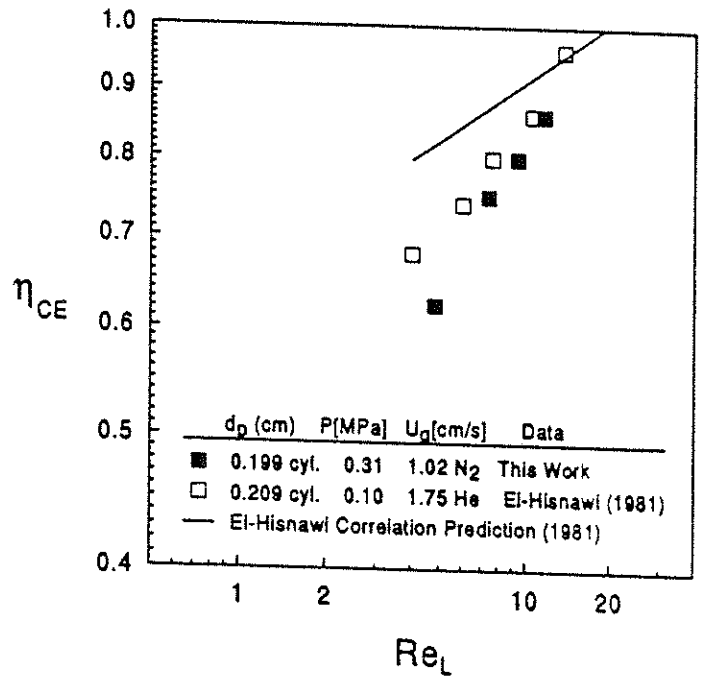

Figure 4.10 : Comparison between the data of this work obtained at low pressure and El-Hisnawi's data obtained at atmospheric pressure. This work data : solvent : hexane ; tracer : heptane , El-Hisnawi's data : solvent : hexane ; tracer : pentane

II - The Developed Model

The liquid-solid contacting efficiency data obtained in this study is used to develop the phenomenological model to predict it at high pressure operation. The result of a nonlinear regression analysis according to equation (4.5) yields the following model:

$$\eta_{CE} = 1.104 \ \mathrm{Re}_L^{1/3} \left[\frac{1 + \dfrac{\Delta P / Z}{\rho_L g}}{Ga_L} \right]^{1/9} \tag{4.11}$$

where $\mathrm{Re}_L = \dfrac{U_L \, \rho_L \, d_p}{\mu_L \, (1 - \varepsilon_B)}$ and $Ga_L = \dfrac{d_p^3 \, \rho_L^2 \, g \, \varepsilon_B^3}{\mu_L^2 \, (1 - \varepsilon_B)^3}$

The mean relative error of this model prediction is 3.7%. A comparison between experimental and predicted liquid-solid contacting efficiency is presented in Figure 4.11. The data are bounded by $\pm$ 10% . Moreover, the developed model predicts properly the trend of the reactor pressure effect and gas flow rate on the contacting efficiency as illustrated in Figure 4.12.

The mean relative error of the developed model prediction to some of El-Hisnawi's data (1981) is 20%. In such evaluation the dimensionless pressure drop term of the developed model is neglected, since El-Hisnawi did not measure the pressure drop across the bed. If pressure drop is incorporated with El-Hisnawi's data based on the interpolation of the current data obtained in a bed and system close to that of El-Hisnawi's work (1981), the mean relative error of the developed model prediction become 13%. However,

El-Hisnawi's correlation (1981) , as shown in Table 4.1 (Form A), failed to predict the effect of reactor pressure and gas flow rate.It did not include the $(1+(\Delta P/Z)/\rho_L g)$ term and its Reynolds and Galileo numbers did not involve the bed voidage parameter. The other form of El-Hisnawi's correlation (1981) (Form B) which expresses the wetting efficiency in terms of dynamic liquid saturation is not compatible with the experimental observations (Figures 4.7-4.9). Since liquid holdup decreases at high pressure and high gas flow rate, it gives an opposite trend for the effect of reactor pressure and gas flow rate.

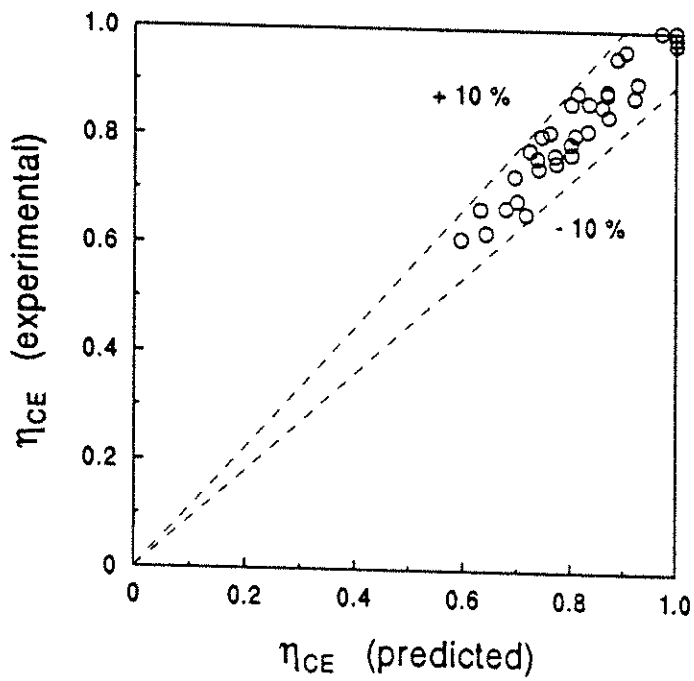

Figure 4.11 : A comparison of the developed model prediction and data for liquid-solid contacting efficiency

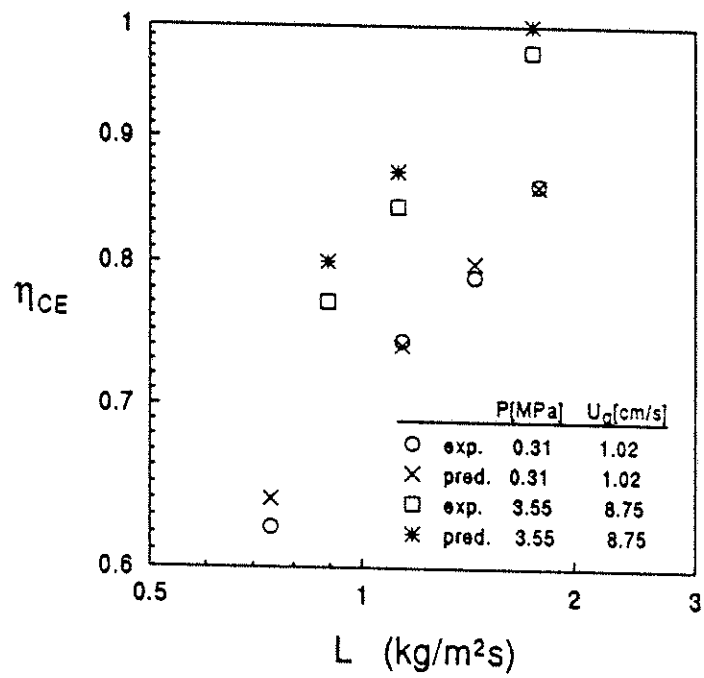

Figure 4.12 : The trend of the developed model prediction of the effect of high pressure and gas flow rate on the contacting efficiency in the extrudate bed ($(d_p)_{eq}$ = 0.199 cm)

5. EFFECT OF FINES ON EXTERNAL LIQUID-SOLID CONTACTING EFFICIENCY, PRESSURE DROP AND LIQUID HOLDUP

5.1 BACKGROUND

The design of commercial trickle-bed reactors, needed for the development and commercialization of novel processes and products, are based on translation of laboratory (bench-scale) data to large scale (i.e. scale-up). On the other hand in some circumstances the commercial process is well established, and laboratory studies are aimed to provide predictive information concerning the behavior of new catalyst, alternative feed stock, etc. (i.e. scale-down). Therefore, scale-up and scale-down of such reactors are very important and laboratory investigations are essential. In laboratory scale reactors often the velocities of gas and liquid are much lower than in a commercial reactor as illustrated in Table 5.1 for typical trickle-flow hydrotreating processes (Sie, 1991). Moreover, the same catalyst sizes, type and shapes employed in the commercial reactor are used in laboratory reactors of inside diameter between 1 cm to 3 cm (Anderson and Pratt, 1985). Hence, the effect of reactor diameter is more pronounced in a laboratory reactor where the criterion of $d_r/d_p \geq 20$ usually is not met to minimize the wall effect.(Dudukovic' and Mills, 1986 ; Sie, 1991). In a reactor of low ratio of d_r/d_p, the bed voidage and specific surface per unit volume near the wall deviates from the statistical fluctuation in the interior of the bed. The bed voidage reaches a value of unity very close to the wall, while the specific area approaches zero close to the wall if only particle surface is considered, but attains a higher value than the average value if the wall surface is also taken into account. These contribute to deviation from ideal plug flow in which all catalyst is utilized equally and where each particle is surrounded by a flowing

film of liquid. Accordingly, such conditions in laboratory reactors cause liquid maldistribution , wall effect and hence insufficient use of the catalyst bed by reducing liquid-solid contacting efficiency (Sie, 1991; Van Klinken, 1979; Van Klinken and Van Dongen, 1980; Dudukovic' and Mills, 1986; Gierman, 1988).

Table 5.1 : Some typical data for reactors of different size

Specification	Commercial	Pilot-plant	Bench-scale	Microflow
Catalyst volume , liter	100000	10	0.15	0.008
Diameter , cm	250	4	2	1
Length , cm	2000	800	50	10
Liquid velocity , cm/s	1.1	0.4	0.03	0.006
Re_L	55	22	1.4	0.3

LHSV = 21 (1/h) , $\upsilon = 3 \times 10^{-7}$ m^2/s , $d_p = 0.15$ cm

The hydrodynamics and reaction kinetics are so closely interlinked that their effects on conversion are inseparable. Thus, if the obtained data in a laboratory reactor is not reliable, this can lead to bad commercial design and improper interpretation and conclusion of the data in case of catalyst , alternative feed stock, testing etc..

Dilution of the laboratory beds with fines (small, inert and nonporous particles of about 0.1 catalyst diameter), as shown in Figure 5.1, has been recommended and utilized to overcome the shortcomings in the hydrodynamics of laboratory scale reactors. In this technique, fines are dispersed among the catalyst particles providing more solid-solid contact points and areas over which liquid flows and hence reducing the voidage in the bed particularly near the reactor wall. This is not the same case as reducing the size of uniform particles in the bed. The later case does not increase the number of contacting points per unit volume as much as the addition of fines does.

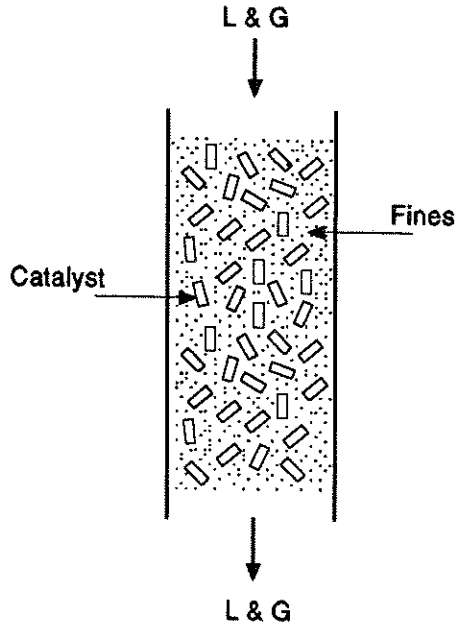

Figure 5.1 : Schematic diagram of diluted bed with fines

Thus the hydrodynamics are largely dictated by the packing of the fines, whereas the catalytic phenomena are governed by the catalyst particle of same shape, size and form as used in industrial practice. This is, in fact a decoupling of hydrodynamics and kinetics to approach the large scale performance by improving the plug flow character of laboratory reactor (Sie, 1991; Van Klinken and Van Dongen, 1980). Such improvement results in better catalyst utilization in a diluted bed with fines due to liquid distribution improvement (increasing liquid holdup as well), reducing wall effect, and minimizing axial dispersion as found by many investigators (Sie, 1991; Sedriks and Kenney, 1973; Koros, 1976; Van Klinken and Van Dongen, 1980; Carruthers et. al., 1988). A qualitative conclusion has been deduced that improving the efficiency of catalyst utilization is the result of improving liquid-solid contacting efficiency. Unfortunately, no

study appeared in the literature which confirms quantitatively the effect of fines on liquid-solid contacting efficiency, the improvement of which affects catalyst utilization.

The catalyst bed dilution technique has found rather wide spread application as a means to produce reliable results for scale-up and scale-down and to allow meaningful testing of commercially used catalyst particle sizes in small scale laboratory reactors. It is noteworthy that the meaningful results of dilution techniques would be negated if the packing method of mixing the bed of catalyst and fines fails to produce reproducible results. All studies in the open literature that utilized fines did not reported how the diluted bed was packed to ensure reproducibility. However, few investigators reported only the amount of fines to catalyst used, which ranges from just filling the voidage of the original catalyst bed (Koros, 1976; Carruthers and DiCamillo, 1988) to 1-10 volumes of fines to one volume of catalyst (Koros, 1976; Gierman, 1988; Carruthers and DiCamillo , 1988; Van Klinken and Van Dongen; 1980; 1979).

5.2 A REPRODUCIBLE PROCEDURE FOR PACKING A LABORATORY TRICKLE-BED REACTOR WITH A MIXTURE OF CATALYST AND FINES

It is important to ensure that the reactor is packed reproducibly with a mixture of catalyst and fines. This is because even if a uniform liquid distribution is achieved at the distributor, significant by-passing (channeling) and/or segregation could occur due to improper way the catalyst and fines are packed (Gierman, 1988). Ensuring an uniform catalyst/fines distribution along the bed, and reproducing such uniformity, is essential to avoid channeling and segregation. In this work different packing procedure for both dry and wet packing has been utilized as shown in Table 5.2 to develop a reproducible procedure (Al-Dahhan, 1991).

Table 5.2 : Methods tested for packing a bed with mixture of catalyst and fines

Type	volume of fines just fill the bed voidage	2 volume fines / 1 volume catalyst
I - Dry method	(A) - Pack portion of catalyst then portion of fines with tapping or vibrating. (B) - Pack the whole bed with catalyst followed by the required amount of fines with tapping and vibrating.	(C) - Repeat (A). (D) - Mix two volumes of fines with one volume of catalyst and pour them into the reactor.
II - Wet method	(E) - Mix portion of catalyst with required portion of fines in the presence of a solvent until the mixture becomes as uniform as possible. Introduce the mixture part by part with pressing each part inside the bed. (F) - Repeat (E) without pressing each introduced part.	(G) - Repeat (E). (H) - Repeat (F).

In order to optimize the effort, the first screening among the above methods was based on reproducing an uniform distribution of catalyst and fines along the bed by employing an acrylic clear reactor. Pressure drop measurements for single phase (gas flow only) and both pressure drop and liquid holdup measurements for two phase flow were used to quantify the reproducibility. Visual observation shows that the dry packing procedure (A and B), where the volume of fines just fills the voidage volume of the actual bed, produces an excellent and reproducible catalyst/fines distribution. All other methods failed to reproduce such uniformity. Dry methods (C) and (D) create clear segregation of fines. Wet method of packing with pressing the bed yields non uniform and not

reproducible fines and catalyst distribution along the bed (either regions with more catalyst or regions with more fines) . If the bed is not pressed the non uniformity becomes worse. Such observations have been confirmed by cutting 3 cm length of the reactor in different positions along the bed, separating fines and catalyst and measuring their distribution. The dry methods (A) and (B) were found to reproduce the fines/catalyst distribution along the different axial positions within relative difference of 2% (vol. fines/vol. cat. at top, middle and bottom of the diluted bed are 0.72, 0.73, 0.72, respectively). In case of the high volumetric ratio of fines to catalyst, as some investigators used, the wet method is better than the dry method but both did not produce uniformity or reproducibility. However, in the wet packing method one can not always use the solvent at room temperature and in an open environment which makes the method inconvenient.

5.2.1 The Developed Procedure

The following is the step-by-step procedure developed to pack the diluted bed reproducibly by dry methods A and B of Table 5.2.

A - Portion of Catalyst by Portion of Fines Packing Procedure

1 - Use dry catalyst and fines.

2 - Load the reactor with the known amount of catalyst to be utilized and determine the bed height.

3 - Calculate the catalyst bed void volume based on the catalyst amount in step (2).

4 - Discharge the catalyst.

5 - Calculate the amount of fines which is required to just fill all the bed voidage volume as :

$$\textit{weight of fines required} = \textit{bed void volume} * \textit{fines bulk density}$$

6 - Divide the amount of catalyst and fines into portions. Number of portions (i.e. amount of each portion) was found not to be critical. The user can chose a number of portions based on convenience.

7 - Load a portion of catalyst to the reactor. Tap or vibrate the reactor until the catalyst bed settles. The duration of the vibrating or tapping period was found not to be critical. A few minutes is adequate.

8 - Load a portion of fines to the reactor . Vibrate or tap the bed gently, which qualitatively means maintaining the original bed of catalyst as stable as possible while the fines migrate to fill its voids. Tapping/vibrating is continued until the top layer of the catalyst becomes visible. This is a critical step which would lead to a segregation if the tapping/vibrating period exceeded the time of the appearance of the catalyst layer. Therefore in case of a stainless steel tube which is frequently used in practice, a light source and/or optical fiber can be utilized to observe the bed surface.

9 - Repeat steps 7 and 8 until the total amount of catalyst and fines are packed.

Note : The expansion in the bed height due to the addition of fines and tapping is within 2 %.

B - Whole Bed Packing Procedure

In a long stainless steel reactor with small inside diameter it is very difficult to observe the bed surface at the bottom by a light source. Moreover, an optical fiber is not always available for this purpose. Therefore, this new procedure of packing the whole bed was utilized and tested. This seemed promising based on the finding of step (6) of the developed procedure (A) that the number of portions used are not critical. Such procedure overcomes the difficulties associated with monitoring the catalyst surface at the reactor bottom. In contrast, the catalyst surface at the upper part of the reactor can be easily observed. The step-by-step procedure is :

1 - Follow step (1), (2), (3), (4), and (5) of procedure (A).

2 - Load the amount of catalyst required portion by portion with associated tapping/vibrating. This is recommended to make the bed stable and reproducible.

3 - Load all fines into the reactor. If there is not enough room to hold all the calculated amount of fines, load it portion by portion. Tap/vibrate until all the fines migrate into the bed and the top catalyst layer becomes visible.

Note :

(1) Based on whether there is a adequate room to accommodate fines at the top of the reactor, the catalyst bed can be loaded in two portions.The first portion is the major one which gives suitable volume to load the fines into it and help observing easily the top of the catalyst surface.

(2) The expansion in the bed height due to the addition of fines and tapping is less than that of procedure (A).

5.2.2 Quantification of Reproducibility of the Developed Procedure

Pressure drop and liquid holdup measurements were used to quantify the reproducibility of the developed procedure to pack a laboratory reactor with a mixture of catalyst and fines. For this purpose, different catalyst shapes and sizes and different reactor diameters have been utilized. Silicon carbide fines of 0.021 cm diameter were used. Figure 5.2 demonstrates the reproducibility of the measured pressure drop with gas flow only in the stainless steel reactor (d_r= 2.19 cm) packed by the developed procedure (A) with a mixture of extrudate catalyst and fines.The bed was repacked three times. The pressure drop reproducibility of both procedures (A) and (B) are shown in Figure 5.3. A comparison of pressure drop reproducibility between the developed procedure (A) and wet method (E) is illustrated in Figure 5.4. In the wet method the bed was dried completely before performing single gas phase flow experiment. The results reveal that the wet method failed to produce a reproducible pressure drop due to the non uniform fines/catalyst distribution along the bed which is not reproducible either. Also the bed height obtained using the same amount of catalyst and fines is higher than that obtained by the developed procedure which causes larger bed voidage. This results in lower pressure drop as shown in Figure 5.4b. Figure 5.5 illustrates a comparison of the pressure drop measured in three different reactor sizes packed by the developed procedure (B) with the same mixture of catalyst and fines. The pressure drop in the smallest reactor (d_r = 0.95 cm) is slightly higher than that of the others. This is because for smaller diameter reactors, the bed voidage close to the wall is higher. As a result the volumetric ratio of fines to catalyst required to fill its voidage is larger. Therefore, the diluted bed voidage in small reactors is low which causes higher pressure drop. The pressure drop obtained in a diluted bed packed by procedure (B) (whole bed packing) is

slightly higher than that in a diluted bed packed by procedure (A) (portion by portion packing) as illustrated by comparing the data of Figure 5.3b and 5.5 (d_r = 2.22 cm). This is because the increase in height of the bed packed by procedure (B) is less than that packed by procedure (A).

In practice, two phase flow operation is of interest. Therefore, the reproducibility of the developed procedure has been also quantified in terms of both pressure drop and liquid holdup measurements. Figure 5.6 confirms the reproducibility achieved by the developed procedure (A) in two phase flow operation. The experimental error is within 5%.

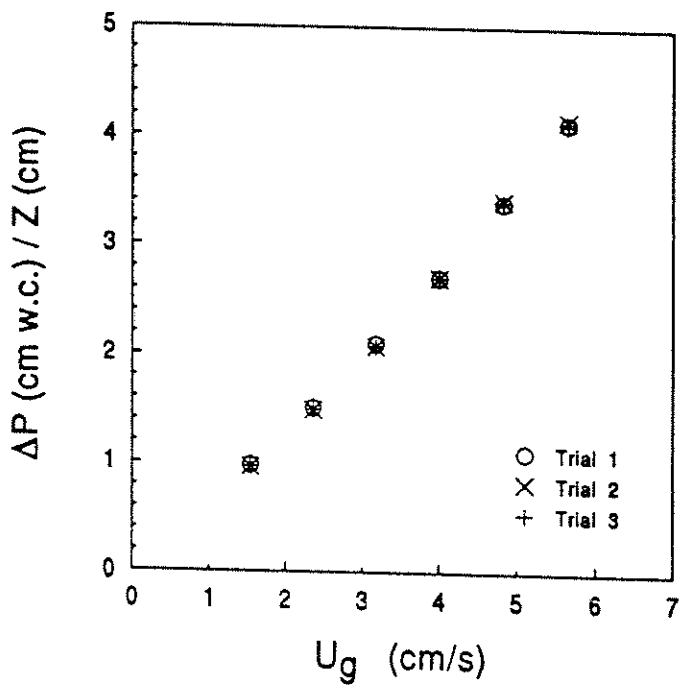

Figure 5.2 : The reproducibility of pressure drop using gas phase flow only in a diluted extrudate bed packed by the developed procedure (A). Gas: nitrogen; catalyst: 0.5% Pd extrudate (0.157x4.3 cm); fines: silicon carbide (d_f=0.21 mm); vol. fines/vol. cat.=0.54; ε_{Bf} = 0.22; reactor: stainless steel (d_r = 2.19 cm), pressure: 0.31 MPa (30 psig). Error bars are contained within the points

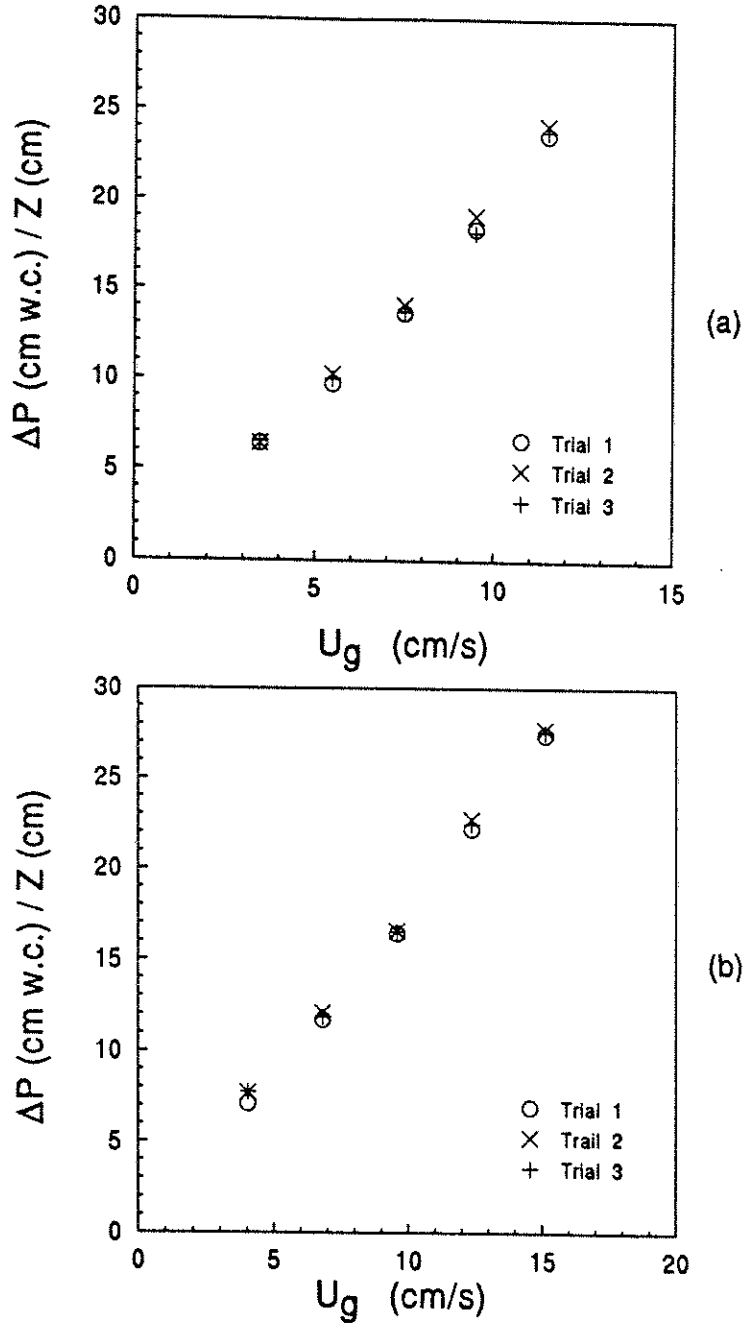

Figure 5.3 : The reproducibility of pressure drop using gas phase flow in a diluted bed packed by the developed procedures (A) and (B).
(a) Portion by portion packing (A). Gas: nitrogen; catalyst: extrudate (0.143x6.14 cm); fines: silicon carbide (d_f=0.21 mm); vol. fines/vol. cat.=0.78; ε_{Bf} = 0.16; reactor: acrylic (d_r = 1.587 cm) , pressure: 0.31 MPa (30 psig).
(b) Whole bed packing (B) . Gas: nitrogen; catalyst: sphere (d_p=0.17cm); vol. fines/vol. cat.=0.7; ε_{Bf} = 0.19; reactor: acrylic (d_r = 0.95 cm), pressure: 0.31 MPa (30 psig). Error bars are contained within the points.

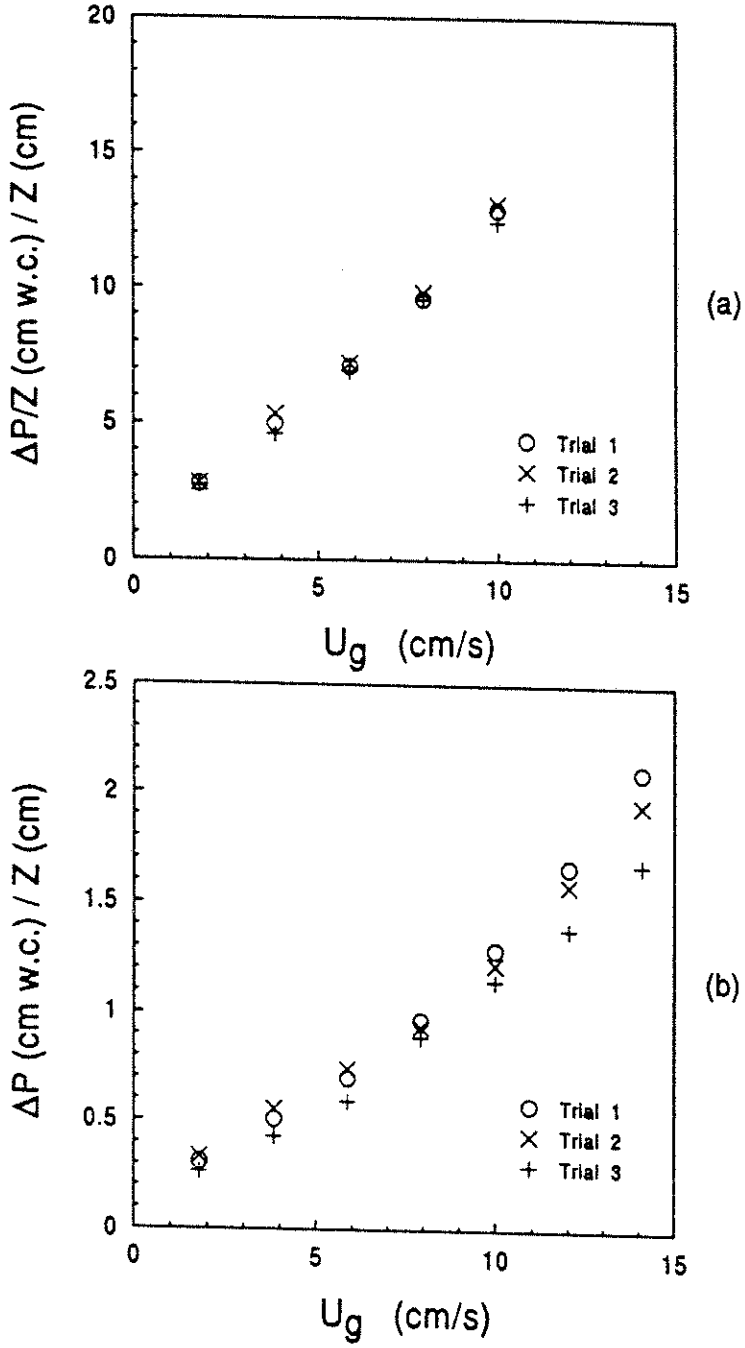

Figure 5.4 : Comparison between the reproducibility of the developed procedure (A) and wet method (E) in pressure drop measurements using gas phase flow only.
(a) Portion by portion dry packing (A). Gas: nitrogen; catalyst: sphere (d_p=0.17cm); fines: silicon carbide (d_f=0.21 mm); vol. fines/vol. cat.=0.62; ε_{Bf} = 0.22; reactor: acrylic (d_r = 2.2 cm) , pressure = 0.31 MPa (30 psig).
(b) Wet method packing (E) . Gas: nitrogen; catalyst: sphere (d_p=0.17cm); vol. fines/vol. cat.=0.62; ε_{Bf} = 0.346; reactor: acrylic (d_r = 2.2 cm), pressure = 0.31 MPa (30 psig). Error bars are contained within the points.

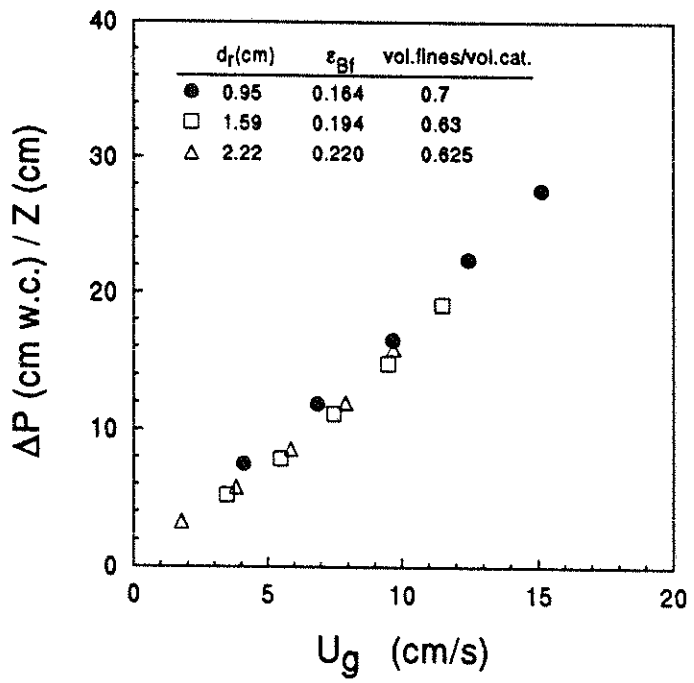

Figure 5.5 : Comparison of pressure drop in different reactor sizes packed by the developed procedure (B) (whole bed packing procedure) with the same mixture of catalyst and fines. Gas: nitrogen; catalyst: sphere (d_p = 0.17 cm); fines: silicon carbide (d_f =0.21 mm); pressure: 0.31 MPa (30 psig). The points represent the average of three experiments with error bars contained within the points

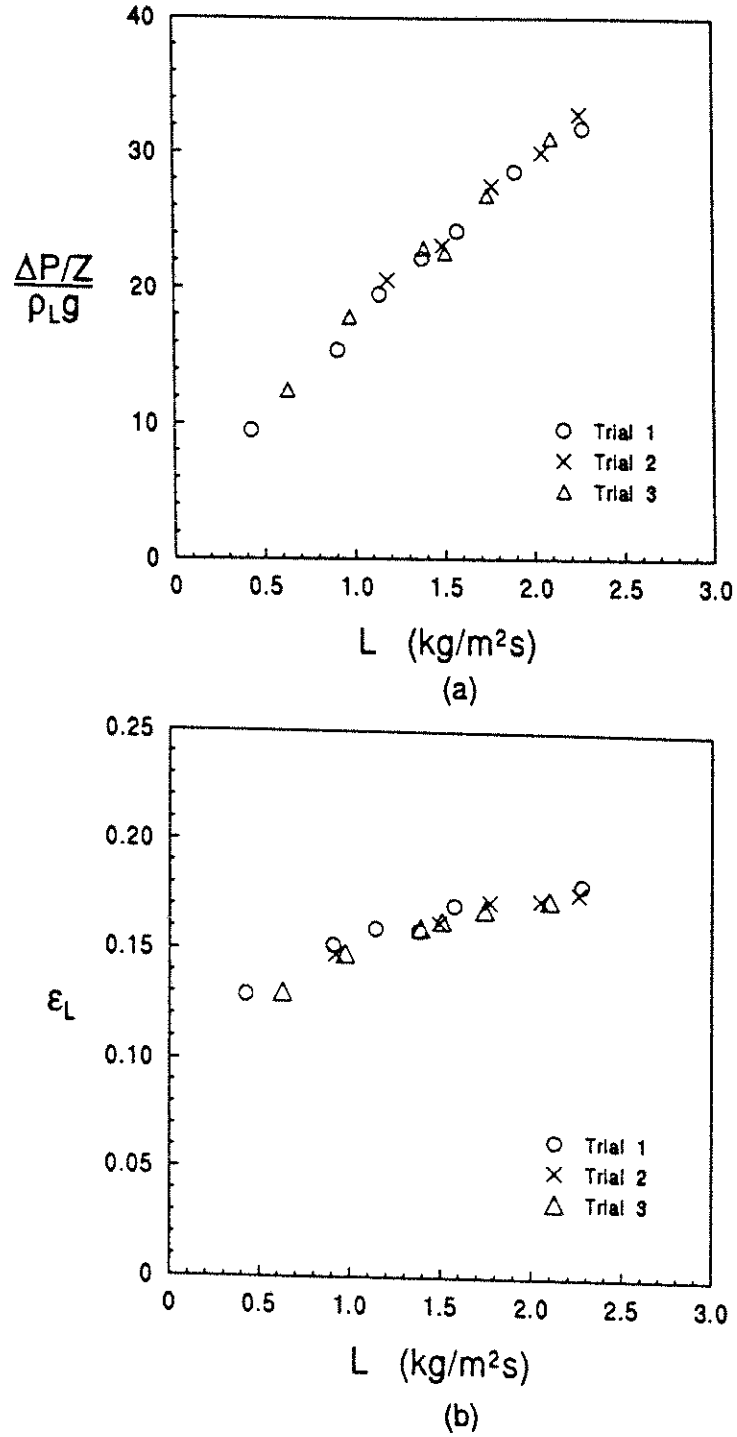

Figure 5.6 : The reproducibility of pressure drop and liquid holdup achieved by the developed procedure (A) in two phase flow operation. System: hexane/nitrogen; catalyst: 0.5% Pd extrudate (0.157x4.3 cm); fines: silicon carbide (d_f =0.21mm); vol. fines/vol. cat. = 0.61; ε_{Bf} = 0.2; reactor: stainless steel (d_r=1.55 cm), pressure: 0.31 MPa (30 psig)

5.3 EXPERIMENTAL INVESTIGATION

The details of the experimental set-up utilized in this investigation have been presented in Chapter 2.

5.3.1 Parameter Determination

I - Pressure Drop and Liquid Holdup Measurements

Pressure drop is measured by high pressure differential pressure transducer (DPT), while liquid holdup is measured by draining (collecting) method. The same procedure and operational consideration discussed in Chapter 3 were implemented.

II - Liquid-Solid Contacting Efficiency Determination

Fines are providing more solid-solid contacting points over which liquid flows, whereby liquid coverage of catalyst particles is improved. The contacting efficiency, η_{CE} , is evaluated by comparing the tracer effective diffusivity into pores of catalyst particles in two phase flow with that in liquid-filled flow according to equation 4.10 as discussed in Chapter 4. For a nondiluted bed, the expressions of moments listed in Tables 4.3 and 4.4, require the bed voidage, ε_B, and particle radius, r_p , to evaluate the effective diffusivities.

For a diluted bed with fines, the expressions of Tables 4.3 and 4.4 can be implemented to evaluate the effective diffusivities based on the following modifications:

(i) The catalyst particle radius , r_p , is used as in the case of the nondiluted bed, since the tracer diffusion occurs only into the pores of the catalyst particles .

(ii) For the expressions of two phase flow, the bed voidage of the catalyst bed, ε_B, is replaced by the following :

$$\bar{\varepsilon}_B = \frac{(Bed\ vol. - Cat.vol.)}{Bed\ vol.} = \frac{(Voidage\ vol. + Fines\ vol.)}{Bed\ vol.} \qquad (5.1)$$

where $\bar{\varepsilon}_B$ in a diluted bed which is packed by the developed procedure (fines just fill its voidage) is equivalent to ε_B of the original nondiluted bed.

This consideration is based on the moment and variance expressions derivation from tracer mass balance given by Mills (1978) and El-Hisnawi (1981). The bed mass balance equation in the interstitial liquid is :

$$D_L \frac{\partial^2 C}{\partial Z^2} - U_L \frac{\partial C}{\partial Z} - a_{LS} N_{LS} = \varepsilon_L \frac{\partial C}{\partial t} \qquad (5.2)$$

The term $a_{Ls} N_{Ls}$ is the rate of tracer loss to particles by liquid-solid mass transfer to liquid filled pores, where a_{LS} is the effective (i.e wetted) liquid-solid area through which mass transfer of tracer may occur from liquid bulk to the catalyst particle surface per unit volume of the reactor. Thus, a_{LS} in the catalyst bed and in the diluted bed is defined as follows :

Catalyst bed only

$$a_{LS} = \frac{S_{ex}}{V_p}\left(\frac{S_{eff}}{S_{ex}}\right)(1-\varepsilon_B)$$

$$a_{LS} = \frac{S_{ex}}{V_p}\,\eta_{CE}\,(1-\varepsilon_B)$$

$$a_{LS} = \left(\frac{\alpha+1}{r_p}\right)\eta_{CE}\,(1-\varepsilon_B)$$

$(1-\varepsilon_B)$ *is cat. vol./Bed vol.*

ε_B : bed void per reactor volume

$$\varepsilon_B = \frac{(Bed\ vol. - Cat.\ vol.)}{Bed\ vol.}$$

r_p : radius of the catalyst particle

$$\alpha = \begin{cases} 0 \text{ for slab} \\ 1 \text{ for cylinder} \\ 2 \text{ for sphere} \end{cases}$$

Diluted bed

$$a_{LS} = \frac{S_{ex}}{V_P}\left(\frac{S_{eff}}{S_{ex}}\right)(1-\bar{\varepsilon}_B)$$

$$a_{LS} = \left(\frac{\alpha+1}{r_p}\right)\eta_{CE}\,(1-\bar{\varepsilon}_B)$$

$(1-\bar{\varepsilon}_B)$ *is cat. vol./Bed vol.*

$$\bar{\varepsilon}_B = \frac{(Bed\ vol. - Cat.\ vol.)}{Bed\ vol.}$$

r_p: radius of the catalyst particle

$$\alpha = \begin{cases} 0 \text{ for slab} \\ 1 \text{ for cylinder} \\ 2 \text{ for sphere} \end{cases}$$

(iii) For the expressions of liquid-filled operation, the liquid holdup , ε_L, in two phase flow expressions is replaced by the diluted bed voidage, ε_{Bf}, which is equal to :

$$\varepsilon_{Bf} = \frac{(Bed\ vol. - Cat.\ vol. - fines\ vol.)}{Bed\ vol.} \tag{5.3}$$

Accordingly , the required expressions for a diluted bed with fines to evaluate effective diffusivities in both liquid filled and two phase flow operations are given in Tables 5.3 and 5.4 for extrudate and spherical particles, respectively.

Table 5.3 : Expressions for the moments in a diluted bed of cylindrical catalyst for a nonvolatile and nonadsorbing tracer

Theoretical expression

I - Two Phase Flow Operation

$$\sigma_D^2 = \frac{\left\{\left(\frac{V_r\,\varepsilon_L}{Q_L}\left[1+\frac{S_{ex}\,r_p}{2\,V_p}\left(\frac{(1-\bar{\varepsilon}_B)\,\varepsilon_p}{\varepsilon_L}\right)\right]\right)-\frac{V_r\,\varepsilon_L}{Q_L}\right\}\frac{r_p^2\,\varepsilon_p}{8(De)_{TF}}}{\left(\frac{V_r\,\varepsilon_L}{Q_L}\left[1+\frac{S_{ex}\,r_p}{2\,V_p}\left(\frac{(1-\bar{\varepsilon}_B)\,\varepsilon_p}{\varepsilon_L}\right)\right]\right)^2}$$

II - Liquid-Filled Operation

In liquid filled operation , liquid holdup (ε_L) is replaced by actual bed voidage (ε_{Bf}). The following is the slope expression of σ_D^2 versus Q_L :

$$slope = \frac{\frac{S_{ex}\,r_p}{2\,V_p}\left(\frac{1-\bar{\varepsilon}_B}{\varepsilon_{Bf}}\right)\frac{r_p^2\,\varepsilon_p^2}{8\,(De)_{LF}}}{V_r\,\varepsilon_{Bf}\left[1+\frac{S_{ex}\,r_p}{2\,V_p}\left(\frac{(1-\bar{\varepsilon}_B)}{\varepsilon_{Bf}}\right)\varepsilon_p\right]^2}$$

Table 5.4 : Expressions for the moments in a diluted bed of spherical catalyst for a nonvolatile and nonadsorbing tracer

Theoretical expression

I - Two Phase Flow Operation

$$\sigma_D^2 = \frac{Q_L}{V_r\,\varepsilon_L}\,\frac{\dfrac{(1-\bar{\varepsilon}_B)\,\varepsilon_p}{\varepsilon_L}\left(\dfrac{r_p^2\,\varepsilon_p}{15\,(De)_{TF}}\right)}{\left[1+\left(\dfrac{(1-\bar{\varepsilon}_B)\,\varepsilon_p}{\varepsilon_L}\right)\right]^2}$$

II - Liquid-Filled Operation

In liquid filled operation , liquid holdup (ε_L) is replaced by actual bed voidage (ε_{Bf}).The following is the slope expression of σ_D^2 versus Q_L :

$$slope = \frac{\dfrac{((1-\bar{\varepsilon}_B)\,\varepsilon_p^2}{\varepsilon_{Bf}}\;\dfrac{r_p^2}{15\,(De)_{LF}}}{V_r\,\varepsilon_{Bf}\left[1+\dfrac{(1-\bar{\varepsilon}_B)\,\varepsilon_p}{\varepsilon_{Bf}}\right]^2}$$

5.3.2 Operating Conditions Investigated

The flow conditions covered in this study are within the trickle flow regime shown in Figure 3.4 on Fukushima and Kusaka (1977) flow map. The range of reactor pressure, liquid and gas superficial velocities covered are listed in Table 5.5 , while the physical properties of the system used are similar to that presented in Table 3.4. Different bed characteristics and degrees of dilution, shown in Table 5.6, have been used to investigate the effect of fines on catalyst contacting efficiency, pressure drop and liquid holdup. Table 5.6 also lists the evaluated liquid-filled effective diffusivities. The higher effective diffusivity obtained in a liquid full highly diluted bed (2 volumes fines / 1 volume catalyst) compared to the one reported for the bed of extrudates in Table 4.7 and compared to the bed with fines packed by the recommended procedure (Table 5.6) is apparently due to increased accessibility of tracer into the pores of catalyst particles. The difference, however, is not large (5.4%).

Table 5.5 : Range of covered operating conditions

Condition	covered Range
Reactor pressure, MPa	$0.31 \leq P \leq 1.8$
Psig	$30 \leq P \leq 250$
Gas superficial velocity, cm/s	$1 \leq U_G \leq 8.5$
Gas superficial mass velocity, kg/m^2 s	$6.64 \times 10^{-3} \leq G \leq 4.0$
Liquid superficial flow rate, ml/min.	$15 \leq Q_L \leq 70$
Liquid Superficial mass flow rate, kg/m^2 s	$0.42 \leq L \leq 2.1$
Temperature , K	≈ 298

Table 5.6 : Packed bed characteristics

Reactor/Packing	Characteristics
<u>Reactor</u> Stainless steel reactor	d_r = 2.19 cm ; Length = 57.31 cm
<u>Packing</u> Fines	Type: nonporous silicon carbide; d_p= 0.021 cm ρ_{bulk} = 1.51 gm/cm^3 ; $\rho_{material}$ = 3.21 gm/cm^3
0.5% Pd extrudate / fines Developed procedure (A)	Type: porous ; $(d_p)_{eq}$=0.199 cm, d_r/d_p=11; Bed length (Z) = 53.81 cm; ε_p = 0.599 ; $\rho_{bulk\ cat.}$ = 1.189 gm/cm^3 vol. fines/vol. cat.=0.54; ε_{Bf} = 0.22; $\bar{\varepsilon}_B$=0.38; $(De)_{LF}$ = 17.979 x 10^{-6} cm^2/s
0.5% Pd extrudate / fines Method (G) - wet method	Type: porous ; $(d_p)_{eq}$=0.199 cm, d_r/d_p=11; Bed length (Z) = 51.51 cm; ε_p = 0.599 ; $\rho_{bulk\ cat.}$ = 1.189 gm/cm^3 vol. fines/vol. cat.= 2; ε_{Bf} = 0.35; $\bar{\varepsilon}_B$=0.767 $(De)_{LF}$ = 18.951 x 10^{-6} cm^2/s
Silica shell sphere / fines Dry method (A) Note: Bed voidage is partially filled with fines.	Type: porous ; d_p= 0.152 cm, d_r/d_p=14.6; Bed length (Z) = 53.51 cm; ε_p = 0.697 ; $\rho_{bulk\ cat.}$ = 0.697 gm/cm^3 vol. fines/vol. cat.=0.4; ε_{Bf} = 0.305; $\bar{\varepsilon}_B$=0.42; (according to the developed procedure, the ratio of vol. fines/vol. cat should be 0.7) $(De)_{LF}$ = 14.277 x 10^{-6} cm^2/s

5.3.3 Results and Data Analysis

I - Effect of Fines on Pressure Drop and Liquid Holdup

In a diluted bed with fines, solid-solid contacting points are increased and liquid flows over them. Therefore, total external liquid holdup increases as indicated by a residence time distribution that shifts to longer times. Since, the actual diluted bed voidage decreases, a larger stationary solid volume tends to retard the flowing fluids. Hence, pressure drop increases. Figure 5.7 demonstrates such effects on pressure drop and liquid holdup in a diluted bed of extrudates packed by the developed procedure (A). The same effect is obtained in a diluted bed of spheres packed with less fines than that determined by the developed procedure (i.e. the spheres bed voidage is partially filled with fines), as shown in Figure 5.8. However, smaller amount of fines produces less pressure drop and less holdup in a particular catalyst bed. The effect of reactor pressure and gas flow rate on pressure drop and liquid holdup obtained in a diluted bed of extrudates is shown in Figure 5.9. It is obvious that as reactor pressure and gas flow rate increases, pressure drop increases significantly while liquid holdup decreases noticeably similar to what was found and discussed in Chapter 3. A comparison of pressure drop and liquid holdup obtained in a non-diluted bed, diluted bed packed according to the developed procedure (A), and diluted bed with a ratio of 2 volumes of fines to 1 volume of extrudates packed by wet method (G) is illustrated in Figure 5.10. The data reveals that the pressure drop in the diluted packed bed with 2 volumes of fines to 1 volume of catalyst is less than that of the developed procedure. This is because the voidage in the first bed (ε_{Bf}= 0.35) is larger than that of the second bed (fines just fill the voidage, ε_{Bf}= 0.22). However, liquid holdup is higher in the bed of 2 volumes of fines to 1 volume of extrudates due to more available void space for the liquid around the solid to solid contacting points.

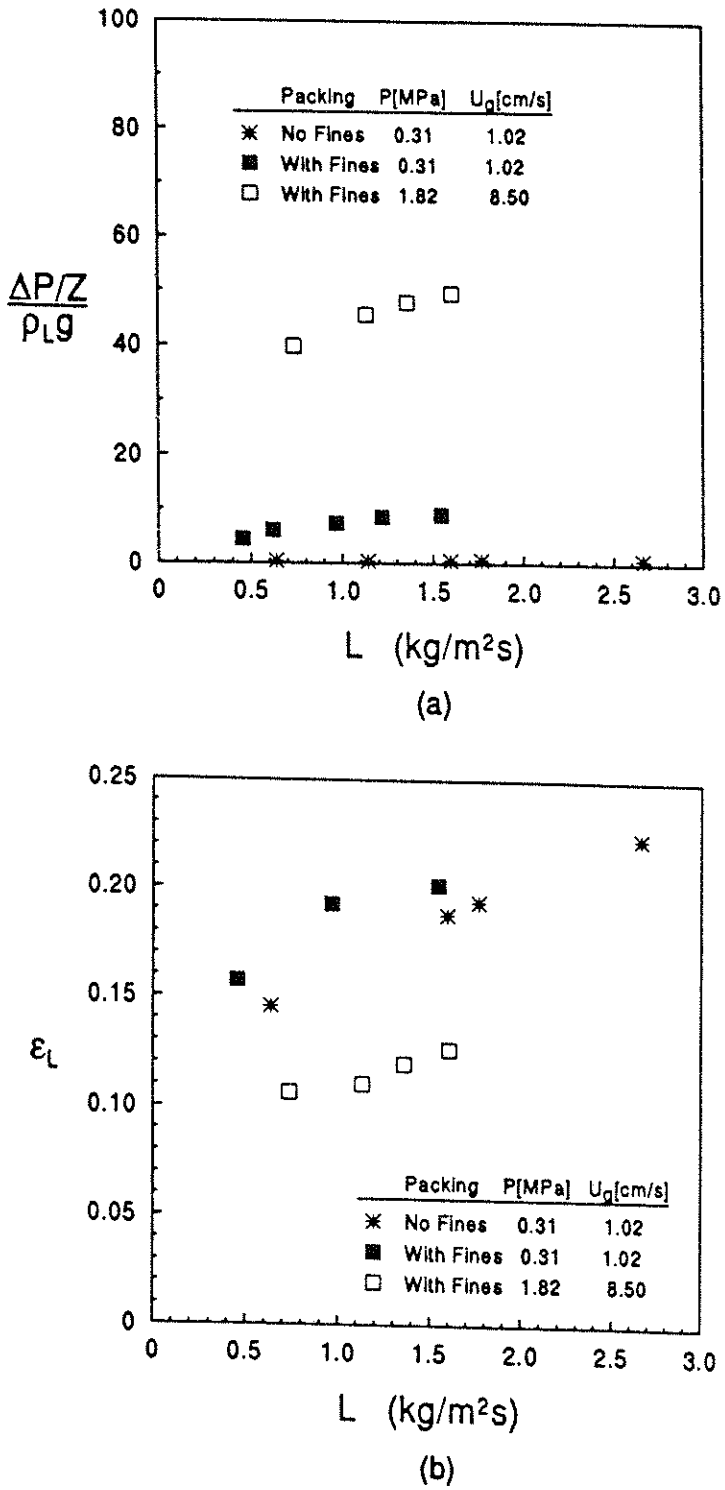

Figure 5.7 : Effect of fines on pressure drop and liquid holdup in a diluted bed of extrudates. System: hexane/nitrogen; porous 0.5% Pd ($(d_p)_{eq}$=0.199 cm); vol. fines/vol. cat.= 0.54 (developed procedure A); ε_{Bf} = 0.22

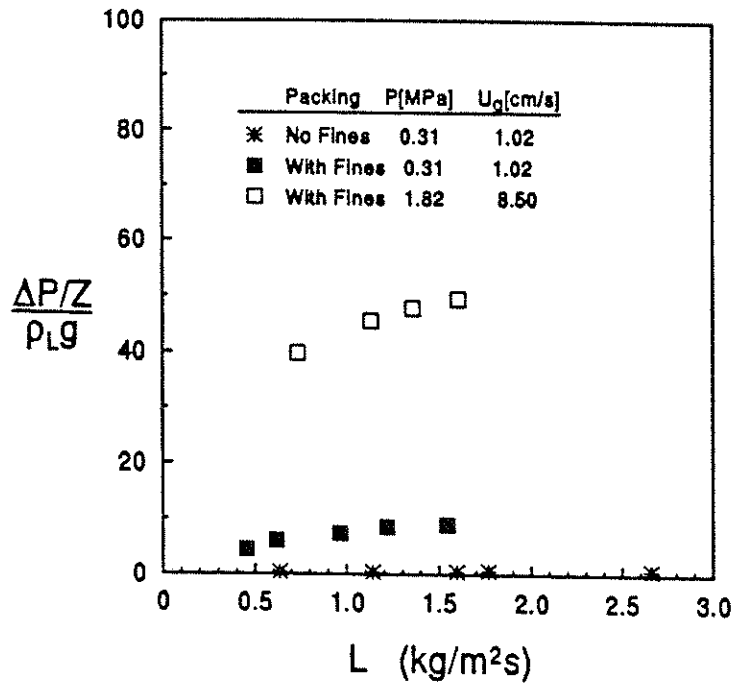

(a)

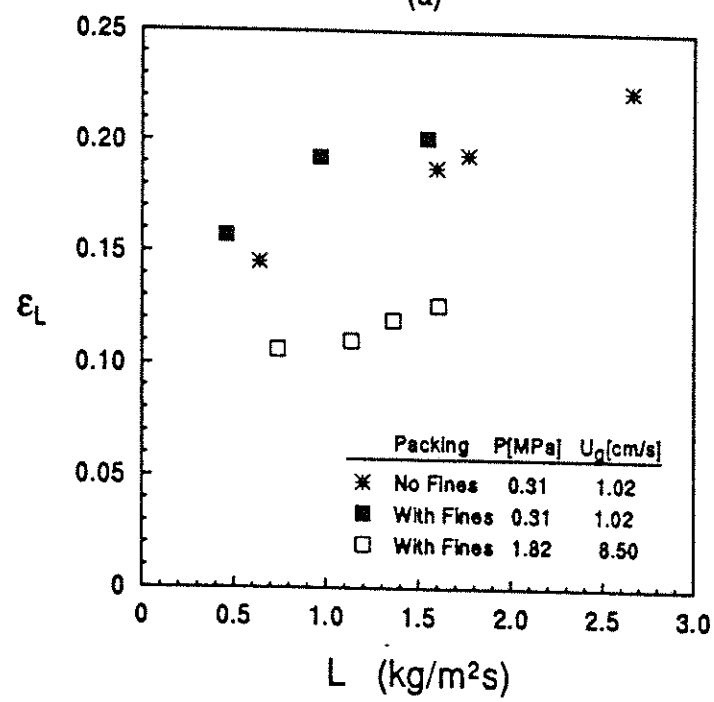

(b)

Figure 5.8 : Effect of fines on pressure drop and liquid holdup in a diluted bed of spheres with less fines than that required by the developed procedure. System: hexane/nitrogen; porous silica shell (d_p=0.152 cm); vol. fines/vol. cat.= 0.4; ε_{Bf} = 0.305 (the developed procedure required vol. fines/ vol. cat. = 0.7)

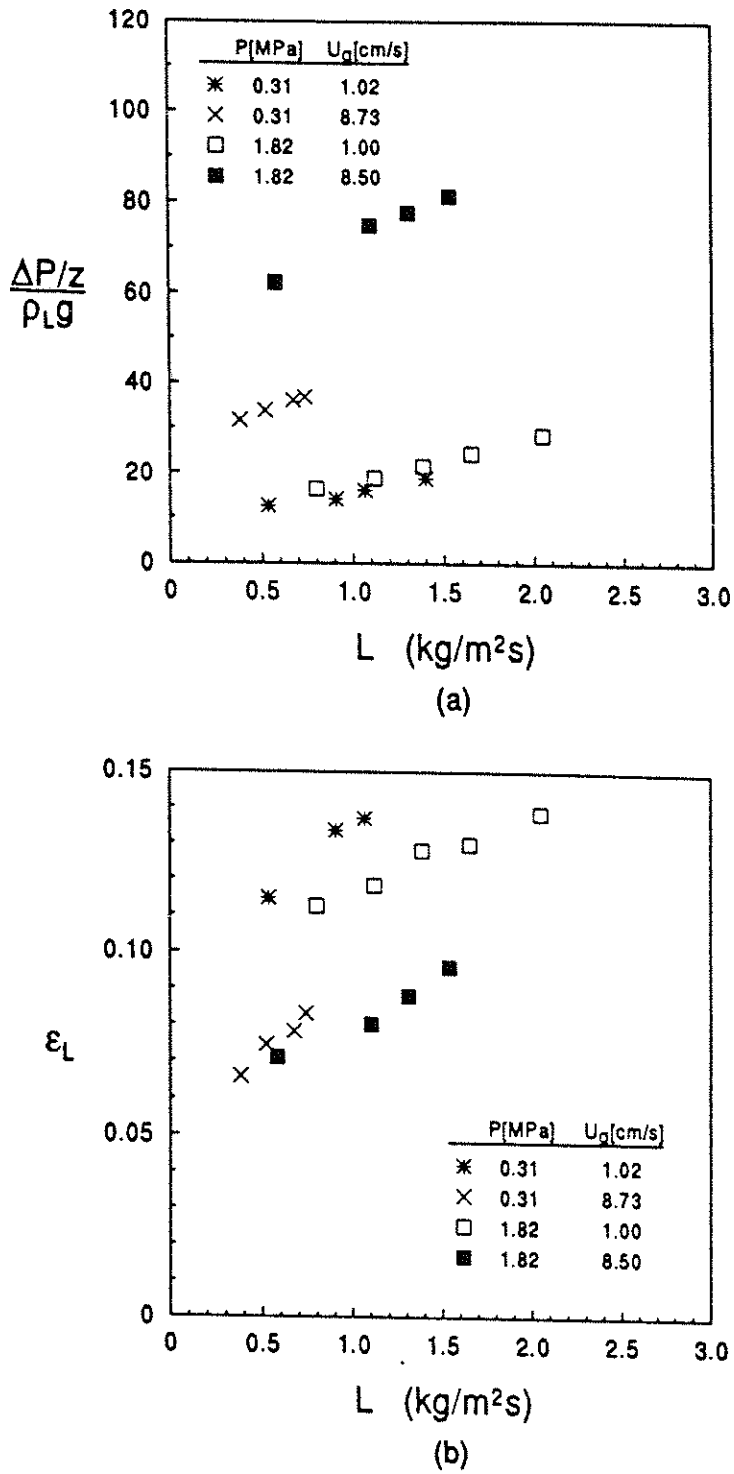

Figure 5.9 : Effect of reactor pressure and gas flow rate on pressure drop and liquid holdup in a diluted bed of extrudates. System: hexane/nitrogen; porous 0.5% Pd ($(d_p)_{eq}$=0.199 cm); vol. fines/vol. cat.= 0.54 (developed procedure A) ; ε_{Bf} = 0.22

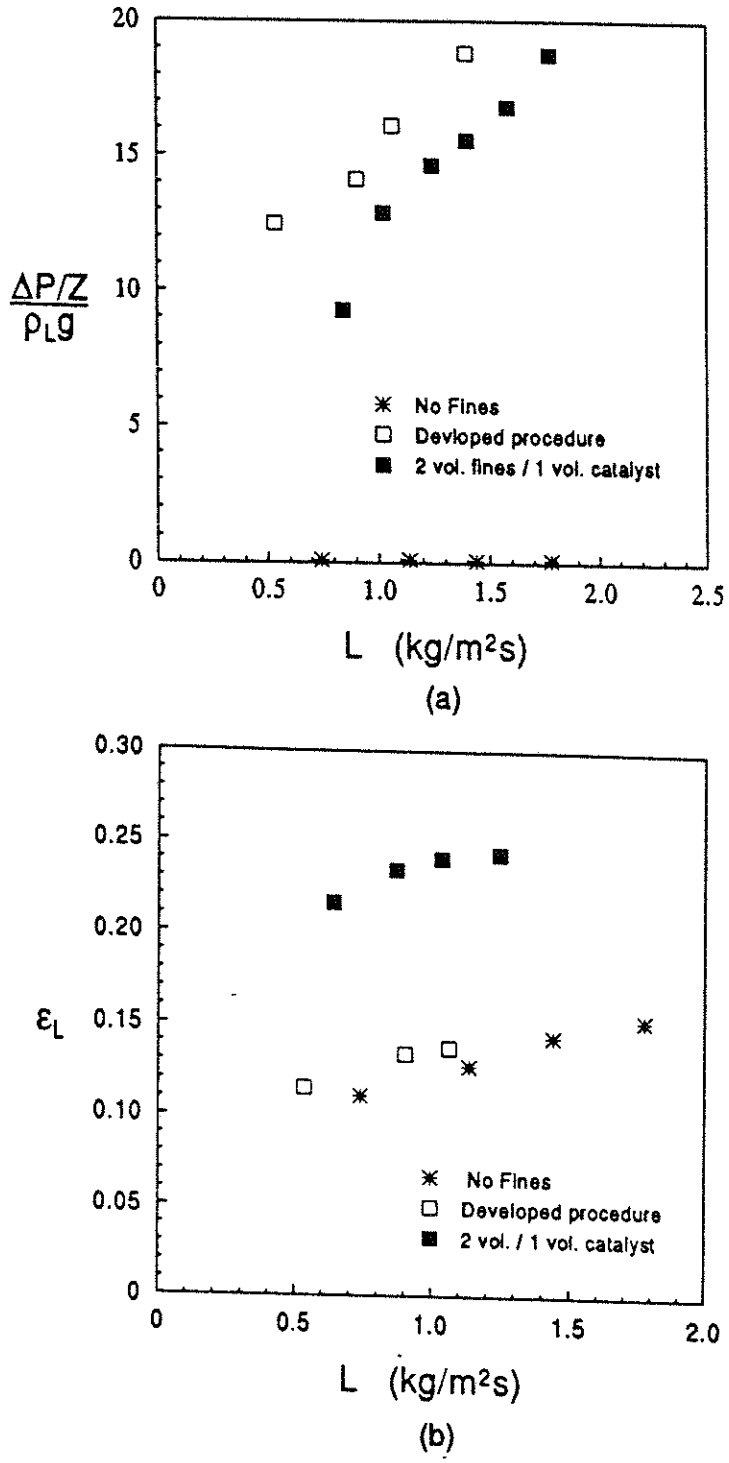

Figure 5.10 : A comparison among pressure drop and liquid holdup obtained in a nondiluted bed of extrudates, diluted bed with vol. fines/vol. cat = 0.54 (developed procedure A) and diluted bed with vol. fines/vol. cat. = 2 packed by wet method (G), pressure : 0.31 MPa (30 psig) ; U_G = 1.0 cm/s

II - Effect of Fines on Liquid-Solid Contacting Efficiency

All the current investigations confirm that diluting the bed with fines improves the efficiency of catalyst utilization, which qualitatively indicates that contacting efficiency is improved. Figure 5.11 compares the contacting efficiency in undiluted bed of extrudates with that of diluted bed packed according to the developed procedure (A). It shows that liquid-solid contacting efficiency, η_{CE} , increases as a result of the dilution with fines. As reactor pressure and gas flow rate increase , pressure drop increases and hence contacting efficiency increases due to better spreading of the flowing liquid. The increase in η_{CE} in a more diluted bed (2 volumes of fines/1 volume of catalyst) was found to be comparable to that of the diluted bed with just enough to fill fines its voidage (the developed procedure) as illustrated in Figure 5.12. This is related to the finding shown in Figure 5.10, where the pressure drop in the diluted packed bed with 2 volumes of fines to 1 volume of catalyst is less than that of the developed procedure, while liquid holdup is higher. Hence, the effect of low pressure drop and high liquid holdup in a diluted bed on the contacting efficiency compensates that in a bed of high pressure drop and low liquid holdup. Figure 5.13 shows as well that η_{CE} is improved in the spherical diluted bed packed with less fines than that determined by the developed procedure. The improvement is approximately similar of that shown in Figure 5.11. In such a bed liquid holdup is higher, while pressure drop is lower than those obtained in diluted bed of extrudates packed by the developed procedure. . However, the catalyst shape, size, and type are different in these two beds which are important factors in determining the contacting efficiency (Koros, 1976; Carruthers and DiCamillo, 1988).

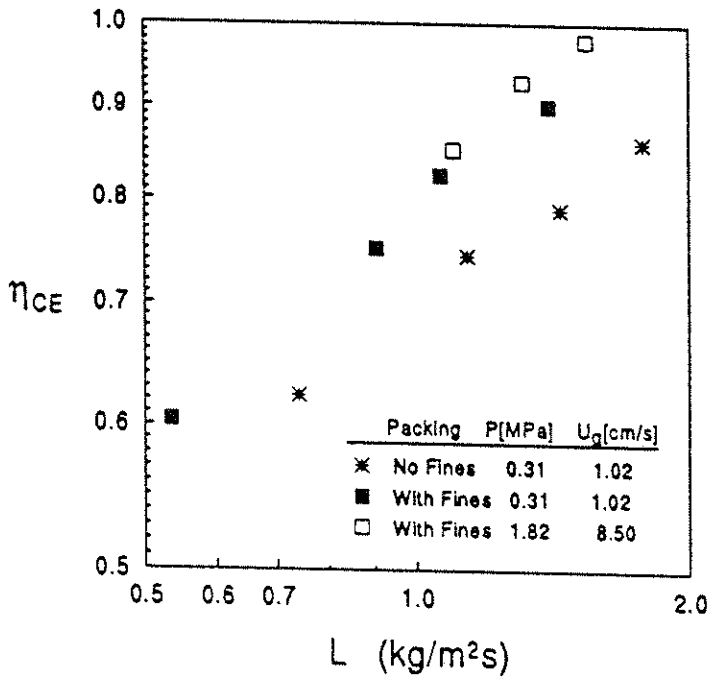

Figure 5.11 : Effect of fines on liquid-solid contacting efficiency. System: hexane / nitrogen; tracer: heptane; porous 0.5% Pd extrudate; vol. fines/vol. cat.=0.54 (developed procedure A)

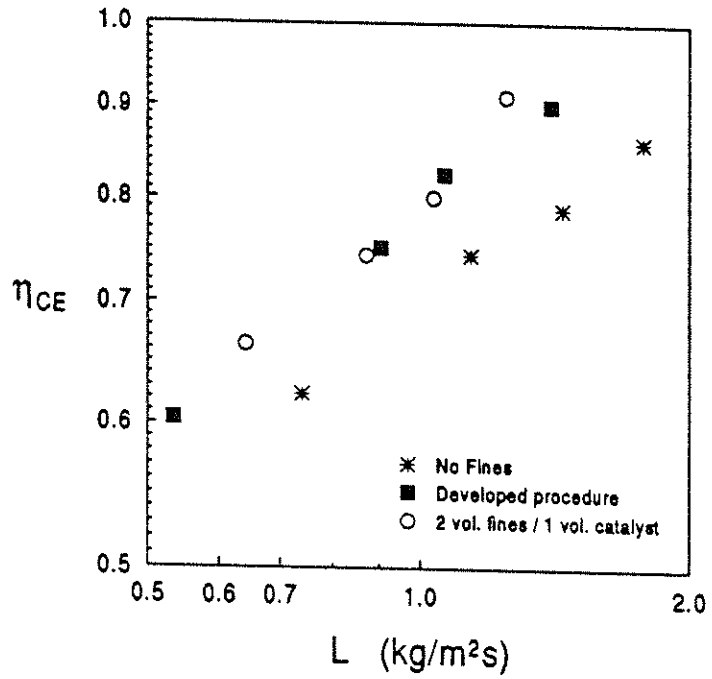

Figure 5.12 : Effect of degree of bed dilution on liquid-solid contacting efficiency. System: hexane / nitrogen; tracer: heptane; porous 0.5% Pd extrudate;

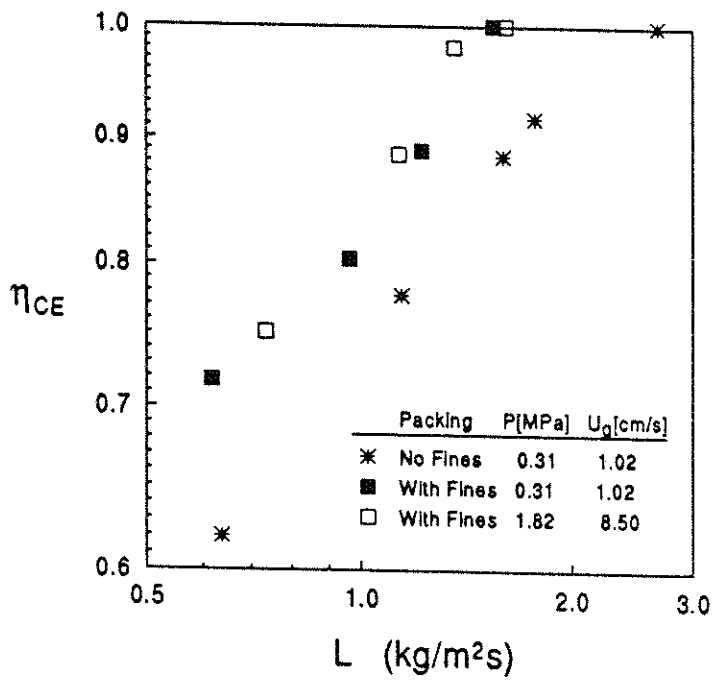

Figure 5.13 : Effect of fines on liquid-solid contacting efficiency in a diluted spherical bed packed according to method (A) with vol. fines/vol. cat. = 0.4 which is less fines than that determined by the developed procedure (vol. fines/vol. cat. = 0.7)

The quantitative improvement of the contacting efficiency in the diluted bed, as shown in Figures 5.11, 5.12 and 5.13, are consistent with Koros's (1976) findings. Koros (1976) utilized hydrogen peroxide decomposition to test the effect of fines (sand) on the catalyst utilization efficiency. He also compared the effect of fines in two diluted beds: (i) diluted bed where the amount of fines just fills the voidage of the original bed and (ii) diluted bed with 10 volumes of fines to 1 volume of catalyst. In both beds the fines (sand) improve the catalyst utilization efficiency by about the same amount as Shown in Figure 5.14.

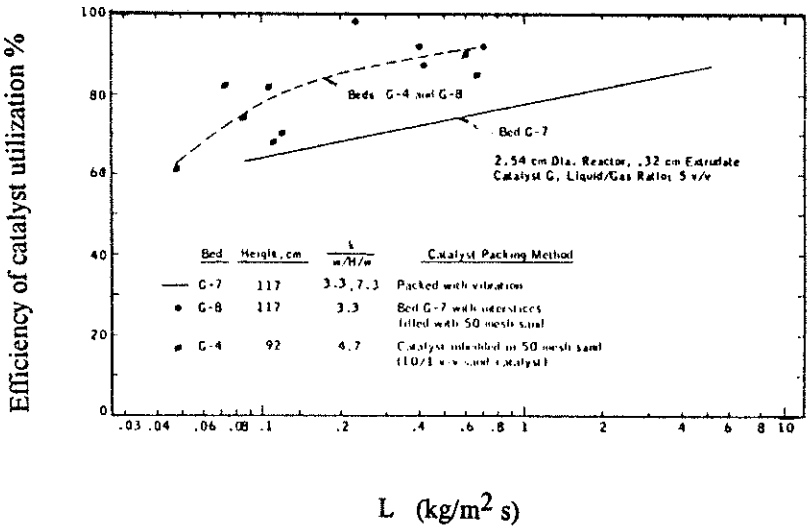

Figure 5.14 : Koros (1976) findings of the effect of fines (sand) on catalyst utilization efficiency

Although the data of Figure 5.14 is scattered, it indicates that in both beds the catalyst was not fully utilized (i.e. not fully wetted). Carruthers and Dicamillo, (1988) found that the best catalyst utilization is in the diluted bed when the amount of fines is just sufficient to fill the voidage of the origin catalyst bed.

It is known that contacting efficiency can have a significant effect on the catalyst effectiveness factor for partially wetted catalyst pellets. This profoundly affects reactor performance where the effectiveness factor is an important parameter in the trickle-bed reactor model. It has been found that incomplete wetting and effectiveness factor are strongly coupled phenomena (Dudukovic′ and Mills, 1986; Zhukova et al., 1990; Dudukovic′, 1977; Herskowitz, and Smith, 1983). Therefore the significance of partial wetting on the global rate of reaction depends on intra and interparticle diffusion and the volatility of the limiting reactants and of the solvent (Herskowitz and Smith, 1983). If the limiting reactant is nonvolatile and Thiele modules is small,ϕ_T, the effect of the wetting efficiency ($0.6 \leq \eta_{CE} \leq 1.0$) on the effectiveness factor is not large (Mills and Dudukovic′, 1979; Herskowitz, 1981; Herskowitz and Smith, 1983; Zhukova et al., 1990). If the limiting reactant is volatile and/or partially volatile, the effect of η_{CE} depends on the interparticle diffusion. Therefore Thiele modules, ϕ_T , which is the ratio of the maximum reaction rate and the maximum rate of internal diffusion transport, determines whether the catalyst effectiveness factor will be primarily affected by external contacting efficiency where the catalyst pores in trickle-bed reactor are usually completely filled with liquid particularly for prewetted bed. For large modulii ($\phi_T >> 1$) η_{CE} is the dominant variable, and the utilization of the catalyst is proportional to the fraction of the external area wetted over which the reactant is supplied to the reaction zone. For small modulii ($\phi_T << 1$) where interparticle diffusion is neglected and the reaction rate is completely kinetically controlled regime, the effect of η_{CE} on effectiveness factor and hence on the catalyst utilization is diminished (Dudukovic′,

1977; Herskowitz and Smith, 1983). The plots in Figure 5.15 (Herskowitz and Smith, 1983) indicate that the effect of partial wetting is very significant at high values of Thiele modules, ϕ_T, and at low liquid superficial flow rate. Moreover small changes in η_{CE} may cause significant change in the effectiveness factor and hence in the catalyst utilization. Accordingly , diluting the laboratory reactor bed with fines improves the reactor performance. The extent of improvements would depend on the type of the reaction.

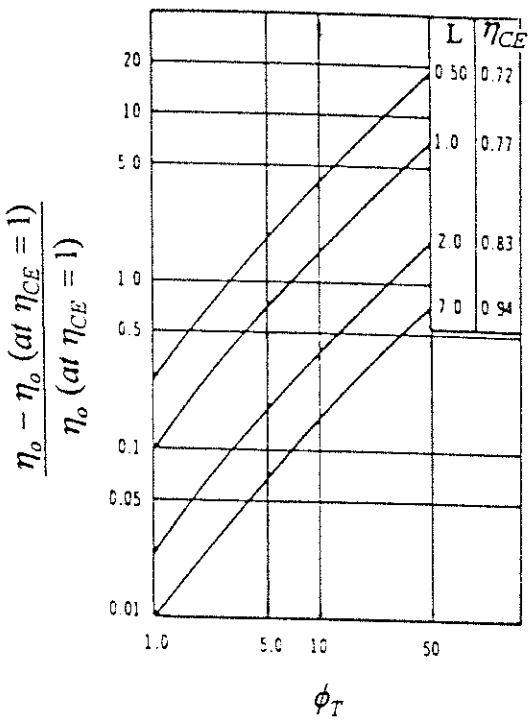

Figure 5.15 : Effect of wetting efficiency on the overall effectiveness factor. d_p= 0.15 cm; ε_B = 0.4 (Herskowitz and Smith, 1983)

6. CONCLUSIONS AND RECOMMENDATIONS

6.1 CONCLUSIONS

Reported studies in the literature on the design and scale-up parameters of trickle-bed reactor have been mainly performed under atmospheric conditions. In industrial practice these reactors are generally operated at elevated pressure. Commercial reactors are usually designed based on data obtained in a bench scale unit. In a laboratory scale trickle-bed reactor, wall effects, axial dispersion and liquid maldistribution are encountered due to low superficial liquid velocities besides utilizing the same catalyst sizes and shapes of the commercial units. Diluting the bed with fines is recommended to overcome such shortcomings.

In this study, a high pressure trickle-bed reactor facility has been designed and developed. The effects of high pressure and fines on pressure drop, liquid holdup and liquid-solid contacting efficiency have been investigated. These hydrodynamic parameters are important for design and scale-up and affect other important parameters as well. According to the findings of this work, the following conclusions are deduced:

(1) At high pressure and high gas flow rate , pressure drop increases significantly, while liquid holdup decreases considerably.

(2) Liquid-solid contacting efficiency improves noticeably at high pressure and high gas flow rate . This is due to the improved spreading of the liquid holdup over the external packing area as a result of increase in the shear stress on the gas-liquid interface by means of higher gas velocity or pressure (gas density).

(3) The influence of pressure on pressure drop, liquid holdup and contacting efficiency is due to the gas phase density which increases at high pressure. At a given superficial gas and liquid velocity, the pressure drop and liquid holdup are about the same for equal gas density.

(4) The effect of gas flow rate on pressure drop, liquid holdup and liquid-solid contacting efficiency is more pronounced at elevated pressure.

(5) The developed phenomenological analysis described properly the experimental observations of the effect of elevated pressure and gas flow rate on the investigated hydrodynamics parameters (pressure drop, liquid holdup and contacting efficiency).

(6) A new model based on phenomenological approach for prediction of liquid-solid contacting efficiency has been developed. The model predicts the trend of the effect of high pressure and gas flow rate on the contacting efficiency properly. El-Hisnawi's correlations (1981) (Table 4.1) Failed to predict the effect of reactor pressure and gas flow rate.

(7) Holub's phenomenological model (1990) predicts the pressure drop and liquid holdup at elevated pressure better than the recently reported correlations. It could be implemented to predict them in trickle-flow regime at operating condition of interest (high pressure). Moreover, it predicts the trend of the effect of elevated pressure and gas flow rate on pressure drop and liquid holdup properly. Besides being based on a phenomenological approach, it is the only model that does not contain any parameter fitted to two phase flow data where wall effects, axial dispersion and liquid maldistribution in laboratory reactors can be encountered. It only requires the Ergun constants for each bed of interest to be measured by single phase pressure drop experiments. In contrast, all other current models need at least two parameters fitted to two phase flow experiments. Furthermore, all the current empirical correlations

developed based on high pressure data failed to predict pressure drop and liquid holdup data closer than the Holub's model (1990) prediction.

(8) A reproducible procedure to pack the laboratory scale trickle-bed reactor with a mixture of catalyst and fines has been developed. The reproducibility has been quantified. The developed procedure is basically based on filling the voidage of the original bed with fines.

(9) Liquid-solid contacting efficiency in a diluted bed with a mixture of catalyst and fines has been measured. The results confirm quantitatively its improvement. Diluting the bed with fines also increases liquid holdup and pressure drop over the bed.

(10) The effect of the degree of dilution with fines on liquid-solid contacting efficiency, pressure drop and liquid holdup has been investigated. If the bed dilution increases (large volumetric ratio of fines to catalyst), the bed voidage and solid to solid contacts points increase. In a bed of 2 volumes of fines to 1 volume of catalyst, pressure drop was found to be smaller due to more voidage, while liquid holdup is larger due to large number of solid to solid contact points than those in a bed packed with less fines (fines just fill the voidage according to the developed procedure).

(11) The improvement of the liquid-solid contacting efficiency in the diluted bed of 2 volumes of fines to 1 volume of catalyst is approximately similar to that obtained in the bed diluted with less fines according to the developed procedure (fines just fills the bed voidage). This would indicate that smaller pressure drop and higher holdup in the first bed compensate the higher pressure drop and less holdup in the second bed for their effects on contacting efficiency in the diluted bed with fines.

(12) According to the findings mentioned in (11) above, the developed procedure to pack the bed with a mixture of catalyst and fines is strongly recommended where both uniform catalyst and fines distribution and reproducibility are ensured over the highly diluted bed and/or other methods described previously as well.

6.2 RECOMMENDATIONS

In addition to the parameters investigated in this work (pressure drop, liquid holdup and contacting efficiency), it is recommended that other design, scale-up and operating parameters, such as flow regimes transition, liquid distribution, volumetric mass transfer coefficients, heat transfer, etc. need to be reevaluated at high pressure operation before any findings at atmospheric pressure are implemented to the operating condition of interest (high pressure). The following recommendations emphasize the parameters that are closely related to the findings of this study.

(1) In order to implement Holub's model (1990) in scale-up, scale-down and design, it is recommended to verify that E_1 and E_2 are independent of reactor diameter and height. Preliminary tests were conducted to evaluate Ergun constants in two reactors of inside diameter 2.2 cm and 7.9 cm using spherical alumina of d_p = 0.3 cm and nitrogen as a gas phase. The initial results indicate that Ergun constants are independent of reactor diameter, height and pressure (E_1 = 210 , 218 ; E_2 =1.7, 2.6 for I.D. = 2.2 and 7.9 cm, respectively). Further work on this part is recommended to include larger reactors, different catalyst shapes and sizes, and different bed heights.

(2) The developed phenomenological analysis indicates that at high pressure operation , liquid film thickness decreases (equation 4.3). Decreasing liquid film thickness affects the transition from trickle to pulse flow regime. The initiation of transition is probably due to collapsing of liquid films in such a way that the gas flow through the pore necks is blocked . Therefore, decreasing liquid film thickness at high pressure operation shifts the transition towards higher liquid throughput. Hence, the operating regime for trickle flow becomes larger (Wammes, 1990). Since all the current flow map and transition model and/or criteria have been developed at atmospheric conditions, further investigations on flow regime transition are recommended to establish a new map and transition model or criteria at operating condition of interest (high pressure operation).

(3) Investigation of the effect of high pressure and gas flow rate on the hydrodynamics parameter in the other flow regimes, particularly the pulse flow regime which is of industrial interest, should be conducted. Yet no study appeared which addressed such effects.

(4) Liquid-solid mass transfer is affected by liquid-solid contacting efficiency, therefore, studying the effect of high pressure and gas flow rate on liquid-solid mass transfer coefficient is recommended. Fines should also be incorporated to investigate their effect. The improvement in liquid-solid mass transfer should be compared with that obtained in this work on contacting efficiency.

(5) Gas-liquid mass transfer need to be studied at high pressure operation . Recently Larachi et al. (1991) and Wammes (1990) found that at high pressure operation gas-liquid interfacial area increases.

(6) Investigation should be performed to study the effect of reactor temperature at high pressure operation on liquid-solid contacting efficiency as well as the other parameters.

(7) It is recommended to investigate the effect of fines on the catalyst utilization efficiency which is related to the liquid-solid contacting efficiency. This can be achieved by utilizing a model reaction such as hydrogen peroxide decomposition in a nondiluted and diluted beds. The result should be compared to the findings of this study

(8) For the purpose of scale-up, investigation of catalyst utilization and/or liquid-solid contacting efficiency in different reactor sizes is recommended. A comparison between the findings obtained in small reactor with fines with that obtained in larger units should be conducted toward establishing scale-up criteria.

(9) It is recommended to extend the models for prediction of pressure drop, liquid holdup and contacting efficiency , to diluted beds with fines. More exprimentes are needed on this part.

7. APPENDICES

APPENDIX 7.1

SAMPLE OF A DATA ACQUISITION PROGRAM

PCLAB library subroutines are utilized to collect data by the developed data acquisition system. The programs have been written in BASIC language and utilize the ADC.VALUE subroutine. All programs are available in the Chemical Reaction Engineering Laboratory (CREL). The following is a simple program called DPT.BAS written to collect data from the differential pressure transducers and to compute the pressure drop in terms of inches of water column.

7.1.1 Getting Started

(1) open PCLAB directory from the C drive

C:\cd\PCLAB ↵

you get the following

C:\PCLAB>

(2) Type PCLLDR PCLDEFL to execute the PCLAB device driver, to place the library into the memory, to establish a BASIC program in line 200 to 300 with the routine locations in the memory and to place the user in the program :

C:\PCLAB>PCLLDR PCLDEFL ↵

You get into the BASIC environment , where the word OK appears at the top left corner. If the user wants to write a data acquisition program, it must not contain lines number from 200 to 300.

(3) Load the desired program :

LOAD"DPT.BAS ↵

(4) To list the program use LIST command. e.g. LIST ↵ , to list all the program ; LIST 1000-1100 , to list only the BASIC statement numbered between 1000 and 1100; LIST 1000- , to list the statements from 1000 to the end of the program.

(5) To Run the program use run command by typing only RUN and hit enter (↵)

7.1.2 DPT.BAS Program

```
1000 'DEPENDING ON THE CONDITIONS, SWITCH DPT DATA
1100 'ACQUISITION CONNECTOR TO THE DPT OF APPROPRIATE RANGE
1200 PRINT "ENTER THE NUMBER REFERRING TO THE SELECTED DPT
1300 PRINT " 1 FOR DPT OF (0-50 w.c.), 2 FOR DPT OF (0-750 w.c.) ? ", NDPT
1400 'ASSIGNING CHANNEL NUMBER AND ITS GAIN
1500 CHAN.DPT% = 1
1600 GAIN.DPT% = 1
1700 'INTRODUCING THE EXPERIMENT AND SAMPLING TIMES
1800 INPUT " ENTER EXPERIMENT TIME (sec) ? ", EXPTIME!
1900 INPUT " ENTER SAMPLING INTERVAL TIME (sec) ? ", SAMPLINTV!
2000 'ASSIGNING DIMENSIONS FOR THE VARIABLES
2100 J% = ( EXPTIME! / SAMPLINTV! ) + 1
2200 DIM TIMSAMPL%(J%) , DIGT.DPT(J%)
2300 'INTRODUCING THE NAME OF THE OUTPUT DATA FILE
2400 INPUT "ENTER THE OUTPUT FILE NAME ? ", FILE1$
2500 'ASSIGNING THE STARTING TIME
2600 INTIALTIME = TIMER
2700 TIMDP(1) = TIMER
```

```
2800 TIMSAMPL%(1) = TIMDP(1) - INTIALTIME
2900 'SAMPLING (COLLECTING DATA) AT THE BEGINNING OF THE FIRST
3000 'INTERVAL (i.e. AT TIMSAMPL%(1) = 0 )
3100 CALL  ADC.VALUE (CHAN.DPT%,GAIN.DPT%,ADIN.DPT%)
3200 DIGT.DPT(1) = ADIN.DPT%
3300 'PRINTING HEADING ONTO THE SCREEN
3400 PRINT  "TIMER" , "SAMPLING TIME" , "DPT DIGIT"
3500 'PRINTING COLLECTED DATA AT BEGINNING OF THE FIRST
INTERVAL
3600 PRINT  TIMDP(1) , TIMSAMPL%(1) , DIGT.DPT(1)
3700 'SAMPLING AT THE END OF EACH INTERVAL
3800 FOR  K=2  TO  J%
3900 INTV! = SAMPLINTV! * (K-1)
4000 TIMSET! = INITIALTIME + INTV!
4100 IF TIMER < TIMSET!  THEN  GO TO  4100
4200 TIMDP(K) = TIMER
4300 TIMSAMPL%(K) = TIMDP(K) - INITIALTIME
4400 CALL ADC.VALUE(CHAN.DPT%,GAIN.DPT%,ADIN.DPT%)
4500 DIGT.DPT(K) = ADIN.DPT%
4600 PRINT  TIMDP(K) , TIMSAMPL%(K) , DIGT.DPT(K)
4700 NEXT
4800 'COMPUTING THE AVERAGE OF DIGIT SIGNAL
4900 SUMDPT! = 0
5000 FOR  K=1  TO  J%
5100 SUMDPT! = SUMDPT! + DIGT.DPT(K)
5200 NEXT
```

```
5300 AVGDPT.DGT = SUMDPT! / J%
5400 'COMPUTING THE PRESSURE DROP AVERAGE IN TERMS OF  VOLT,
5500 'MILLIAMPER, AND WATER COLUMN (w.c.)
5600 AVGDPT.VLT = AVGDPT.DGT * (10! / 4096)
5700 AVGDPT.MA = AVGDPT.VLT * (16! / 10!) + 4
5800 IF  NDPT = 1  THEN  AVGDPT.WC =  - 12.4896 + (3.125 * AVGDPT.MA)
5900 IF  NDPT = 2  THEN  AVGDPT.WC = - 188.132 + (47.039 * AVGDPT.MA)
6000 'OPENING THE OUTPUT DATA FILE
6100 OPEN  FILE1$  FOR  OUTPUT  # 1
6200 'PRINTING  TO THE FILE
6300 PRINT  #1 ,  FILE1$
6400 PRINT  #1  ,  "                    "
6500 PRINT  #1  ,  "PRESSURE DROP IN WATER COLUMN = ",AVGDPT.WC
6600 PRINT  #1  ,  "                    "
6700 PRINT  #1  ,  "AVERAGE DIGIT SIGNAL                    = ",AVGDPT.DGT
6800 PRINT  #1  ,  "AVERAGE VOLTAGE SIGNAL                  = ", AVGDPT.VLT
6900 PRINT  #1  ,  "AVERAGE MILLIAMPER SIGNAL               = ", AVGDPT.MA
7000 PRINT  #1  ,  "                    "
7100 PRINT  #1  ,  "TIMER" , "SAMPLING TIME" , "DPT DIGIT"
7200 FOR  K = 1  TO  J%
7300 PRINT  # 1  ,  TIMDP(K) , TIMSAMPL%(K) , DIGT.DPT(K)
7400 NEXT
7500 END
```

Note : DPT output signal is 4-20 mA

APPENDIX 7.2

TRICKLE-BED REACTOR OPERATING PROCEDURE

A step-by-step operating procedure for high pressure trickle-bed reactor facility is listed below. It is assumed that the liquid phase has met the purification requirements and that the storage tanks have been charged with the desired liquid phase (organic or aqueous).

Operating Procedure :

1. Pack the reactor with the desired catalyst and determine the catalyst weight being charged to the reactor. If diluted bed with fines is utilized, follow the developed procedure in this work to pack the reactor with a mixture of catalyst and fines.
2. Attach the reactor head, and connect the reactor bottom to the on/off valve that is connected to the gas/liquid separator.
3. Pressurize the liquid feed tank with helium or nitrogen if the pressurized tank is utilized. In case that the high pressure pump is used, pressurize the small tank at the discharge line of the pump. Flood the bed with the desired liquid phase to be used. Turn the reactor inlet and outlet valves off, and keep the bed flooded at least overnight. Relieve the pressure in the feed tank by opening the vent line valve.

(4) If the differential refractometer is used in tracer experiments for liquid-filled operation, turn it on for at least twelve hours prior to any experiment. It is recommended to leave it on during the period of use. More details, procedure and recommendations about how to utilize the differential refractometer can be found in its manual posted in the trickle-bed reactor laboratory.

(5) Upon completion of step (3) and (4), set the feed tank supply pressure regulator to a pressure of about 50 psig higher than the operating pressure of the experiment.

(6) Fill the two bubblers (saturators) with the liquid phase being utilized. The pressurized feed tank and/or high pressure pump can be used to fill these saturators .

(7) Turn on the computer and the data acquisition system. Load the required data acquisition program.

(8) If tracer experiment is to be executed , switch the injection valve into non injection mode . Flush and fill the tracer loop with the desired tracer.

(9) Open the reactor outlet and inlet on/off valves. Let liquid phase flow to the reactor by adjusting the liquid inlet needle valve to the desired setting on the rotameter. (If liquid filled operation is used, allow the refractometer base line to reach steady state).

(10) Set the pressure regulator of the feed gas cylinder to a desired pressure. Open the needle valve of the gas inlet slowly. Pressurize the system gradually.

(11) Adjust the gas pressure at the gas rotameters outlet to the rotameter's calibration pressure. In the meantime set the gas rotameter to the desired gas flow rate. These can be achieved by both pressure regulators at the rotameter inlet (i.e. at the gas outlet from the separator) and at the rotameter outlet. The gas flow rate measured at the gas rotameter outlet need to be corrected to the actual flow rate inside the reactor which is at a particular pressure. In this case the compressibility factor need to be considered based on the gas and the range of employed pressure. It is noteworthy to mention that the gas rotameters need to be recalibrated from time to time and for each gas phase being utilized.

(12) Increase liquid flow rate to the level which assumes the high interaction regime and operate in this regime for several minutes.

(13) Reduce the liquid flow rate back to the desired flow.

(14) Maintain the liquid level at the bottom of the gas/liquid separator as constant as possible. Two valves at the outlet liquid stream (between the liquid pressure regulators and the rotameters) are adjusted for this purpose.

(15) Measure the mass liquid flow rate by using the on line calibration lines at the waste and sampling outlet streams.

(16) Open the valves to the high and low pressure port of the differential pressure transducer.

(17) Start the data acquisition, and monitor the pressure drop, gas outlet rotameter reading and pressure (i.e. gas flow rate), reactor pressure, liquid flow rate, liquid level at the gas/liquid separator, pressure indicators. The operation is considered to be stable (steady state) if these conditions are met and controlled properly for at least 5 minutes.

Note : Maintaining a constant level of the liquid at the bottom of gas/liquid separator is essential to stabilize the pressure drop particularly at high pressure and high gas flow rate operation and is required for tracer experiment.

(18) When operating conditions reach steady state according to step (17), the desired measurements can be taken as follows :

(19) For pressure drop and liquid holdup experiments only :

Start sampling the pressure drop measurements and monitor the multimeter signal for about few minutes. The average value of the pressure drop is computed at the end. Then close the valves to the differential pressure transducer. If the draining method is used to measure liquid holdup , close the inlet and outlet valves on the liquid streams simultaneously followed by closing the gas inlet valve. Drain the separator , then open the outlet reactor valve and collect the draining liquid. Static liquid holdup can be measured by the increase in the weight of the reactor at the end of draining over that of the dry reactor. This weight represent both the external static liquid holdup and the liquid that fills the pores of the catalyst in case that porous catalyst is utilized.

(20) For tracer experiment associated with the pressure drop and liquid holdup measurements:

Inject the tracer by converting tracer valve into injection mode (If liquid-filled operation is used, start sampling the differential refractometer signal at the same injection time). For two phase flow operation, start the stop watch at the same time the tracer is injected, collect samples in suitable intervals from the liquid separator outlet. In this operation , keep the liquid level at the bottom of the separator constant and as low as possible. Monitor the operating condition to maintain stability of the unit during tracer experiment period. Shortly after the tracer is injected , open the valves to the differential pressure transducer ports. Pressure drop measurements are sampled at the same sampling interval time of the differential refractometer. The average value of the pressure drop is computed at the end. After the tracer experiment is completed , liquid holdup by the draining method is measured according to step (20).

Shut Down Procedure :

Upon completion of the experiments, the facility is shut down in the following sequence :

(1) Turn off the data acquisition system

(2) Terminate both liquid and gas flow to the reactor.

(3) Relieve the gas line feed pressure by closing the main gas cylinder valve.

(4) Relieve the feed liquid tank.

8. NOMENCLATURE

a_{LS}	Effective liquid-solid mass transfer area per unit reactor volume, cm^2/cm^3
a_S , a_t	Total particles surface area per unit reactor volume, cm^2/cm^3
C	Tracer concentration, $mole/cm^3$
d_p	Particle diameter, cm
d_r	Reactor diameter, cm
$(De)_{LF}$	Effective diffusivity in liquid-filled operation, cm^2/s
$(De)_{TF}$	Effective diffusivity in two phase flow operation, cm^2/s
D_L	Axial dispersion coefficient , cm^2/s
$E(t)$	Normalized tracer response curve
Fr_L	Dimensionless liquid Froud number , $a_t L^2 / \rho^2_L g$
g	Gravitational acceleration, cm/s^2
G	Superficial gas mass velocity , $kg/m^2 s$
Ga_L	Dimensionless liquid Galileo number, $d^3_p \rho^2_L g \varepsilon_B^3 / \mu^2_L (1-\varepsilon_B)^3$
Ga_G	Dimensionless gas Galileo number, $d^3_p \rho^2_G g \varepsilon_B^3 / \mu^2_G (1-\varepsilon_B)^3$
k_{Ls}	Liquid-solid mass transfer coefficient, cm / s
L	Superficial liquid mass velocity , $kg/m^2 s$
N_{LS}	Mass transfer flux of tracer from liquid to catalyst surface, g-mole / cm^2 s
$\Delta P / Z$	Pressure drop per unit bed length, $g/cm^2 s^2$

Pe_L	Dimensionless Peclet number, $U_L d_p / De_L$
Q_L	Liquid volumetric flow rate, cm^3 / s
r_p	Particle radius, cm
Re_L	Dimensionless liquid Reynolds number, $U_L \rho_L d_P / \mu_L(1-\varepsilon_B)$
Re_G	Dimensionless gas Reynolds number, $U_G \rho_G d_P / \mu_G(1-\varepsilon_B)$
S_{ex}	External area of catalyst pellet, cm^2
t	Time , s
T	Tortuosity
U_L	Superficial liquid velocity, cm / s
U_G	Superficial gas velocity , cm/s
V_p	Particle volume , cm^3
V_r	Reactor bed volume , cm^3
We_L	Dimensionless liquid Weber number , $U^2_L d_p \rho_L / \sigma_L$
We_G	Dimensionless gas Weber number , $U^2_G d_p \rho_G / \sigma_L$
Z	Packed-bed length, cm

Greek Letters

β_d , ω_d	Dynamic liquid saturation (liquid volume per void volume)
β_t	Total liquid saturation
δ	Liquid mean film thickness, cm
ε_B	Packed-bed void per reactor volume (bed porosity)
ε_{Bf}	Diluted bed (catalyst and fines) void per reactor bed volume (equation 5.3)

$\bar{\varepsilon}_B$	Diluted bed void per reactor volume + volume of fines per reactor volume (equation 5.1)
ε_{Ld}	Dynamic liquid holdup per reactor bed volume
ε_{Ls}	Static liquid holdup per reactor bed volume
ε_L	External liquid holdup per reactor bed volume ($\varepsilon_{Ld} + \varepsilon_{Ls}$)
ε_{Li}	Internal liquid holdup per reactor bed volume (inside the pores) for porous particles
ε_{Lt}	Total liquid holdup (external and internal) per reactor bed volume ($\varepsilon_L + \varepsilon_{Li}$)
ε_p	Particle porosity
η_{CE}	External liquid-solid contacting efficiency
μ_1	First moment, s
μ_2	Second moment, s^2
μ_L	Liquid viscosity, g/cm s
μ_G	Gas viscosity , g/cm s
ρ_L	Liquid density, g/cm^3
ρ_G	Gas density , g/cm^3
σ^2	Variance of second central moment, s^2
σ^2_D	Dimensionless variance
Ψ_L	Liquid dimensionless pressure drop $((\Delta P/Z)/(\rho_L g)+1)$
Ψ_G	Gas dimensionless pressure drop $((\Delta P/Z)/(\rho_G g)+1)$

9. REFERENCES

Al-Dahhan, M. , " Effects of High Pressure and Fines on the Hydrodynamics of Trickle-Bed Reactors ", D.Sc. Proposal , Washington University , St. Louis , MO , (1992).

Anderson, J. R. and K. C. Pratt ," Introduction to Characterization and Testing of Catalysts ", Academic Press , (1985) .

Basic', A. , " Liquid Holdup and Hydrodynamics of Rotating Packed Beds ", D.Sc. Thesis, Washington University, St. Louis, Missouri, (1992).

Blok, J. R., J. Varkevisser and A. A. H. Drinkenburg, " Transition to Pulsing Flow, Holdup and Pressure Drop in Packed Columns with Cocurrent Gas-Liquid Downflow" , Chem. Eng. Sci. , 38, 687, (1983).

Carruthers D. J., and D. J. DiCamillo, " Pilot Plant Testing of Hydrotreating Catalyst Influence of Catalyst Condition , Bed Loading and Dilution " , Applied Catalysis, 43, (1988).

Charpentier, J. C., C. Prost et P. LeGoff , " Ecoulement Ruisselant de Liquid Dans Une Colonne a Garnissage ", Chimie et Industrie - Genie Chimique , 100, 653, (1968).

Charpentier, J.C. and M. Favier , " Some Liquid Holdup Experimental Data in Trickle Bed Reactors for Foaming and Nonfoaming Hydrocarbons", AIChE J. , 21 ,1213, (1975).

Charpentier, J. C. , " Recent Progress in Two Phase Gas-Liquid Mass Transfer in Packed Beds. " The chem. Eng. J., ,11,161, (1976) .

Charpentier, J. C , " New Trends in Gas-Liquid Reaction Engineering " , Int. Chem. Eng., 28, 2 , 285 , (1988).

Charpentier, J. C., M. Bakos and P. Le Goff, " Hydrodynamics of Two-Phase Cocurrent Down Flow in Packed-Bed Reactors. Gas-Liquid Flow Regime, Liquid Axial Dispersion, and Dead Zones " , Proc. 2nd Conference on Applied Physical Chemistry, Veszprem , Hungary, 2 , 31, (1971).

Clements, L. D. and P. C. Schmidt , " Two-Phase Pressure Drop in Cocurrent Downflow in Packed Beds : Air-Silicone Oil System ", AIChE J. , 26, 314, (1980).

Clements, L. D. and P. C. Schmidt , " Dynamic Liquid Holdup in Two-Phase Downflow in Packed Beds: Air-Silicon Oil System ", AIChE J. , 26, 317, (1980).

Crine, M. D. and G. A. L'Homme , " The Percolation Theory : A Powerful Tool for a Novel Approach to the Design of Trickle-Bed Reactors and Columns ", ACS symp. ser. No. 196,Chemical Reaction Engineering - Boston (Am. Chem. Soc.), Washington D.C., (1982).

Crine, M. and P. Marchot , " Measuring Dynamic Liquid Holdup in Trickle-Bed Reactors Under Actual Operating Conditions", Chem. Eng. Comm., 8, 365, (1981).

Chou, T. S, F. L. Worley Jr. and D. Luss, " Transition to Pulsed Flow in Mixed-Phase Cocurrent Downflow Through a Fixed Bed " , Int. Eng. Chem. Process. Des. Dev.,16, 424, (1977).

Colombo, A. J. , G. Baldi and S . Sicardi ," Solid-Liquid Contacting Effectiveness in Trickle Bed Reactors ", Chem. Eng. Sci. , 31, 1101 , (1976).

Danckwerts P. V. , " Continous Flow System Distributions of Resistence Times", Che. Eng. Sci. , 2, 1, (1953).

Dudukovic, M. P. and P. L. Mills ," Contacting and Hydrodynamics in Trickle-Bed Reactors", in Encyclopedia of Fluid Mechaics (N. P. Cheremisinoff, ed.), Gulf pub. Co., Ch.32, 969, (1986).

Dudukovic, M. P.," Catalyst Effectiveness Factor and Contacting Efficiency in Trickle-Bed Reactors " , AIChE J. , 23, 6, (1977).

Dudukovic, M. P.and R. M Felder, " Mixing Effects in Chemical Reactors- III Dispersion Model " , AIChE Modular instruction , Series E, Vol. 4, Reactor Stability, Sensitivity and Mixing Effects, (Module E4.7), AIChE, New York, (1983).

Dudukovic, M. P. and R. M Felder," Mixing Effects in Chemical Reactors-IV Residence Time Distributions " , AIChE Module instruction, Vol. 4 , series E-kinetics , E4.7.

Dudukovic, M. P., N. Devanathan and R. Holub " Multiphase Reactors : Models and Experimental Verification. " Revue De L'Inistitut Francais -Du Petrole , 46, 4, (1991).

El-Hisnawi, A. A. , " Tracer and Reaction Studies in Trickle Bed Reactors " , D.Sc. Thesis, Washington University, St. Louis , Missouri, (1981).

El-Hisnawi, A. A., M. P. Dudukovic and P. L. Mills, " Trickle-Bed Reactors: Dynamic Tracer Tests , Reaction Studies , and Modeling of Reactor Performance ", ACS Sym. Series,196, 431, (1982).

Ellman, M. J., N. Midoux, A. Laurent , and J. G. Charpenteir, "A New Improved Pressure Drop Correlation for Trickle-Bed Reactors " , Chem. Eng. Sci., 43 , 2201, (1988).

Ellman, M. J., N. Midoux, G. Wild, A. Laurent and J. C. Charpentier, " A New Improved Liquid Hold-up Correlation for Trickle-Bed Reactors" , Chem .Eng. sci., 45, 7, 1677,(1990).

Ergun, S. , " Fluid Flow Through Packed Columns ", Chem. Eng. Prog., 48, 89, (1952)

Fukushima, S. and K. Kusaka, " Interfacial Area and Boundary of Hydrodynamic Flow Region in Packed Column with Cocurrent Downward Flow ", J. of chem. Eng of Japan, 10, 6, (1977).

Fukushima, S. and K. Kusaka, " Liquid Phase Volumetric and Mass Transfer Coefficient, and Boundary of Hydrodynamic Flow Region in Packed Volume with Cocurrent Downword Flow " , J. of chem. Eng. of Japan ,10 , 6, 468, (1977).

Fukushima, S. and K. Kusaka , " Boundary of Hydrodynamic Flow Region and Gas-Phase Mass Transfer Coefficient in Packed Column with Cocurrent Downword Flow ", J.of chem. Eng. of Japan ,11, 3, 241, (1978).

Fukushima, S. and K. Kusaka ," Gas-Liquid Mass Transfer and Hydrodynamics Flow Region in Packed Columns with Cocurrent Upward Flow ", J. of chem. Eng. of Japan, 12, 4 , 296 , (1979).

Gianetto, A. and P. L. Silveston , (ed.) , " Multiphase chemical Reactors, Theory, Design, Scale-up " , Hemisphere Pub. Corp., (1986).

Gianetto, A. and V. Specchia, " Trickle-Bed Reactors : State of Art and Perspectives" Chem. Eng. Sci. , 47 , 13/14 , 3197 , (1992).

Gierman H. , " Design of Laboratory Hydrotreating Reactors Scaling Down of Trickle-Flow Reactors ", Applied Catalysis , 43, 285, (1988).

Goto, S. and J. M. Smith , " Trickle-Bed Reactor Performance ", AIChE J. , 21, 4, (1975).

Goto, S. , J. Levec and J. M. Smith, " Trickle-Bed Oxidation Reactors ", Catal. Rev. Sci. Eng., 15, 187, (1977).

Hanratty, P. J. , " Dynamic Modelling of Trickle Bed Reactors " , M.Sc. Thesis,Washington University, St. Louis , Missouri , (1988).

Herskowitz, H. and J. M. Smith , " Liquid Distribution in Trickle-Bed Reactors . Part I: Flow Measurements ,Part II: Tracer Studies " AIChE J., 24 ,439 ,(1978).

Herskowitz, M. , R. G. Carbonell and J. M. Smith, " Mass Transfer and Wetting in Trickle-Bed Reactors ", AIChE J. , 25, 272, (1979).

Herskowitz, H. and J. M. Smith," Trickle-Bed Reactors: A Review ", AIChE J. , 29, 1, 1, (1983).

Hewitt, G. F. , Measurement of Two Phase Flow Parameters , Academic Press, N.Y., (1978).

Hofmann, H. P., " Multiphase Catalytic Packed-Bed Reactors ",Catal. Rev. Sci. Eng., 17, 21, 71, (1978).

Holub, R. ," Hydrodynamics of Trickle Bed Reactors ", D.Sc.Thesis,Washington University , St. Louis, Missouri, (1990).

Holub, R. A. , M. P. Dudukovic' and P. A. Ramachandran, " A Phenomenological Model of Pressure Drop, Liquid Holdup and Flow Regime Transition in Gas-Liquid Trickle Flow", Chem. Eng. Sci. , 47, 9/11, 2343, (1992).

Hutton, B. E. T. and L. S. Leung , " Cocurrent Gas-Liquid Flow in Packed Columns ", Chem. Eng. Sci. , 29, 1681, (1974).

Jones, O. C. and N. Zuber , " X-ray measurement of void fraction in gas-liquid columns " , Int. J. Multiphase Flow, 2, 273, (1975).

Kan, K. and P. E. Greenfield, " Pressure Drop and Holdup in Two-Phase Cocurrent Trickle Flows Through Beds of Small Packings ", Ind. Eng. Chem. Process Des. Dev.,18, 740, (1979).

Koros, R. M. , " Catalyst Utilization in Mixed-Phase Fixed Bed Reactor " 6th European Symposium on Chemical Reaction Engineering, Heidelberg, Germany, (1976).

Krauze, R. and M. Serwinski , " Moisted Surface and Fractional Wetted Area of Ceramic Raschig Rings ." Inzyneria chemicana , 1, 415, (1971).

Lakota, A. and J. Levec, " Solid-Liquid Mass Transfer in Packed Beds with Cocurrent Downward Two-Phase Flow ", AIChE J., 36, 9, 1444, (1990).

Larachi, F., A. Laurent, G. Wild and N. Midoux , " Some Experimental Liquid Saturation Results in Fixed-Bed Reactors Operated Under Elevated Pressure in Cocurrent Upflow and Downflow of the Gas and Liquid ", Ind. Eng. Chem. Res. , 30 , 2404, (1991).

Larachi F., A. Laurent , G. Wild and N. Midoux , " Pressure Effect on Gas-Liquid Interfacial Areas in Cocurrent Trickle-Flow Reactor", Chem. Eng. sci., 47, 9/11, 2325, (1992).

Larachi, F. , A. Laurent , N. Midoux and G. Wild , " Experimental Study of A Trickle-Bed Reactor Operating at High Pressure : Two-Phase Pressure Drop and Liquid Saturation " , Chem. Eng. Sci. , 46, 5-6, 1233, (1991).

Larkins, R. P., R. R. White and D. W. Jeffrey ," Two-Phase Cocurrent Flow in Packed Beds", AIChE J. , 7, 231, (1961).

Lazzaronni, C. L., H. R. Keselman and H. S. Figoli, " Calorimetric Evaluation of the Efficiency of Liquid-Solid Contacting in Trickle Flow ", Ind. Eng. Chem. Res., 27, 1132, (1988).

Levec, J. and S. Goto , "Mass Transfer and Kinetics in Three-Phase Reactors ", in handbook of heat and mass transfer , (Chereisinoff, N. P. , ed.), Gulf Pub. Co. , vol.2, Ch.19, (1986).

Levec , J., A. E. Saez and R.G. Carbonell , " Hydrodynamics of Trickling Flow in Packed Beds", AIChE J., 32, 3, 369, (1986).

Levec, J., K. Grosser and R. G. Carbonell , " The Hysteretic Behavior of Pressure Drop and Liquid Holdup in Trickle Bed Reactor ", AIChE J. , 34, 1027, (1988).

Levenspiel, O., The Chemical Reactor OmniBook+ , Oregon State University, Book Store Inc., (1986).

L'Homme , G. A. (ed.), Gas-Liquid-Solid Catalyst Reaction , CEBEDOC, Liege , Belgium , (1979).

Macdonald, I. F., M. S. El-Sayed, K. Mow and F. A. L. Dullien, " Flow Through Porous Media - the Ergun Equation Revisited" , Ind. Eng. Chem. Fundam. , 18, 3, (1979).

Marques, A. L., F. Larachi , G. Wild and A. Laurent, " Mass Transfer Characteristics of Fixed Beds with Cocurrent Upflow and Downflow. A Special Reference to the Effect of Pressure", chem .Eng. Sci., 47, 13/14, 3485, (1992).

Matsuura, A., T. Akehata and T. Shirai, " Axial Dispersion of Liquid in Cocurrent Gas-Liquid Downflow in Packed Beds ", J. Chem. Eng. Japan , 9, 294, (1976).

Melli, T. R. and L. E. Scriven, " Theory of Two-Phase Cocurrent Down Flow in Networks of Passages " , Ind.Eng.Chem .Res.,30, 951, (1991).

Midoux, M. , M. Favier and J. C. Charpentier, " Flow Pattren, Pressure Loss and Liquid Holdup Data in Gas-Liquid Downflow Packed Beds with Foaming and Nonfoaming Hydrocarbon ", J. Chem. Eng. of Japan, 9, 350, (1976).

Mills , P. L., " Catalyst Effectiveness and Solid-Liquid Contacting in Trickle-Bed Reactors ", D.Sc.Thesis, Washington University , St. Louis, Missouri, (1978).

Mills, P. L. and M. P. Dudukovic, " Evaluation of Liquid-Solid Contacting in Trickle by Tracer Methods ", AIChE J., 27 , 893, (1981).

Mills, P. L. and M. P. Dudukovic , " Integral Equation Solution for the Effectiveness Factor of Partially Wetted Catalysts " , Ind. Eng. Chem., 21, 1, (1982).

Mills, P. L. and M. P. Dudukovic, " Evaluation of Liquid-Solid Contacting in Trickle Bed Reactors by Tracer Methods " , AIChE J. , 28 , 52, (1982).

Morsi, B. I. , N. Midoux, A. Laurent , J. C. Charpentier ," Hydrodynamics and Interfacial Areas-Liquid Flow Through Fixed Beds. Influence of the Nature of the Liquid ", Inter. Nat. Eng. , 22, 1, 142, (1982).

Morsi, B. I., A. Laurent, N. Midoux, G. Barthole-Delaunay, A. Strock and J. C. Charpentier, " Hydrodynamics and Gas-Liquid-Solid Interfacial Parameters of Cocurrent Downward Two Phase Flow in Trickle-Bed Reactors ", Chem. Eng. Comm., 25, 267, (1984).

Ng , K. H. and C. F. Chu, " Trickle-Bed Reactor ", Chem. Eng. Progress, 55, (1987).

Onda, k., H. Takeuchi and Y. Kayama, " Effect of Packing Materials on Wetted Surface Area", K. Kagaku Kogaku, 31, 126, (1967).

Patil, V. K. and M. M. Sharma , " Packed Tube Columns : Hydrodynamics and Effective Interfacial Area; Pall Rings and Multifilament Wire Gauze Packings ", Can. J. Chem. Eng. , 59, 606, (1981).

Puranik, S. S. and V. Vogelphl ," Effective Interfacial Area Irrigated Packed Columns", Chem.Eng.Sci. , 29, 501, (1974).

Ramachandran, P. A. and R. V. Chaudhari , Three Phase Catalytic Reaction, Gordon and Breach Science Publishers ,(1983).

Ramachandran, P. A. , M. P. Dudukovic and P. L. Mills , "A New Model For Assessment of External Liquid-Solid Contacting in Trickle-Bed Reactors From Tracer Response Measurements", Chem. Eng. Sci., 42, 4855 , (1986).

Ramachandran, P. A. , M. P. Dudukovic and P. L. Mills, " Recent Advances in the Analysis and Design of Trickle bed Reactors ", A special Issue of Sadhana,10, 269, (1987).

Rao, V.G. , M. S. Ananth and Y. B. G. Varma ," Hydrodynamics of Two-Phase Cocurrent Downflow Through Packed Beds ", AIChE J. , 29, 467, (1983).

Rao, V. G. and A. A. H. Drinkenburg , " Pressure Drop and Hydrodynamic Properties of Pulses in Two-Phase Gas-Liquid Down Flow Through Packed Columns ", Can. J. Chem. Eng., 61, 158, (1983).

Rao, V. G. and A. A. H. Drinkenburg , " A Model for Pressure Drop in Two-Phase Gas-Liquid Downflow Through Packed Columns ", AIChE J. , 31, 1010, (1985).

Reiss, L. P. , " Cocurrent Gas-Liquid Contacting in Packed Columns ", Ind. Eng. Chem. Proc. Des. Dev., 6, 486, (1967).

Reynier, J. P. , and J. C. Charpentier , " Hold-up Prediction in Packed Columns for Co-current Gas-Liquid Downflow ", Chem. Eng. Sci. , 26, 1781, (1971).

Ring. Z. E. and R. W. Missen, " Trickle-Bed Reactors : Tracer Study of Liquid Holdup and Wetting Efficiency at High Temperature and Pressure ", Can. J. Chem. Eng. , 69, 1016, (1991).

Rodrigues, B. A. , J. M. Calo and N. H. Sweed (ed.), Multiphase Chemical Reactors,Volume I: Fundamentals, Volume II: Design Methods , NATO ASI, Series E , Sijthoff and Noordhot International Publisher ,(1981).

Ruecker, C. M. and A. Akgerman, " Determination at Wetting Efficiencies For a Trickle-Bed Reactor at High Temperature and Pressure " , Ind . Eng. Chem. Res. , 26, 164, (1987).

Saez, A. E. and R. G. Carbonell, " Hydrodynamic Parameters for Gas-Liquid Cocurrent Flow in Packed Beds " , AIChE J., 31, 52, (1985).

Saze, A. E., R. G. Carbonell and J. Levec ," The Hydrodynamics of Trickling Flow in Packed Beds ", AIChE J. , 32, 3, 353, (1986).

Sai , P. S. T. and Y. G. B. Varma, "Pressure Drop in Gas-Liquid Downflow Through Packed Beds" , AIChE J., 33 , 2027, (1987).

Sato, Y. , T. Hirose, F. Takahashi and M. Toda ," Pressure Loss and Liquid Holdup in Packed Bed Reactor with Cocurrent Gas-Liquid Downflow " , J. chem. Eng. Japan, 6, 147, (1973).

Satterfeild, C. N. ," Trickle-Bed Reactors " , AIChE J., 21, 2, 209, (1975).

Sedriks W. and C. N. Kenney , " Partial Wetting in Trickle Bed Reactors ", Adv. Chem. 109, 251, (1972).

Sedriks W. and C. N. Kenney , " Partial Wetting in Trickle-Bed Reactors: The Reduction of Crotonaldehyde Over A Palladium Catalyst ", Chem. Eng. Sci. , 38, 559, (1973).

Schubert, C. N., J. R. Linder and R. M. Kelly, " Experimental Methods For Measuring Static Liquid Holding in Packed Columns" , AIChE J. , 32, 1920, (1986).

Schwartz, J. G., E. Weger, M. P. Dudukovic, "A New Tracer Method for Determination of Liquid-Solid Contacting Efficiency in Trickle-Bed Reactors ", AIChE J. , 22, 5, (1976).

Shah,Y. T. , " Gas-Liquid-Solid Reactor Design ", McGraw Hill, (1979).

Shulman, H. L., C. F. Ullrich , A. Z. Proulx and J. O. Zimmerman ," Performance of Packed Column II : Wetted and Effective Interfacial Area , Gas and Liquid Mass Transfer Rates " AIChE J., 1, 2, 253, (1955).

Sicardi, S. , G. Baldi , A.Gianetto and V. Specchia," Catalyst Areas Wetted by Flowing and Semistagnant Liquid in Trickle-Bed Reactors " , Chem. Eng. Sci. , 35, 67, (1980).

Sicardi, S., G. Baldi, V. Specchia , I. Mazzarino and A. Geianetto ," Packing Wetting in Trickle Bed Reactors : Influence of the Gas Flow Rate " , Chem. Eng. Sci. , 36, 226, (1980).

Sie, S. T. ," Scale Effects in Laboratory and Pilot-Plant Reactors For Trickle-Flow Processes ", Revue De L'Institut Français Du Petrole , 46, 4, (1991).

Specchia,V. and G . Baldi , " Pressure Drop and Liquid Holding For Two Phase Cocurrent Flow in Packed Beds " , Chem. Eng. Sci. , 32 , 515 (1977).

Specchia, V., G. Baldi and A. Gianetto , " Solid-Liquid Mass Transfer in Cocurrent Two-Phase Flow Through Packed Beds ", I & CE Proc. Des. Dev. , 17 , 3, 372, (1978).

Sweeney, D. E. " A Correlation for Pressure Drop in Two-Phase Cocurrent Flow in Packed Beds " , AIChE J. , 13, 4, 663, (1967).

Talmor, E. , " Two-Phase Downflow Through Catalyst Beds. I : Flow Maps " , AIChE J., 22 , 868, (1977).

Tosun, G . "A Study of Co-Current Downflow of NonFoaming Gas-Liquid Systems in Packed Bed. I: Flow Regimes ; Search for A Generalized Flow Map. II: Pressure Drop; Search for A Correlation " , Ind . Eng. Chem. Process. Des. Dev., 23, 79, (1984).

Tukac, C.V. and J. Hanika , " Influence of Catalyst Particles Orientation on the Pressure Drop and the Liquid Dispersion in the Trickle-Bed Reactor " , 47, 9-11 , 2227, (1992).

Turpin, T. L. and R. L. Huntington , " Prediction of Pressure Drop for Two Phase, Two-Component Cocurrent Flow in Packed Beds ", AIChE J. , 13, 1196, (1967).

Van Klinken, J. , in Chemical Engineering of Gas-Liquid-Solid Catalyst Reactions (G. L. L' Homme, ed.), CEBEDOC , Ch.6, 172, (1979).

Van Klinken, J. and R. H. Van Dongen ," Catalyst Dilution for Improved Performance of Laboratory Trickle-Flow Reactors" Chem. Eng. Sci. , 35, 59 , (1980).

Wammes, W. J. A. , " Hydrodynamics in Cocurrent Gas-Liquid Trickle-Bed Reactor at Elevated Pressure ", Ph. D. Thesis ,University of Twente , Enschede, Netherlands , (1990).

Wammes, W. J. and K. R. Westerterp, " The Influence of the Reactor Pressure on the Hydrodynamics in A Cocurrent Gas-Liquid Trickle-Bed ", Chem. Eng. Sci. , 45, 8, 2247, (1990).

Wammes, W. J. A., S. J. Mechielsen and K. R.Westerterp, " The Transition Between Flow and Pulse Flow in A Cocurrent Gas-Liquid Trickle-Bed Reactor at Elevated Pressures " , Chem. Eng. Sci. , 45, 3149, (1990).

Wammes, W. J. A. , S. J. Mechielsen and K. R.Westerterp, " The Influence of Pressure on The Liquid Hold-up in A Cocurrent Gas-Liquid Trickle-Bed Reactor Operating at Low Gas Velocities ", Chem. Eng. Sci. , 46, 409, (1991).

Wammes, W.J.A. , J. Middelkamp, W. J. Hulsman, C. M.deBaas, and K. R.Westerterp , " Hydrodynamics in A Cocurrent Gas-Liquid Trickle Bed at Elevated Pressures", AIChE. J., 37, 12, 1849, (1991).

Weekman, W. V. and J. E. Myers " Fluid-Flow Characteristics of Cocurrent Gas-Liquid Flow in Packed Beds " , AIChE J., 10, 6, 951, (1964)

Wijffels, J. B., J. Verloop and F. J. Zuiderweg , " On the Wetting of Catalyst Particles under Trickle Flow Conditions " Paper Presented at the Third International Symposium on Chemical Reaction Engineering, Evanston, August, (1974).

Zhukova, T. , B.V. N. Pisarenko and V. V. Kafarov, " Modeling and Design of Industrial Reactors with A Stationary Bed of Catalyst and Two-Phase Gas-liquid Flow - A Review ", Int. Chem. Eng., 30,1 ,57, (1990).

10. ACKNOWLEDGMENTS

I would like to express my sincere appreciation and deep sense of gratitude to my advisor professor M. P. Dudukovic′ for the help, constructive suggestions, continued encouragement and freedom given to me during the course of this research. The knowledge that I acquired under his guidance is a considerable asset to my career.

I wish also to thank my co-advisor professor P. A. Ramachandran for his advise and help during this work and I am grateful to the members of my committee, Professors J. L. Kardos, R. L. Motard , R. Gardner and Dr. P. Mills for their input to this research.

I am also indebted to Professors J. L. Kardos and R. L. Motard for having me appointed as an instructor in the Chemical Engineering Department.

The financial support, partially from the Ministry Higher Education of Iraq, Chemical Reaction Engineering Laboratory (CREL) funds, and Chemical Engineering Department is gratefully acknowledged.

I am grateful to Mr. Y. X. Wu and Robert Brown for helping me in some of the experiments.

My thanks are due to all the graduate students, post doctorate fellows, and friends for their help and encouragement. In Particular I wish to acknowledge Henry Erk, Jay Turner, Waleed Al-Eisa, Baisheng Zou, Peter Hanratty, Alain Choné , Anjelko Basic′, Yubo Yang , Sujatha Degaleesan, Sriganesh Karur, Severine Choné, Jean Michel Mercier, Sailesh Kumar and Milind Kulkarni for their help and friendship.

My thanks go also to Steve Picker and Pat Harkins for their suggestions and help on the design and development of the experimental facility.

Appreciation is due to all the chemical Engineering Department Faculty members and secretaries for their cooperation and encouragement.

I am greatly indebted to my wife Etihad for her patience, understanding, support, and continued encouragement. She was the one who suffered from the hard work that I went through this accomplishment.

My parents, wife, kids, brothers and sisters deserve much more than thanks who are the happiest to see this journey come to a successful completion. I am very grateful for them for their love, moral support and patience.

11. VITA

Muthanna H. Al-Dahhan

* Born on May 4, 1957 in Al-Samawa , Iraq
* Attended University of Baghdad, Chemical Engineering Department from August 1975 to June 1979.
* Trained in Yugoslavia and Italy during the year of 1978 and 1980 on different engineering aspects.
* Worked in both Industry and Chemical Engineering Department / University of Baghdad from 1980 - 1985.
* Attended Oregon State University from 1986 to 1988 , Received M.S. in Chemical Engineering.
* Attended Washington University in St. Louis from September 1988 to September 1993.
* Appointed as an instructor in the Chemical Engineering Department from 1990 to 1993. Taught " Introduction to Computing and Computer Applications " for eight semesters

December, 1993

Short Title : Trickle-Bed Reactor / Hydrodynamics Al-Dahhan, D.Sc. 1993